

**Closing the Loop: Designing an Advanced Hydrometallurgical Lithium-Ion Battery
Recycling Facility**

Joseph Fink, Benson Harlan, Gaurav Kapoor, Nikolai Kosinski, Connor Dight

Table of Contents

Executive Summary	1
Section 1: Introduction	3
Section 2: Prior Works	5
Section 3: Discussion	7
3.0 Process Overview	7
3.1 Leaching Reactor	9
3.1.1 Reactions Overview	11
3.1.2 Standard Reactor Design	12
3.1.2.1 Impeller Choice and Design	13
3.1.2.2 Standard Reactor Power Requirements	15
3.1.2.3 Cooling Jacket Design	16
3.2 Precipitator	19
3.2.1 Impurity Removal Precipitator	20
3.2.1.1 Reactions Overview	21
3.2.1.2 Impurity Removal Precipitator Design	22
3.2.1.3 Cooling Jacket Design	23
3.2.2 Manganese Carbonate Precipitator	24
3.2.2.1 Reactions Overview	24
3.2.2.2 Manganese Carbonate Precipitator Design	25
3.2.3 Cobalt Hydroxide Precipitator	26
3.2.3.1 Reactions Overview	26
3.2.3.2 Cobalt Hydroxide Precipitator Design	26
3.2.4 Nickel Hydroxide Precipitator	27
3.2.4.1 Reactions Overview	28
3.2.4.2 Nickel Hydroxide Precipitator Design	28
3.2.5 Lithium Carbonate Precipitator	29
3.3 Packed Bed Reactor	30
3.3.1 H ₂ O ₂ Decomposition Packed Bed Reactor	30
3.3.1.1 Cooling Jacket Design	32
3.4 Liquid-Liquid Extraction Columns	33
3.4.1 Manganese Liquid-Liquid Extraction Columns	34
3.4.1.1 Reactions Overview	35
3.4.1.2 Manganese Liquid-Liquid Extraction Column Design	36
3.4.2 Cobalt Liquid-Liquid Extraction Column	38
3.4.2.1 Reactions Overview	40
3.4.2.2 Cobalt Liquid-Liquid Extraction Column Design	42

3.5 Stripping Column	42
3.5.1 Manganese Stripping Column	42
3.5.2 Cobalt Stripping Column	43
3.6 Scrubbing Column	45
3.6.1 Manganese Scrubbing Column	45
3.6.2 Cobalt Scrubbing Column	46
3.7 Waste Stream Gas Scrubber	47
3.7.1 Waste Stream Gas Scrubber Design	48
3.8 Saponification Reactor	54
3.8.1 Reaction Overview	54
3.8.2 Cobalt Saponification Reactor Design	55
3.9 Rotary Vacuum Drum Filter	55
3.9.1 Rotary Vacuum Drum Filter Design	56
3.10 Rotary Drum Dryer	59
3.10.1 Rotary Drum Dryer Design	60
3.11 Ancillary Equipment	62
3.11.1 Mass Transport Design	62
3.11.1.1 Pump Design	65
3.11.1.2 Blower Design	65
3.11.1.3 Bucket Elevator Design	66
3.11.1.4 Conveyor Belt Design	66
3.11.1.5 Transport Power Requirements	66
3.11.2 Heat Exchanger Design	69
3.11.3 Storage Equipment	70
3.11.4 Air Heaters	72
Section 4: Final Design	73
4.1 Leaching Block	73
4.1.1 Final Design Description	76
4.1.2 Material Balances	78
4.2 Impurity Removal Block	80
4.2.1 Final Design Description	82
4.2.2 Material Balances	84
4.3 Manganese Extraction Block	87
4.3.1 Final Design Description	91
4.3.2 Material Balances	94
4.4 Cobalt Extraction Block	99
4.4.1 Final Design Description	102
4.4.2 Material Balances	105

4.5 Nickel Extraction Block	112
4.5.1 Final Design Description	114
4.5.2 Material Balances	116
4.6 Lithium Extraction Block	118
Section 5: Economics	119
5.1 Capital Costs	119
5.1.1 Leaching Block	121
5.1.2 Impurity Removal Block	122
5.1.3 Manganese Extraction Block	123
5.1.4 Cobalt Extraction Block	124
5.1.5 Nickel Extraction Block	125
5.1.6 General Costs	126
5.1.7 Fixed Capital Investment and Lang Factor	127
5.1.8 Working Capital	128
5.2 Operating Cash Flow	129
5.2.1 Raw Materials	129
5.2.2 Utility Costs	130
5.2.3 Waste Disposal	131
5.2.4 Labor and Maintenance	132
5.3 Process Viability	133
Section 6: Environmental, Social, and Safety Considerations	135
6.1 Environmental Considerations	135
6.2 Societal Considerations	137
6.3 Safety Considerations	137
6.3.1 Piranha Solution	138
6.3.2 Hydrofluoric acid	139
6.3.3 Organic Solvents	140
6.3.4 Kerosene	142
6.3.5 Airborne Powders	143
6.3.6 Contaminated Water	144
6.3.7 Natural Gas	145
Section 7: Conclusions and Recommendations	148
7.1 Conclusions	148
7.2 Future Work Recommendations	149
Acknowledgments	152
References	153
Appendix A: Design and Operating Calculations	157
Leaching Reactor Just Suspension Speed Calculation	157

Leaching Reactor Impeller Power Calculations	157
RDC Column Power Calculation	157
Rotary Vacuum Drum Filter Calculation	158
Rotary Drum Dryer Area Calculation	158
Heat Exchanger Cooling Water Mass Flow Rate Calculation	159
Heat Exchanger Area Requirement Calculation	159
Hot Air Furnace Heater Natural Gas Requirement Calculation	160
Cooling Jacket Area Sufficiency Validation Calculation	161
Waste Stream Gas Scrubber Column Height Calculation	162
Pump Energy Requirements - P-101	164
Capital Cost Estimation - PLEACH-101	165
Appendix B: Full Stream Tables	166
Leaching Block	166
Impurity Removal Block	170
Manganese Extraction Block	174
Cobalt Extraction Block	184
Nickel Extraction Block	191

Executive Summary

The electrification of processes is becoming a growing trend when developing technology. This demand has brought about the development of lithium-ion batteries (LIBs) for many different devices including cell phones, computers, and other small electronic devices. However, the most notable use of LIBs is in the electric vehicle (EV), with thousands of lithium-ion cells in each car. LIB technology has brought about a revolution in moving away from fossil fuels in the transportation industry, but still lacks proper infrastructure. Currently, there is demand for a safe LIB waste disposal option, which gives rise to the opportunity to recycle valuable metals in the cathodes of LIBs. This project aims to develop an LIB recycling plant to extract manganese, cobalt, nickel, and lithium from spent LIBs.

The process of extracting metals from spent LIBs follows the common practice of hydrometallurgy. Mechanically and thermally treated black mass, which is composed of cathode and anode material (with the casing removed), enters the process and is leached using a solution of sulfuric acid and hydrogen peroxide, otherwise known as Piranha solution. Leached metals are then separated from the unleached metals and gas generated by the reaction. The aqueous metals then go through a series of extraction steps which separate out individual components in the following order: impurities (aluminum, iron, and copper), manganese, cobalt, nickel, and lithium. Each valuable metal is then precipitated as an insoluble hydroxide or carbonate to be sold. This report covers all of the design logistics of unit operations, simulations, economics, and safety analysis that comes with the process.

Final results were obtained through a mixture of ASPEN simulations and literature reviews. ASPEN was always considered the primary option and literature was only used when ASPEN lacked data. Overall, the process successfully converts 12,678 kg/hr of black mass into

3,943 kg/hr of MnCO_3 , 1,339 kg/hr of Co(OH)_2 , and 4,297 kg/hr of Ni(OH)_2 . This is accomplished through leaching, extracting, and precipitating each metal from black mass. Lithium recovery was unsuccessful due to the vast amount of sodium ions present compared to the lithium ions entering the lithium block. The 555 kg/hr of lithium ions, that could be extracted as a valuable product, was treated as hazardous waste. Unfortunately, the process is not economically viable, as the process loses 1.8 billion dollars per year. The main issue with the current design is the large amount of water in the aqueous streams which causes all unit operations to be at their maximum dimensions and run in parallel multiple times. Additionally, the process is not optimized and disposes of 1.6 billion dollars of waste per year. To make this process economically viable, leaching would need to be done at a high molar concentration of acid to limit the water as well as allow water to evaporate at points in the process when heat is generated through reactions.

Section 1: Introduction

The global demand for lithium ion batteries (LIBs) has been accelerating over the past several years as countries begin to use them as an effective means of storing renewable energy and powering electric vehicles (EVs). Critical to the performance and longevity of these batteries are key metals, particularly lithium, cobalt, nickel, and manganese. For example, cobalt, often used as part of the cathode material, enhances the stability, energy density, and overall lifespan of the battery.

Today, lithium and cobalt are among the most valuable materials used in LIBs, primarily due to their limited global supply and mining challenges. Over 70 percent of cobalt is currently extracted from the Democratic Republic of the Congo, while most lithium is sourced from brine deposits in Australia and Chile.¹ These methods of acquiring the materials are extremely harmful to local environments and are often extracted unethically or in volatile regions.

Additionally, the surge in LIB usage has led to an escalating accumulation of electronic waste (e-waste), such as batteries and circuit boards, which poses a serious environmental challenge. Currently, without effective recycling processes, vast quantities of LIBs end up in landfills, contributing to environmental hazards, mainly fires. This pressing issue is our primary motivation for designing a hydrometallurgical LIB recycling plant to extract and recycle lithium, cobalt, manganese, and nickel from black mass sourced from spent LIBs.² Our approach aims to recover these essential metals in the form of lithium carbonate, cobalt (II) hydroxide, alongside potentially valuable byproducts like manganese (II) carbonate and nickel (II) hydroxide. By reintegrating these recovered materials into EV manufacturing, consumer electronics, and energy storage solutions, we can significantly reduce resource strain and the environmental impact of LIBs.

The amount of end-of-life electric vehicle batteries in the US is expected to increase rapidly over the next couple of decades. To ensure that the US has the recycling capacity for LIBs batteries, various battery recycling plants have been opened across the country. As of September 2023, the US is capable of recycling over 100,000 tons of electric vehicle batteries. Many of these facilities are on the pilot scale, but upcoming facilities are expected to operate at the commercial scale where a single plant can process up to 100,000 tons of batteries in a year. The majority of facilities are concentrated where EV and LIB manufacturers are located. Virginia currently has about 85,000 EVs, with the majority being situated in Northern Virginia. The plant will be located in central Virginia to capitalize on the spent batteries from the DC, Maryland, Virginia Metropolitan Area (DMV) as well as importing batteries from nearby states.

Assuming that the average Tesla Model S battery weighs about 550 kg, that translates to 50,000 tons of EV batteries in current use. Assuming that at least a third of these batteries are recycled every year of operation, the plant should be designed to process about 15,000 tons of spent EV batteries a year. This number is expected to rapidly increase so the final processing expectation is 100,000 tons of black mass per year. Black mass is shredded cathode and anode material and is roughly 40-50 weight percent of a LIB. The remaining parts of the battery, plastics and electrolytes, are not recycled.

Section 2: Prior Works

Lithium-ion battery (LIB) recycling has undergone extensive research, leading to the development of various recovery methodologies including hydrometallurgical, pyrometallurgical, and direct recycling techniques. Among these, hydrometallurgical processing has emerged as a preferred approach due to its superior metal recovery efficiency and reduced environmental footprint compared to pyrometallurgical methods.³ This process leverages aqueous chemistry to selectively extract lithium and transition metals from spent cathodes, ensuring high-purity material recovery.⁴

Aspen Technology developed a simulation of hydrometallurgical recycling of LIBs titled “Li-ion Battery Recycling Process with TEA and LCA Analysis”. Prior research has demonstrated that process modeling enhances the predictive capabilities of metal recovery systems by integrating thermodynamic equilibria, reaction kinetics, and mass transfer phenomena.⁵ The Aspen Plus framework implemented in this work incorporates detailed electrolyte equilibrium chemistry, enabling accurate predictions of precipitate formation as a function of key operating parameters such as pH, temperature, and reagent concentration.

To ensure model accuracy, feed stream compositions were defined based on industrially relevant cathode and anode chemistries, particularly NMC-111 formulations. The model includes critical unit operations such as acid leaching, selective precipitation, and solvent extraction, all calibrated using experimentally validated thermodynamic data. Leaching reactions were simulated using yield-based reactor modules, with yields being determined by various literature papers; the leaching reactions were those of lithium and transition metal oxides in acidic media.⁶ Subsequent purification steps were optimized via parametric sensitivity analyses to maximize metal recovery efficiency while minimizing reagent consumption.

The section of the previous work that was most vital was the integration of laboratory-scale data with separation mechanisms within the Aspen Plus. By leveraging established thermodynamic models, phase equilibria predictions were refined to accurately simulate solid-liquid interactions, thereby allowing for the optimization of lithium and transition metal precipitation yields. Heat and mass balance calculations were validated against empirical data from laboratory-scale hydrometallurgical recycling trials, reinforcing the model's applicability to industrial-scale operations.⁷ Furthermore, an economic evaluation was incorporated, assessing the material cost implications and energy consumption profiles of the proposed process.

This work advances prior efforts in LIB recycling modeling by incorporating detailed mass transfer limitations and refining reaction pathways for enhanced predictive accuracy. The improvements in computational process simulation contribute to the ongoing development of scalable, economically viable, and environmentally sustainable recycling solutions for lithium-ion batteries.

Section 3: Discussion

3.0 Process Overview

The following work describes the process for recycling nickel-manganese-cobalt (NMC) lithium-ion batteries (LIBs). The final products, MnCO_3 , Co(OH)_2 , and Ni(OH)_2 are collected through a series of operations including solvent extraction, precipitation, and purification steps. Figure 3.0-1 details the overall block flow diagram this process entails. It is worth noting that Li_2CO_3 is a final product but was not isolated in this process.

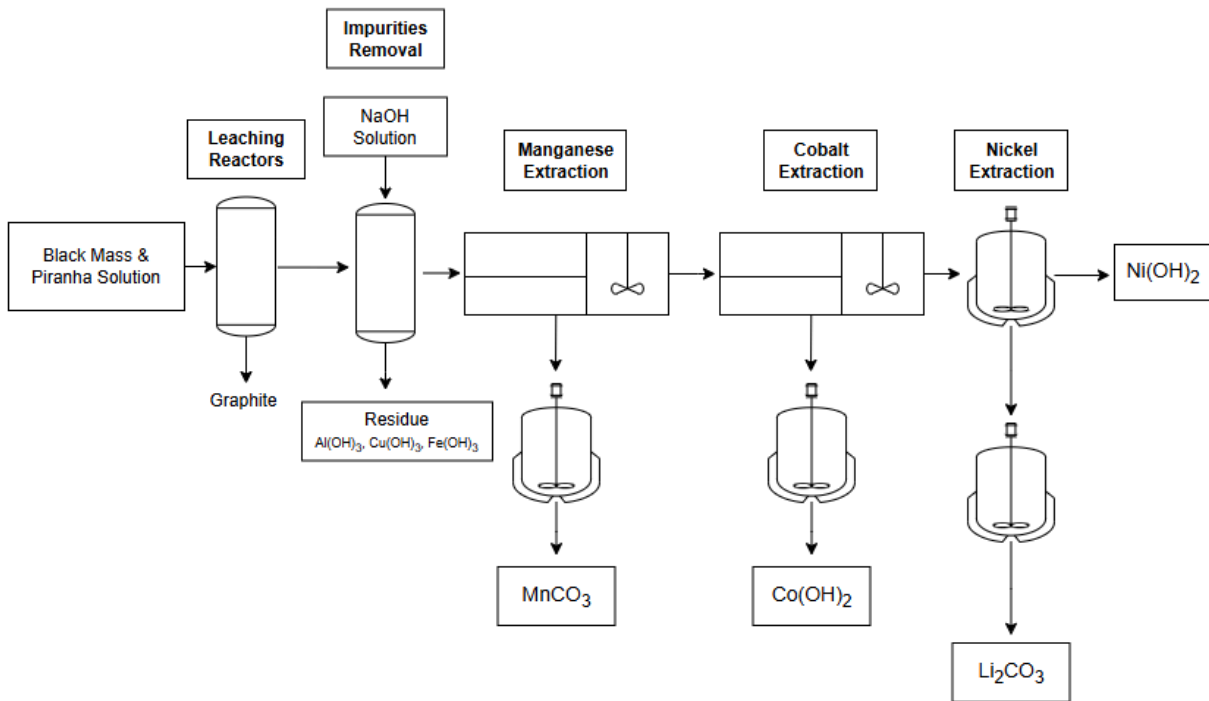


Figure 3.0-1 General process flow diagram

Black mass is introduced with Piranha solution in a batch reactor to dissolve the metals into an aqueous form. Table 3.0-1 details the component makeup of our black mass feed stream.

Table 3.0-1 Black Mass Composition by Component			
Component	Weight Percent	Component (cont'd)	Weight Percent
C	32.28	LiF(s)	1.53
Ni	20.9	Al	1.02
Mn ₃ O ₄	18.35	Fe	0.81
Co	13.1	CoLiO ₂	0.61
Li ₂ O	8.45	LiMn ₂ O ₄	0.61
Cu	1.73	LiNiO ₂	0.61

The aqueous metals stream is sent through several process blocks including impurity removal, manganese extraction, cobalt extraction, and nickel extraction. Each process block uses a combination of precipitation reactions, extraction columns, stripping columns, and scrubbing columns to extract and improve the purity of the final products. Precipitated final products are sent through both a washing step and a drying step, to remove water and other impurities. The order of the process blocks listed above is relevant, as the pH is raised in each process block to allow the next product to crash out. Greater detail on the design and operation conditions for each of these process blocks and their respective unit operations are provided in the sections to follow.

3.1 Leaching Reactor

The first step in the process is leaching the metals from their oxide or pure metal state in black mass to solution. Section 4.1 details the streams and compositions around the leaching reactor (PLEACH-101). The leaching solution is a mixture of sulfuric acid (H_2SO_4), water, and hydrogen peroxide (H_2O_2) (102-PIR). H_2SO_4 is the main component as most metals in black mass are only soluble in acidic solutions. Additionally, H_2SO_4 does not produce harmful byproducts. For example, leaching with hydrochloric acid (HCl) would produce chlorine gas (Cl_2) as a byproduct. H_2O_2 acts as an oxidizing agent that helps dissolve metals into solution. Additionally, it is used to reduce some transition metals present in black mass (for example Co^{3+} to Co^{2+}) to reach more favorably leachable valence states and to decrease the need for more concentrated acid solutions to obtain similar efficiencies.⁸

Due to the novelty of the process, experimental results from research papers were used to determine the leaching conditions. The key variables for leaching are pulp density (concentration of black mass in acid), reactor temperature, acid (H_2SO_4) concentration, oxidizing agent (H_2O_2) concentration, impeller speed, and the residence time required for the resulting yield. The conditions for all literature reviewed are displayed in Table 3.1-1 below. The reported yield is the conversion of the desired metals (Li, Ni, Mn, and Co) into solution (103-EFF). This leaching reactor was used directly from the ASPEN file mentioned above in Section 2: Prior Works, and adjusted for the inlet feeds, based on experimental data, to complete the material and energy balances.

Table 3.1-1 Literature Review of Optimized Leaching Reactor Conditions							
Pulp Density (g/mL)	Reactor Temperature	H ₂ SO ₄ Conc.	H ₂ O ₂ (vol %)	Impeller Speed	Time (min)	Yield (%)	Reference number
1:20	50°C	2M	3	300 RPM	60	100	⁸
1:10	70°C	2M	4	250 RPM	120	99	⁹
1:25	40°C	1M	1	400 RPM	60	99.7	¹⁰
1:1.25	70°C	4M	4.5	300 RPM	70	100	¹¹

The choice for operating conditions was done on a conservative approach due to the likelihood of unideal conditions including uncalculated impurities like the presence of plastics, incorrect scale-up assumptions, and incorrect research data. The chosen operating conditions for the leaching reactor (bolded in Table 3.1-1) were a 1:25 ratio of kg of black mass to liter of Piranha solution, reactor temperature of 70°C, 2M H₂SO₄ concentration, 4 vol % of 50 wt% H₂O₂, and 120 minute residence time resulting in 100% conversion of all metals into solution.

Table 3.1-2 Leaching Reactor Tag Legend	
Tag Number	Brief Description
PLEACH-101	Black Mass Leaching Reactor

3.1.1 Reactions Overview

The reactions that occur in the leaching process are listed along with their heat of reaction in Table 3.1.1-1 below. All reactions are highly exothermic so each reactor was equipped with a cooling jacket to maintain a constant temperature of 70°C. All components in the black mass feed enter as solids and react with H₂SO₄ and H₂O₂ to become aqueous. Additionally, water and oxygen are generated as a byproduct. It is important to note that the reaction of LiF creates HF as a byproduct which is highly toxic and must be targeted as an environmental, health, and safety hazard.

Table 3.1.1-1 Chemical Reactions and Heat in the Leaching Process ¹²	
Reaction Stoichiometry	Heat
$2\text{LiCoO}_2 (\text{s}) + 3\text{H}_2\text{SO}_4 + 3\text{H}_2\text{O}_2 \rightarrow 2\text{CoSO}_4 (\text{aq}) + \text{Li}_2\text{SO}_4 (\text{aq}) + 2\text{O}_2 + 6\text{H}_2\text{O}$	-10,873 J/g LiCoO ₂
$2\text{LiNiO}_2 (\text{s}) + 3\text{H}_2\text{SO}_4 + 3\text{H}_2\text{O}_2 \rightarrow 2\text{NiSO}_4 (\text{aq}) + \text{Li}_2\text{SO}_4 (\text{aq}) + 2\text{O}_2 + 6\text{H}_2\text{O}$	-11,405 J/g LiNiO ₂
$2\text{LiMn}_2\text{O}_4 (\text{s}) + 5\text{H}_2\text{SO}_4 + 3\text{H}_2\text{O}_2 \rightarrow 4\text{MnSO}_4 (\text{aq}) + \text{Li}_2\text{SO}_4 (\text{aq}) + 3\text{O}_2 + 8\text{H}_2\text{O}$	-9,849 J/g LiMn ₂ O ₄
$\text{Mn}_3\text{O}_4 (\text{s}) + 3\text{H}_2\text{SO}_4 + \text{H}_2\text{O}_2 \rightarrow 3\text{MnSO}_4 (\text{aq}) + \text{O}_2 + 4\text{H}_2\text{O}$	-2,408 J/g Mn ₃ O ₄
$\text{Co} (\text{s}) + \text{H}_2\text{O}_2 + \text{H}_2\text{SO}_4 \rightarrow \text{CoSO}_4 (\text{aq}) + \text{H}_2\text{O}$	-9,431 J/g Co
$\text{Ni} (\text{s}) + \text{H}_2\text{O}_2 + \text{H}_2\text{SO}_4 \rightarrow \text{NiSO}_4 (\text{aq}) + \text{H}_2\text{O}$	-9,280 J/g Ni
$\text{Li}_2\text{O} (\text{s}) + \text{H}_2\text{SO}_4 \rightarrow \text{Li}_2\text{SO}_4 (\text{aq}) + \text{H}_2\text{O}$	-12,250 J/g Li ₂ O
$\text{LiF} (\text{s}) + \text{H}_2\text{SO}_4 \rightarrow \text{Li}_2\text{SO}_4 (\text{aq}) + 2\text{HF}$	-5,145 J/g LiF
$2\text{Fe} (\text{s}) + 3\text{H}_2\text{SO}_4 + 3\text{H}_2\text{O}_2 \rightarrow \text{Fe}_2(\text{SO}_4)_3 (\text{aq}) + 6\text{H}_2\text{O}$	-14,429 J/g Fe
$2\text{Al} (\text{s}) + 3\text{H}_2\text{SO}_4 + 3\text{H}_2\text{O}_2 \rightarrow \text{Al}_2(\text{SO}_4)_3 (\text{aq}) + 6\text{H}_2\text{O}$	-47,738 J/g Al
$\text{Cu} (\text{s}) + \text{H}_2\text{SO}_4 + \text{H}_2\text{O}_2 \rightarrow \text{CuSO}_4 (\text{aq}) + 2\text{H}_2\text{O}$	-6,930 J/g Cu

3.1.2 Standard Reactor Design

The leaching reactors were designed to react 12,684 kg/hr of black mass pseudo-continuously by running 12 batch reactors in parallel. To support the inlet feed of black mass, 36 reactors are required. The volume of each reactor is 35.3 m³ at a height of 5 meters and diameter of 3 meters (Figure 3.1.2-1). A 1-meter-diameter pitched-blade turbine with 4 blades rotating at 60 RPM is used to suspend the solids and ensure turbulent mixing. Additionally, each reactor is fitted with 4 baffles, all 0.3 meters in width and extending to the height of the tank. All reactors in the process fill to roughly 80-85 percent of the total volume to prevent overflow. Finally, to prevent a build up of pressure from the oxygen and HF being generated in the reaction, each reactor is equipped with a vent stream on top to allow gas to exit the reactor independent of the batch schedule (104-VAP).

The highly corrosive and exothermic nature of the leaching reaction requires a material of construction that is capable of resisting corrosion, compatible with the reactants, and can withstand high temperatures. Therefore, the reactors are constructed from Titanium Grade 7 Alloy. Titanium alloy is very expensive compared to other materials, such as stainless steel; but, the increased corrosion resistance will decrease lifetime maintenance costs. It should be noted that these reactors are referenced throughout the report as they are used for other unit operations. The material of construction does change based on the corrosivity of the materials within.

The leaching reactor was modeled in Aspen using an RSTOIC block that set the conversion based on yield values found in research papers, which were 100%. Additionally, the reactor was held at a constant temperature of 70°C and a constant pressure of 1 atm.

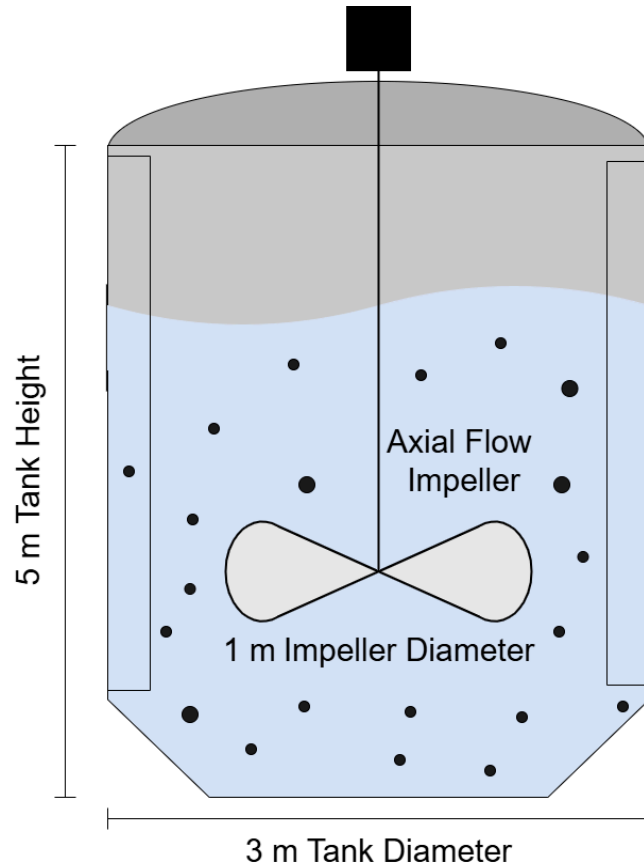


Figure 3.1.2-1 Diagram of Standard Reactor Design

3.1.2.1 Impeller Choice and Design

The purpose of the impeller in the standard reactor is to promote solid suspension and turbulent mixing. As such, an axial flow impeller, specifically a 4-blade pitched-blade turbine, was chosen. The impeller diameter is $\frac{1}{3}$ the diameter of the tank at 1 meter. The Zwietering correlation for just suspension was used to determine the minimum impeller speed to achieve solid suspension.

$$N_{js} = Sv^{0.1} \left[\frac{g(\rho_s - \rho_l)}{\rho_l} \right]^{0.45} X^{0.13} d_p^{0.2} D^{-0.85}$$

Equation 3.1.2.1-1 Zwietering Correlation for Just Suspension Speed

N_{js} , impeller speed	rps
S , zwietering constant	
ν , kinematic viscosity	m^2/s
g , gravitational constant	m/s^2
ρ_l , liquid density	kg/m^3
ρ_s , solid density	kg/m^3
X , solid mass fraction * 100	%
d_p , median particle diameter	m
D , impeller diameter	m

Here, S is a dimensionless constant that is dependent on tank geometry.

$$S = 10.42 \left(\frac{C}{T} \right)^{0.455} \left(\frac{H}{T} \right)^{-0.107}$$

Equation 3.1.2.1-2 Zwietering Constant of Pitched Blade Turbine

C , impeller clearance	m
T , tank diameter	m
H , tank height	m

Typical ratios of impeller clearance to tank diameter vary from 0.33 to 0.5, therefore a clearance of 1 m is used for calculation of S . Although solid density and particle diameter vary between reactors, other parameters, such as kinematic viscosity, are approximated to be similar due to dilute conditions and low amounts of solid loading. The required speeds for standard reactors vary between 35 and 45 RPM.

Table 3.1.2.1-1 Impeller Speed Design Specifications			
Reactor	Just Suspension Speed (RPM)	Re (*10 ⁵)	Designed Speed (RPM)
Leaching	36.3	6.1	60
PRCP- 201 (Impurity Removal)	42.7	7.1	60
PRCP- 301 (Manganese)	44.5	7.4	60
PRCP - 401 (Cobalt)	34.2	5.7	60
PRCP - 501 (Nickel (Ni(OH) ₂))	39.5	6.6	60

For consistency, each impeller is operated at 60 RPM to ensure complete suspension of solid particles. This impeller speed is also sufficient for turbulent mixing ($Re \gg 10^3$).

3.1.2.2 Standard Reactor Power Requirements

Because all standard reactors are operated in turbulent regimes, power consumption is independent of viscosity.

$$P = N_p \rho n^3 D^5$$

Equation 3.1.2.2-1 Power Consumption of Turbulent Mixing

P ,	power consumption	W
N_p ,	power number	dimensionless
ρ ,	fluid density	kg/m ³
n ,	impeller speed	rps
D ,	impeller diameter	m

For a pitched blade turbine, power number is constant when $Re > 10^3$ ($N_p \sim 1.3$). Due to identical impeller geometry and speed for all standard reactors ($n = 1$ rps, $D = 1$ m), differences in power consumption are only dependent on the density of the fluid in the reactor.

Table 3.1.2.2-1 Power Consumption of Standard Reactors		
Reactor	Fluid Density (kg/m ³)	Power Consumption (kW)
PLEACH - 101 (Leaching)	1107	1.44
PRCP - 201 (Impurity Removal)	1249	1.62
PRCP - 301 (Manganese)	1118	1.45
PRCP - 401 (Cobalt)	1212	1.58
PRCP - 501 (Nickel)	1231	1.60

Although the power requirements are estimated to be between 1 and 2 kW, each impeller is designed with a power capacity of 10 kW. This is done for two reasons: contingencies and cost estimation. Neglected parameters such as frictional losses are likely to increase power requirements, therefore it stands to reason to design impeller drivers more conservatively. Additionally, establishing driver power at a higher value places reactor impeller design within the bounds of purchased equipment cost estimation obtained from Towler and Sinnott, allowing for a more reliable capital cost estimation.

3.1.2.3 Cooling Jacket Design

The leaching reactors operate at a temperature of 70°C. However, the exothermic nature of the reactions means that heat must be removed via cooling jackets. The cooling jacket design goals are the determination of the mass flow rate of cooling water needed to maintain constant reactor temperature, as well as an assessment of the viability of a cooling jacket in providing

adequate cooling. To elaborate on the viability metric, this is a determination of the overall heat transfer coefficient of the system, followed by a determination of the heat transfer area required for the system; if this area is less than the actual jacketed surface area of the vessel, then a cooling jacket is sufficient.

Each leaching reactor is fitted with a cooling jacket, in which cooling water (CW) flows in at 30°C and exits at 45°C. Each individual leaching reactor, during operation, has a heat removal requirement of 385 kW. Determination of the mass flow rate of CW can be done via Equation 3.1.2.3-1 below.

$$m = \frac{Q}{C_p * \Delta T}$$

Equation 3.1.2.3-1 Cooling Water Mass Flow Rate Requirement

m,	cooling water flow rate	kg/s
Q,	heat removal requirement	W
C _p ,	cooling water specific heat capacity	J/kg*K
ΔT,	cooling water temperature change	°C

The required mass flow of CW for the leaching reactor cooling jacket is 6.14 kg/s. Next, the overall heat transfer coefficient of the system was determined via Equation 3.1.2.3-2 below.

$$U = \left[\frac{1}{h_o} + \frac{r_o \ln(r_o/r_i)}{k_{pipe}} + \frac{r_o}{h_i r_i} \right]^{-1}$$

Equation 3.1.2.3-2 Overall Heat Transfer Coefficient

U,	overall heat transfer coefficient	W/m ² K
h _o ,	convective heat transfer of CW	W/m ² K
h _i ,	convective heat transfer coefficient of reactor fluid	W/m ² K

k_{pipe} ,	conductive heat transfer coefficient of vessel wall	W/mK
r_o ,	outer vessel radius	m
r_i ,	inner vessel radius	m

The convective heat transfer coefficients h_o and h_i were calculated using Equations 3.1.2.3-3 and 3.1.2.3-4 below.

$$h_o = \left(\frac{k_{\text{fluid}}}{2r_o} \right) \left(\frac{(f/2)(Re-1000)Pr}{1.0+12.7\sqrt{f/2}(Pr^{2/3}-1)} \right)$$

Where $(f/2) = 0.125[0.79\ln(Re) - 1.64]^{-2}$

Equation 3.1.2.3-3 Gnielinski Correlation for Turbulent Flow in a Circular Pipe¹³

$$h_i = \left(\frac{k_{\text{fluid}}}{2r_i} \right) a Re^b Pr^{1/3}$$

Equation 3.1.2.3-4 Correlation for Convective Heat Transfer Coefficient in Agitated Vessel¹⁴

Re,	Reynold's Number	
Pr,	Prandtl Number	
k_{fluid} ,	thermal conductivity of reactor fluid	W/mk
a,	coefficient based on turbine geometry	(=0.53)
b,	coefficient based on turbine geometry	(=2/3)

Following a determination of U, an assessment of the available heat transfer area was performed. The cooling jacket is considered sufficient for the removal of the required heat if the inequality in Equation 3.1.2.3-5 below is satisfied.

$$A_{available} > A_{required} = \frac{Q}{U * LMTD}$$

Equation 3.1.2.3-5 Determination of Viability of Cooling Jacket

$A_{available}$,	available jacketed surface area	m^2
$A_{required}$,	minimum area to remove heat U	m^2
LMTD,	logarithmic mean temperature difference	$^{\circ}C$

The LMTD is the logarithmic mean temperature difference between the vessel and the cooling water calculated via Equation 3.1.2.3-6 below.

$$LMTD = \frac{(T_{vessel} - T_{CW, cold}) - (T_{vessel} - T_{CW, hot})}{\ln\left(\frac{T_{vessel} - T_{CW, cold}}{T_{vessel} - T_{CW, hot}}\right)}$$

Equation 3.1.2.3-6 LMTD Calculation

T_{vessel} ,	temperature of the vessel	$^{\circ}C$
$T_{CW, cold}$,	temperature of CW entering	$^{\circ}C$
$T_{CW, hot}$,	temperature of CW leaving	$^{\circ}C$

For the leaching reactor, it was determined that a cooling jacket is indeed sufficient to maintain the reactor temperature at the desired $70^{\circ}C$. $T_{CW, cold}$ was assumed to be $30^{\circ}C$ and $T_{CW, hot}$ was assumed to be $45^{\circ}C$.

3.2 Precipitator

After the leaching step, several precipitation reactions are performed to remove target metal ions from the solution by converting them into solid forms, which are later separated during the solid washing step. These reactions are pH-controlled by adding NaOH and various salts to selectively raise the solution’s pH, causing the desired metal ions to precipitate as insoluble salts in each unit operation. All heat duties and solubility modeling were calculated

using the ELECNRTL method in ASPEN, either by directly utilizing or modifying the ASPEN file referenced earlier in Section 2: Prior Works. The required inlet NaOH flow rates were determined based on the target pH for each reaction.

The inlet to the Impurity Reactor Precipitator is the aqueous, metal-rich outlet stream from the leaching reactor. For the Manganese Carbonate and Cobalt Hydroxide Precipitators, the inlets are the aqueous phases from their respective stripping columns. Similarly, the Nickel Hydroxide Precipitator receives its aqueous feed from the Cobalt Liquid-Liquid Extraction Column. These inlet streams are further discussed in the Discussion section. The following sections provide detailed descriptions of the specific precipitation reactions and the design of the associated unit operations.

Table 3.2-1 Precipitator Tag Legend	
Tag Number	Brief Description
PRCP-201	Impurity Removal Precipitator
PRCP-301	Manganese Carbonate Precipitator
PRCP-401	Cobalt Hydroxide Precipitator
PRCP-501	Nickel Hydroxide Precipitator

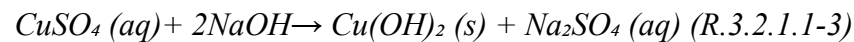
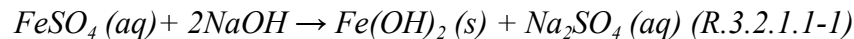
3.2.1 Impurity Removal Precipitator

The following section details the design process around the Impurity Removal Precipitator. This includes necessary reaction data and operating conditions. This precipitator was adapted from the ASPEN file mentioned above in Section 2: Prior Works, with inlet feeds scaled up to meet our process requirements.

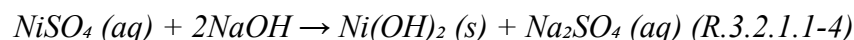
3.2.1.1 Reactions Overview

Within our leachate stream (106-LCH/201-LCH), multiple low-value metal ions—specifically Iron (III) (Fe^{3+}), Aluminium (III) (Al^{3+}), and Copper (II) (Cu^{2+})—are present and will precipitate as metal hydroxides alongside our high-value metal products (MnCO_3 , $\text{Co}(\text{OH})_2$, $\text{Ni}(\text{OH})_2$, Li_2CO_3) if not removed. Since the majority of our desired products will be fine, white powders, these target components would be visually indistinguishable from the lower-value impurities, making physical separation difficult.

To achieve the high product purity required for battery-grade material, this unit operation is designed to selectively precipitate these impurities as solid metal hydroxides using the double displacement reactions outlined in Reactions 3.2.1.1-1 through 3.2.1.1-3.¹⁵ These precipitated impurities can then be separated from the aqueous solution and removed as waste, minimizing contamination of the target metals in downstream processing.

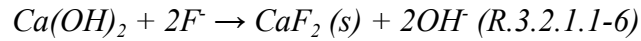
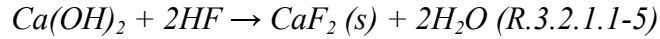


To accomplish this, the pH of the solution will be raised by adding in a solid stream of 90 wt% NaOH and 10 wt% $\text{Ca}(\text{OH})_2$. Fe^{3+} and Al^{3+} are completely precipitated at pH 4.5. Cu^{2+} , on the other hand, completely precipitates at pH 7. Raising the pH above 6 begins to precipitate Ni^{2+} in the form of solid $\text{Ni}(\text{OH})_2$, as seen in Reaction 3.2.1.1-4.¹⁵ To maximize the removal of Cu and minimize the amount of Ni product becoming waste, the reactor will operate at a pH of 5.9.



The basic feed stream contains 10 wt% $\text{Ca}(\text{OH})_2$ as a means of precipitating the majority of fluoride ions that are present after the leaching step. As seen in Reactions 3.2.1.1-5 and

3.2.1.1-6, Ca(OH)_2 reacts with hydrofluoric acid (HF) and fluoride ions within the solution to form calcium fluoride (CaF_2), which precipitates as a solid, from pH 6-8.¹⁶



This unit operation precipitates 100 mol% of the Fe^{3+} and Al^{3+} , 98 mol% of the Cu^{2+} , and 80 mol% of the F^- as solid residue. Additionally, the AspenPlus model calculated these exothermic reactions to generate 385 kW of heat duty, therefore, a cooling jacket will be used to maintain temperature at 70 C. Also, a solubility analysis was modeled on AspenPlus, finding that the solubility of the solids weren't significantly affected by the changes in temperature that warranted the solution to be cooled below 70 C.

3.2.1.2 Impurity Removal Precipitator Design

This precipitation step uses our standard reactor design detailed in Section 3.1.2. The material of construction, reactor size, impeller size, and impeller speed will all remain the same. To accommodate for the high inlet flow rate of leachate solution, this unit operates with 12 parallel processing streams. This determination was made using the Aspen-generated density, from which the total number of required parallel streams was calculated.

The longest precipitation reaction takes 6 hours to complete.¹⁵ To maintain a pseudo-continuous flow, 84 reactors are needed. More information on this is detailed in Section 4.2. Figure 3.2.1.2-1 below details the material balance of a single processing stream, while highlighting the key components and products, which includes the reactor, filter, and drying unit operations.

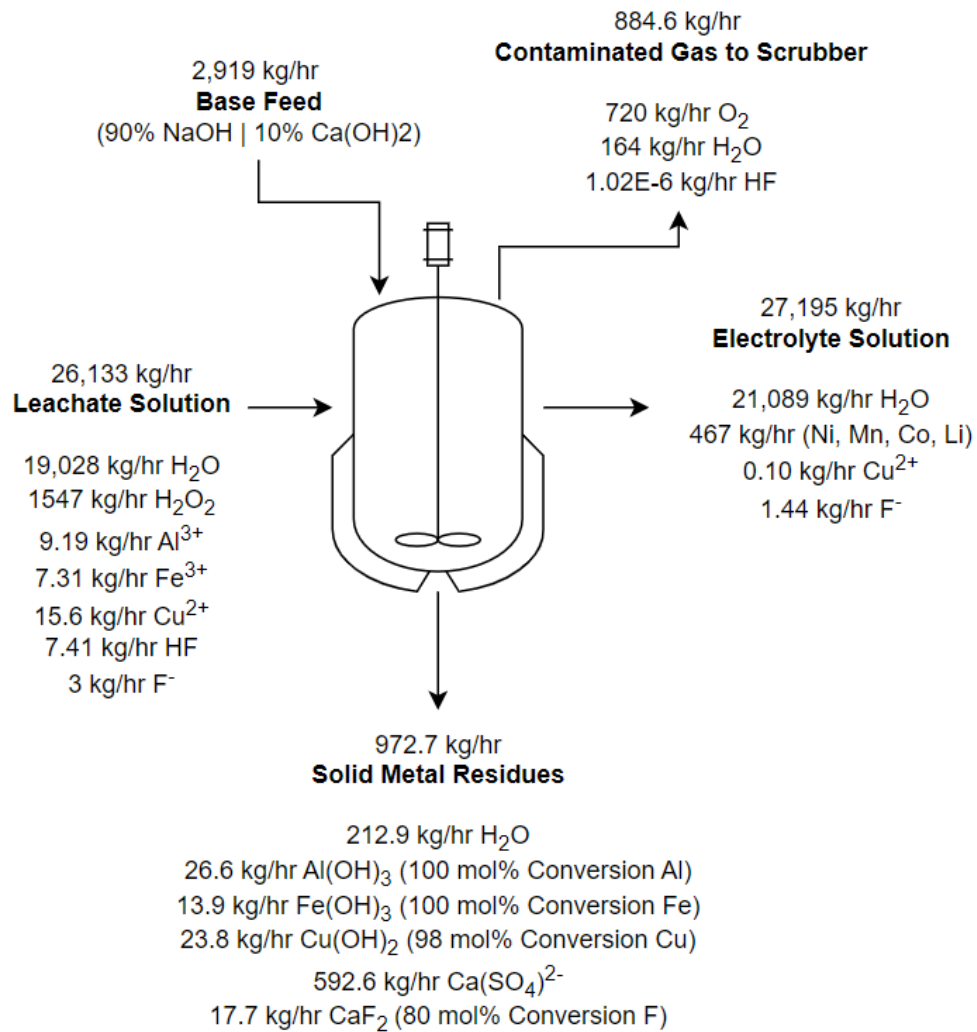


Figure 3.2.1.2-1 Impurity removal material balance for a single processing stream

3.2.1.3 Cooling Jacket Design

Similar to the leaching reactors, the impurity removal precipitation reactors are maintained at 70°C via a cooling jacket. Each individual impurity removal reactor generates 350 kW of heat which must be removed. Using the same process as the one described in Section 3.1.2.3, the required mass flow of CW was determined to be 5.56 kg/s. Additionally, by the same

process, the cooling jacket was determined to indeed provide sufficient cooling to maintain the reactors at 70°C given the available jacketed area.

3.2.2 Manganese Carbonate Precipitator

The following section details the design process around the manganese (II) carbonate (MnCO₃) precipitator. This includes the necessary reaction data and operation conditions. This precipitator was adapted from the ASPEN file mentioned above in Section 2: Prior Works, with inlet feeds scaled up to meet our process requirements.

3.2.2.1 Reactions Overview

The purpose of this precipitation step is to convert the manganese ions (Mn²⁺) from the Mn-rich, aqueous stream from the Manganese Stripping Column (312-AQTE) into manganese (II) carbonate (MnCO₃) by using the following double displacement reactions, Reactions 3.2.2.1-1 and 3.2.2.1-2, to return a product purity of 88 wt%.



These reactions precipitate the most manganese at pH 9.6.¹⁷ Therefore, an inlet stream of solid sodium hydroxide (NaOH) is used to make the solution basic, followed by solid sodium carbonate (Na₂CO₃). These conditions were chosen based on experimental data from Sayilgan et al., where 99.9% of the Mn²⁺ ions precipitated as MnCO₃ after a 3 hour residence time.¹⁶ Additionally, this reaction generates negligible amounts of heat and the solubility of the components are not temperature dependent.

3.2.2.2 Manganese Carbonate Precipitator Design

This precipitation step uses our standard reactor design detailed in Section 3.1.2. The material reactor size, impeller size, and impeller speed will all remain the same, but the material of construction will change to 316 stainless since the H_2O_2 has been removed. To accommodate for the high inlet flowrate of electrolyte solution, this unit operates 4 parallel processing streams. This determination was made using the Aspen-generated density, from which the total number of required parallel streams was calculated. To maintain a pseudo-continuous flow, a total of 20 reactors are required. More information on this is detailed in Section 4.3. Figure 3.2.2.2-1. below details the material balance of a single processing stream, while highlighting the key components and products, which includes the reactor, filter, and drying unit operations.

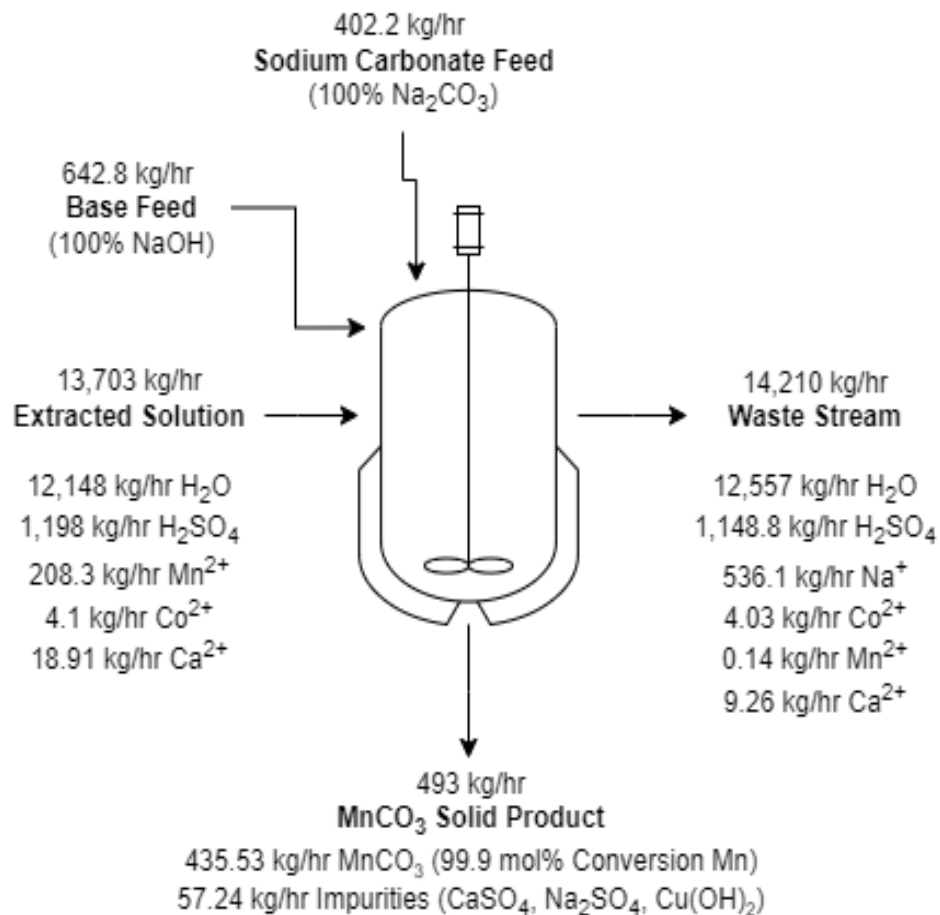


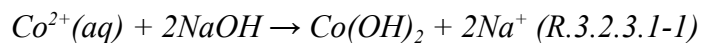
Figure 3.2.2.2-1 $MnCO_3$ material balance for a single processing stream

3.2.3 Cobalt Hydroxide Precipitator

The following section details the design process around the cobalt (II) hydroxide ($\text{Co}(\text{OH})_2$) precipitator. This includes the necessary reaction data and operating conditions. This precipitator was adapted from the ASPEN file mentioned above in Section 2: Prior Works, with inlet feeds scaled up to meet our process requirements.

3.2.3.1 Reactions Overview

The purpose of this precipitation step is to convert the cobalt ions (Co^{2+}) in the Co-rich, aqueous stream from the Cobalt Stripping Column (415-AQTE) into cobalt (II) hydroxide ($\text{Co}(\text{OH})_2$) by utilizing the following double displacement reaction, Reaction 3.2.3.1-1, to return a product purity of 91 wt% $\text{Co}(\text{OH})_2$.



These reactions precipitate the most cobalt at pH 11.¹⁸ Therefore, an inlet stream of solid sodium hydroxide (NaOH) is used to increase the solution pH to 11. These conditions were chosen based on experimental data from Yuzer et al., where 100% of the Co^{2+} ions precipitated as $\text{Co}(\text{OH})_2$ after a 1 hour residence time.¹⁹ Additionally, this reaction generates negligible amounts of heat and the solubility of the components are not temperature dependent.

3.2.3.2 Cobalt Hydroxide Precipitator Design

This precipitation step uses our standard reactor design detailed in Section 3.1.2. The reactor size, impeller size, and impeller speed will all remain the same but the material of construction, which is 316 stainless steel. To accommodate for the high inlet flow rate of aqueous solution, this unit operates 8 parallel processing streams. This determination was made using the Aspen-generated density, from which the total number of required parallel streams was calculated.

The precipitation reaction takes 1 hour to complete.¹⁹ To maintain a pseudo-continuous flow, a total of 16 reactors are needed. More information on this is detailed in Section 4.4. Figure 3.2.3.2-1 below details the material balance of a single processing stream, while highlighting the key components and products, which includes the reactor, filter, and drying unit operations.

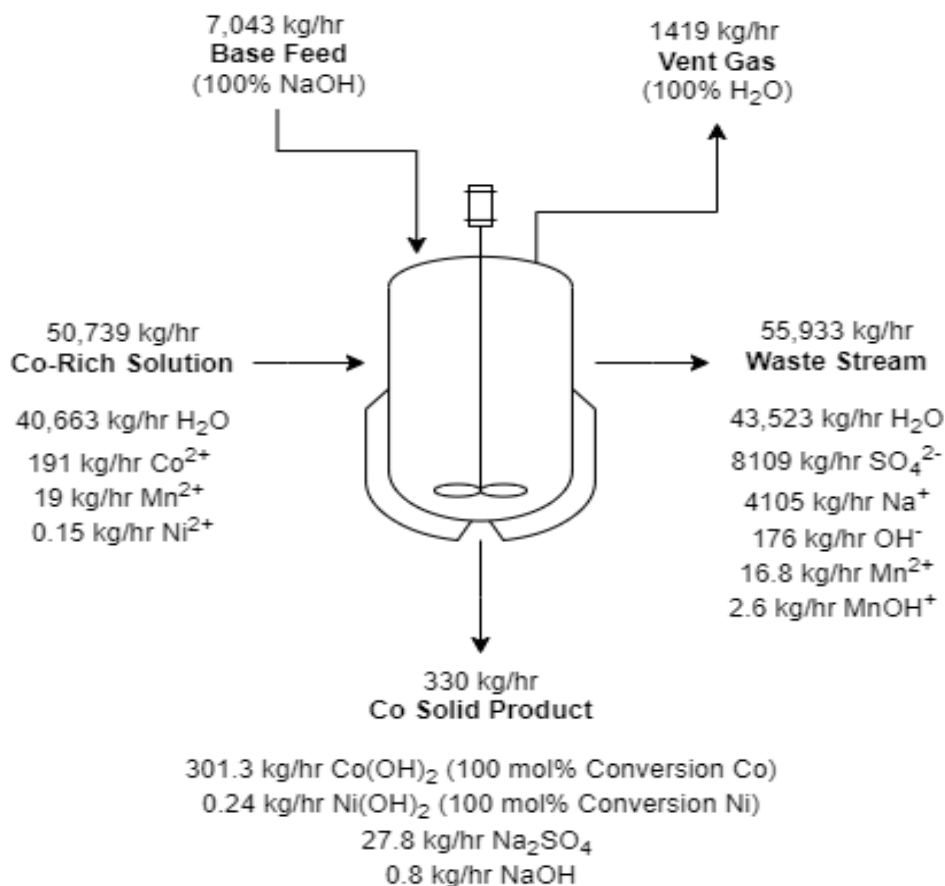


Figure 3.2.3.2-1 Co(OH)₂ material balance for a single processing stream

3.2.4 Nickel Hydroxide Precipitator

The following section details the design process around the nickel (II) hydroxide (Ni(OH)₂) precipitator. This includes the necessary reaction data and operating conditions. This precipitator was adapted from the ASPEN file mentioned above in Section 2: Prior Works, with inlet feeds scaled up to meet our process requirements.

3.2.4.1 Reactions Overview

The purpose of this precipitation step is to react the Ni²⁺ ions in the Ni-rich, aqueous phase from the Cobalt Liquid-Liquid Extraction Columns (407-AQEE/501-EFF) into Ni(OH)₂. This is done by using NaOH in a double displacement reaction to create Ni(OH)₂. NaOH is added in to raise the pH of the solution to 10. This comes out to 100% conversion of Ni²⁺ into Ni(OH)₂. The overall reaction is displayed in Reaction 3.2.4.1-1.



pH 10 and a lower temperature facilitated better Ni²⁺ conversion from the liquid phase to the solid phase.¹⁹ This stream goes in at 35 °C. The research paper tested 30 °C as their lowest temperature and reported near 100% conversion.²⁰ Using the ELECNRTL property method, the Aspen file calculated nearly 100% of the Ni²⁺ ions, which matches the research paper. A 4 hour residence time was also extracted from research data.¹⁸ Additionally, this reaction generates negligible amounts of heat which results in a change of roughly 2 °C.²⁰

3.2.4.2 Nickel Hydroxide Precipitator Design

This precipitation step uses the standard reactor design detailed in Section 3.1.2. The reactor size, impeller size, and impeller speed will all remain the same but the material of construction will be stainless steel. The number of necessary reactors was calculated by using the mass of our incoming stream, the Aspen-generated density, and the 4 hour residence time mentioned above. To maintain a pseudo-continuous flow rate, 60 reactors are needed. More information on batch scheduling is detailed in Section 4.5. Figure 3.2.4.2-1 below details the flows in and out of one single reactor, filter, and dryer unit operations, while highlighting the key ions and products.

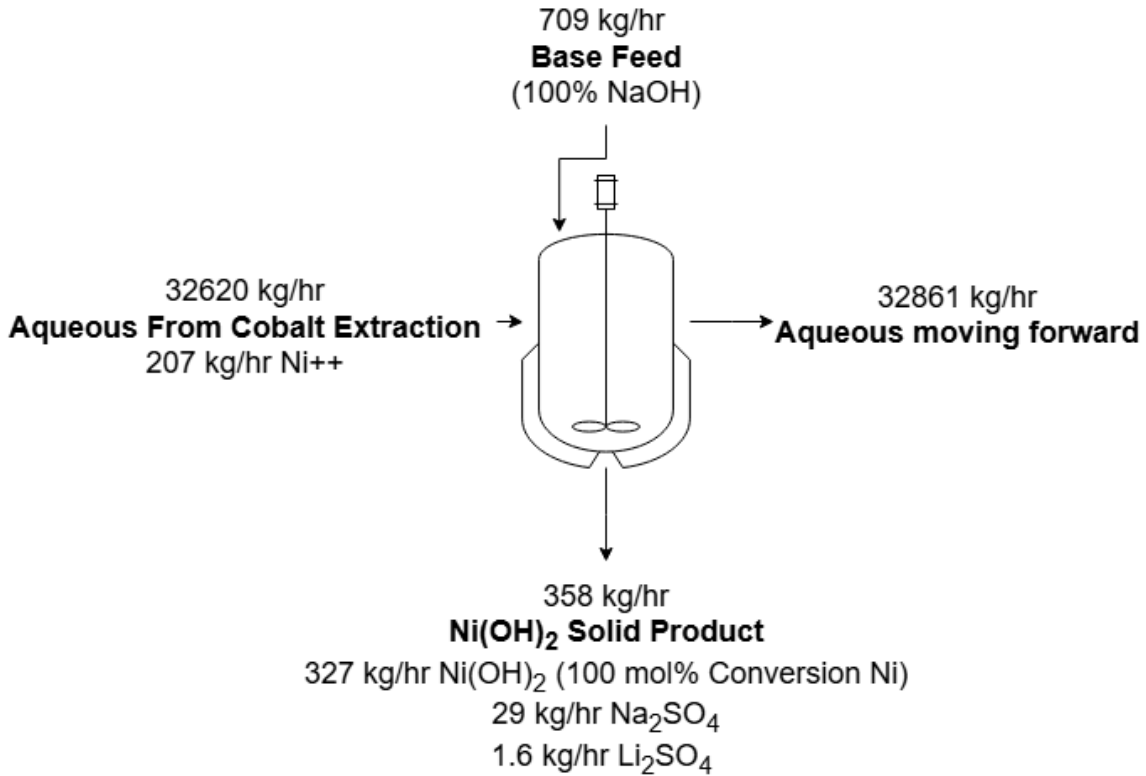


Figure 3.2.4.2-1 Ni(OH)₂ material balance for a single processing stream

3.2.5 Lithium Carbonate Precipitator

Due to excess amounts of sodium ions in stream 504-AQ, selective precipitation of Li₂CO₃ is not currently feasible. The current approach attempts to operate at higher temperatures to decrease Li₂CO₃ solubility and increase Na₂SO₄ solubility. By adding water until nearly all Na₂SO₄ is dissolved, some amount of Li₂CO₃ should remain with the desired purity. However, when examining the material balance in 504-AQ in addition with the sodium carbonate needed to precipitate residual lime and nickel, the water needed to achieve desired purity results in negligible yield of lithium carbonate. Consequently, the design of equipment surrounding lithium extraction is excluded from final design and instead proposed as an avenue for future work in Section 7.2.6.

3.3 Packed Bed Reactor

The leaching process requires that H_2O_2 be used to reduce the metal-ions in black mass to make them more soluble in H_2SO_4 . This, like all solvents, is fed in excess to ensure a fast time for total leaching. Although H_2O_2 is not an immediate concern in the aqueous environment, it becomes a safety hazard when it enters the first liquid-liquid extraction column and is contacted with the organic phase (kerosene). As such, a packed bed reactor was implemented to catalytically decompose H_2O_2 into H_2O and O_2 (PBR-201). Section 4.2 details the streams and compositions around the hydrogen peroxide decomposition packed bed reactor.

Table 3.3-1 Packed Bed Reactor Tag Legend	
Tag Number	Brief Description
PBR-201	H_2O_2 Decomposition Packed Bed Reactor

3.3.1 H_2O_2 Decomposition Packed Bed Reactor

The design of the packed bed reactor for H_2O_2 decomposition was only proposed in theory and has no true mechanical design. One catalyst that decomposes H_2O_2 is Fe^{3+} which is a component that is leached out of black mass. Fe^{3+} operates as a homogeneous catalyst which will decompose H_2O_2 gradually throughout the leaching block and impurity removal block. Equation 3.3.1-1 shows the rate equation for the decomposition of H_2O_2 with Fe(III) where k_d is the second-order rate constant and was found to be equal to $0.47 M^{-1} s^{-1}$ at pH 3.0.²¹ Since Fe^{3+} is in low concentration relative to H_2O_2 , it is assumed that it will not decompose entirely without another catalyst.

$$\frac{-d[H_2O_2]}{dt} = k_d[H_2O_2][Fe(III)]$$

Equation 3.3.1-1 Rate of catalytic decomposition of H₂O₂ using a Fe³⁺ catalyst

A packed bed reactor was implemented after the impurity removal solid washer and immediately before any contact with the organic streams in liquid-liquid extraction to remove the remaining H₂O₂. The packed bed reactor uses MnO₂ as the heterogeneous catalyst and is assumed to decompose the remaining H₂O₂. Equation 3.3.1-2 shows the pseudo first-order equation for the decomposition with a MnO₂ catalyst. Figure 3.3.1-1 shows the values of k_{obs} based on the ratio of the concentration of H₂O₂ to MnO₂. Additionally, the process is tolerant of Mn leaching into solution as the next unit operation removes the manganese. The reaction is highly exothermic so the reactor requires a cooling jacket, as getting to temperatures above 80°C will start to precipitate out CaSO₄.

$$\frac{-d[H_2O_2]}{dt} = k_{obs}[H_2O_2][MnO_2]$$

Equation 3.3.1-2 Rate of catalytic decomposition of H₂O₂ using a MnO₂ catalyst

Experiments	[H ₂ O ₂] (mM)	[≡MnO ₂] (mM)	Ratio of [H ₂ O ₂]/ [≡MnO ₂]	k _{obs} (±r.a.e.) ^a (min ⁻¹)	k _{MnO₂} ^b (mM ⁻¹ min ⁻¹)
1	29.4	7.5	3.92	0.461 (±0.11)	0.061
2	58.8		7.48	0.275 (±0.11)	0.037
3	147		19.6	0.212 (±0.03)	0.028
4	294		39.2	0.162 (±0.08)	0.022
5	441		58.8	0.132 (±0.08)	0.018
6	294	5	58.8	0.072 (±0.05)	0.014
7		7.5	39.2	0.166 (±0.06)	0.022
8		10	29.4	0.232 (±0.07)	0.023
9		15	19.6	0.352 (±0.05)	0.023
10		25	11.8	0.741 (±0.05)	0.030

^a Relative average error (average absolute error/average measured value).

^b Pseudo first-order rate constants ($k_{\text{MnO}_2} = \frac{k_{\text{obs}}}{[\text{≡MnO}_2]}$).

Figure 3.3.1-1 Observed and pseudo first-order rate constants of hydrogen peroxide decomposition on manganese oxide²²

H₂O₂ decomposition was modeled in Aspen using an RSTOIC block. It is predicted that the presence of Fe³⁺ ions in solution would act as a homogeneous catalyst, decomposing some of the H₂O₂ throughout the leaching and impurity removal block. However, this behavior was not predicted by Aspen Plus, so the H₂O₂ decomposition reactor was designed to decompose all of the remaining H₂O₂ after the leaching step. This also results in the most heat being generated, so the cooling jacket was designed with the worst-case scenario in mind.

3.3.1.1 Cooling Jacket Design

The packed bed reactor for hydrogen peroxide decomposition is to be maintained at 70°C. The proposed method for temperature control is via a cooling jacket around the reactor, although this method was not confirmed to provide adequate heat transfer. Theoretically, using equation 3.1.2.3-1, the mass flow rate of water to remove the 1290 kW of heat generated in the

decomposition can be determined as 20.5 kg/s of CW. To determine the viability of a cooling jacket in providing adequate heat transfer, the geometry of the packed bed reactor must be known. The geometry is currently unknown and was determined to be outside the scope of this project

3.4 Liquid-Liquid Extraction Columns

The main method for separating the valuable metals from the mixed brine solution is through the process of liquid-liquid extraction (LLE). The technique takes advantage of certain compounds being more soluble in one solvent than another, in this case an organic phase and an aqueous phase. Both solvents are well-mixed with one another to ensure adequate transport of the metal ions. Additionally, one solvent needs to be aqueous and the other be organic so that they can phase separate. In industry, the process takes advantage of differences in density between the heavier aqueous phase and lighter organic phase to flow countercurrent to one another.

In both the manganese extraction block and the cobalt extraction block, the extraction columns are the first operation processing the aqueous inlet stream to the block. The extraction columns remove the majority of the block's respective target metal into the organic phase, which is then processed in the scrubbing and stripping columns. The outlet aqueous phase from manganese extraction goes to the cobalt extraction block, and the aqueous outlet from the cobalt extraction goes to the nickel extraction block.

Table 3.4-1 Liquid-Liquid Extraction Column Tag Legend	
Tag Number	Brief Description
EXT-301	Manganese Extraction Column
EXT-302	Manganese Extraction Column
EXT-401	Cobalt Extraction Column

3.4.1 Manganese Liquid-Liquid Extraction Columns

Manganese is the first metal ion to be targeted for removal in LLE. Section 4.3 details the streams and compositions around LLE. To remove Mn from the aqueous metals, the stream (303-AQEF) is contacted with bis(2-ethylhexyl) phosphoric acid (D2EHPA), shown in Figure 3.4.1-1, in kerosene.

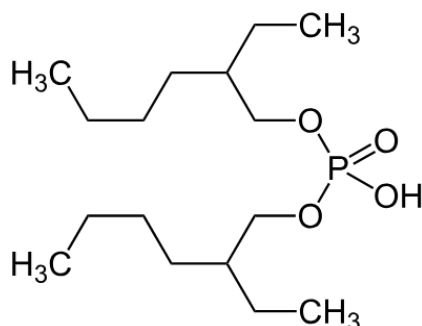


Figure 3.4.1-1 Molecular Structure of D2EHPA

This creates two distinct phases: a kerosene-rich organic phase that is selective to manganese and a water-rich aqueous phase containing the other dissolved metals. The reaction is done at ambient temperature and pressure as both variables have little to no effect (Figure 3.4.1-2). The main variables in this process are D2EHPA concentration in the organic phase, organic to aqueous volume ratio (O:A), and contact time. An optimization study done by Nathália Vieceli modeled the effect of process variables on the extraction of manganese and cobalt from a dissolved metals solution. Under optimized conditions (O:A of 1.25:1, pH 3.25,

and 0.5 M D2EHPA), extractions of 70% Mn were reached with a coextraction of 5% Co after 10 minutes of contact time.²³ Additionally, these results can be achieved after two theoretical contact stages. It is important to note that higher O:A ratios, lower pH, and higher concentrations of D2EHPA increases the yield of Mn to 99% but also increases the yield of Co to 35% which is far too much Co to lose.

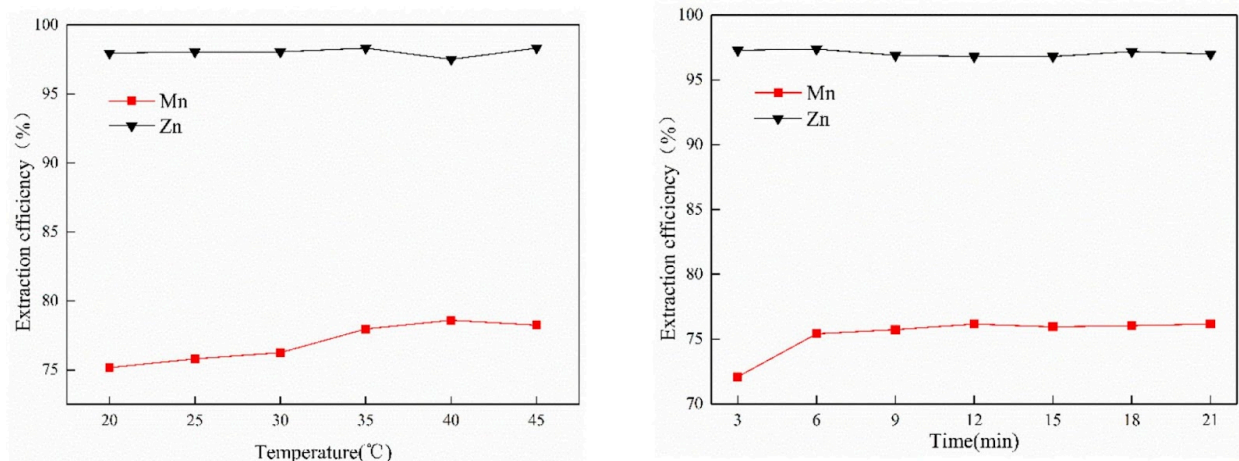


Figure 3.4.1-2 Factors affecting Mn Extraction

3.4.1.1 Reactions Overview

Bis(2-ethylhexyl) phosphoric acid (D2EHPA) is the most widely used extractant to recover Mn from LIBs. The metal ion replaces the acidic proton and forms a complex with the conjugate base. Unfortunately, the extraction of metals in D2EHPA follows the order of $Fe^{3+} > Ca^{2+} > Fe^{2+} > Cu^{2+} \approx Mn^{2+} > Co^{2+} \approx Ni^{2+} > Li^+$.²⁴ Therefore, it is appropriate to assume any remaining Al, Ca, and Fe are removed in the process and Cu is assumed to be extracted at a 91% yield mirroring Mn. The reactions have negligible heats of reaction so no heating or cooling is required.

Table 3.4.1.1-1	Manganese LLE Chemical Reactions ²⁵
	$2D2EHPA + Mn^{2+} + 2H_2O \rightarrow Mn-D2EHPA + 2H_3O^+$
	$2D2EHPA + Co^{2+} + 2H_2O \rightarrow Co-D2EHPA + 2H_3O^+$
	$2D2EHPA + Cu^{2+} + 2H_2O \rightarrow Cu-D2EHPA + 2H_3O^+$
	$2D2EHPA + Ca^{2+} + 2H_2O \rightarrow Ca-D2EHPA + 2H_3O^+$
	$3D2EHPA + Fe^{3+} + 3H_2O \rightarrow Fe-D2EHPA + 3H_3O^+$
	$3D2EHPA + Al^{3+} + 3H_2O \rightarrow Al-D2EHPA + 3H_3O^+$

Manganese extraction was modeled in ASPEN with two blocks, an RSTOIC block that performs the reaction and a SEP block that separates the organic and aqueous phases. This decision was based on the ASPEN Technology modeling of solvent extraction for Mn (Section 2). The phase separation is assumed to be perfect. Both blocks run adiabatically at a constant pressure of 1 atm.

3.4.1.2 Manganese Liquid-Liquid Extraction Column Design

The extractor for LLE is a rotating disc contactor (RDC) column (EXT-301, EXT-302) (Figure 3.4.1.2-2). The reactor takes advantage of counter-current flow where the heavy aqueous phase is fed at the top and the light organic phase is fed at the bottom. The total volume of the column is 9.42 m³. This was determined by the 10-minute contact (or residence) time and a 1.57 m³ section at the top and bottom of the column to allow for phase separation. The column, in total, is 12 meters in height and 1 meter in diameter. The column is designed to operate at 1/24 the capacity of the total flowrate requiring 24 LLE systems operating in parallel. The two liquids then go through a series of stages where mixing is promoted by a rotating disc. The process requires 2 theoretical stages for adequate mixing (Figure 3.4.1.2-1) and the RDC column was

assumed to have a 25% stage efficiency, which requires 8 stages. Each stage has circular stator rings 0.2 meters in width to separate the stages and contain a 0.6 diameter rotor disc. The column shaft, and subsequently the rotor disc, rotates at 200 RPM to ensure adequate mixing and phase separation.²⁶⁻²⁸ The power to operate the shaft is 43.3 kW which is calculated in Appendix A using the power required to spin a 0.2 meter diameter cylinder in turbulent flow.²⁹ The material for the columns is stainless steel as the pH ranges between 1-6 with no Cl⁻ and relatively low temperatures.

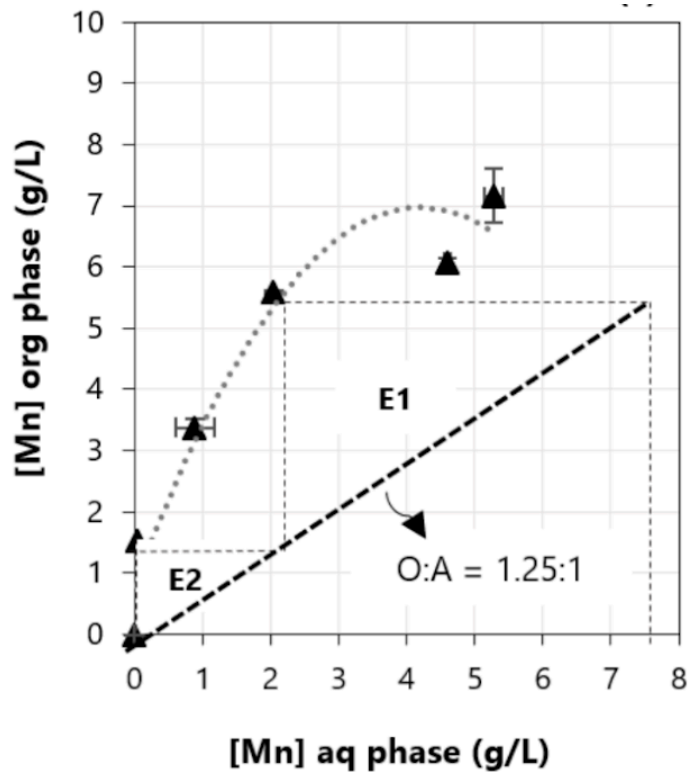


Figure 3.4.1.2-1 McCabe–Thiele diagram of the Mn extraction³⁰

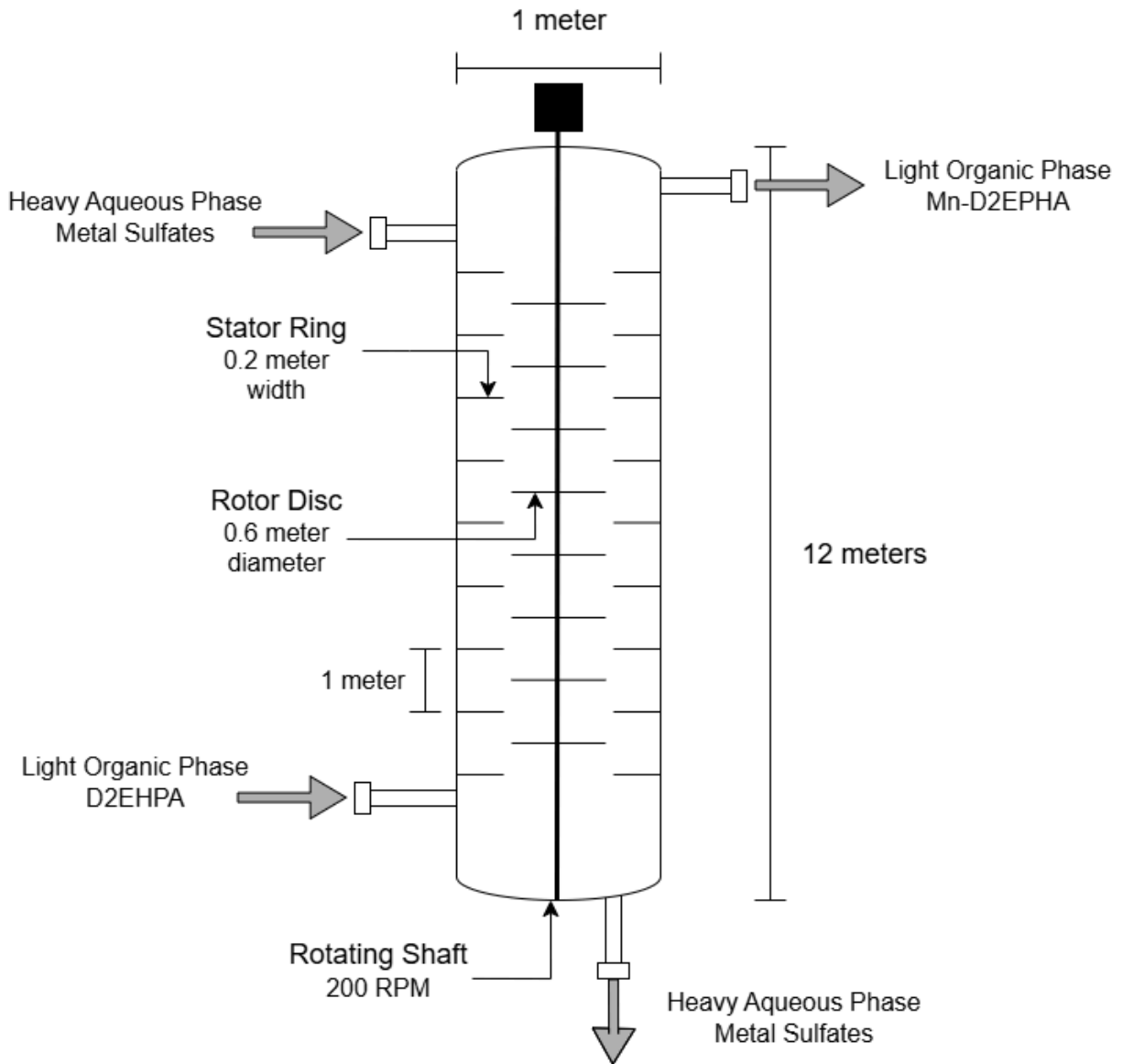


Figure 3.4.1.2-2 RDC Column Diagram

3.4.2 Cobalt Liquid-Liquid Extraction Column

The Cobalt Extraction block follows the Manganese Extraction block, taking the aqueous metal-rich effluent from the second set of manganese extraction columns as feed. Cobalt extraction occurs via a similar liquid-liquid process as manganese extraction, but with a different

extractant: Bis(2,4,4-trimethylpentyl)phosphinic acid, also called Cyanex-272. The structure of Cyanex-272 is depicted in Figure 3.5.2-1 below. Cyanex-272 is a Co-selective extractant.

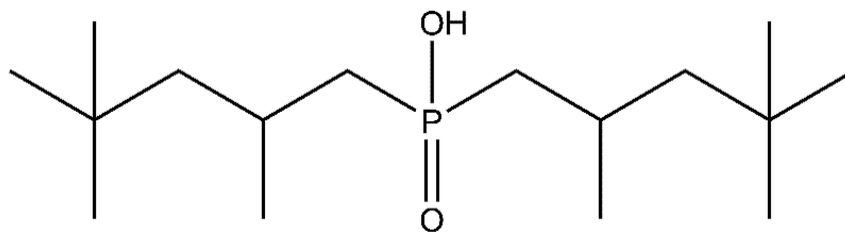


Figure 3.4.2-1 Bis(2,4,4-trimethylpentyl)phosphinic acid, Cyanex-272.

The organic inlet stream to the extraction columns (containing the fresh extractant) is 406-OREF. The aqueous feed is the aqueous output of the manganese block mixed with NaOH pellets, 403-AQEF. The metal-loaded organic effluent is stream 408-OREE. The aqueous effluent is sent forward to the nickel extraction block via 407-AQEE.

The important variables to be considered in the Cobalt extraction column design are residence time, organic:aqueous volume phase ratio (O:A), concentration of Cyanex-272 in kerosene, and equilibrium pH. Several literature sources were considered in the design. These sources are all based on experiments conducted at lab scale, so there are accuracy concerns when predicting scale-up; thus, conditions chosen using the most conservative variable from various papers.

Most literature sources agreed on a volume phase ratio, O:A, of 1 to be effective for extraction of Co^{2+} with saponified Cyanex in an organic diluent.^{31,32} Contact times varied from 5 minutes^{29,32} to 30 minutes³³ in the literature, so a 30 minute residence time is used for the design in our process. The concentration of Cyanex in kerosene was conservatively taken as 20 vol%, though some papers reported successful recovery of cobalt with concentrations as low as 0.2 M (6 vol%).^{23,30}

Equilibrium pH of the extraction column is important to maximize the extraction of cobalt ions into the organic phase. The optimal equilibrium pH was found to be 5.^{29,32,34} To accomplish this, the aqueous feed to the block (which is initially acidic) must be neutralized with NaOH pellets before feeding to the extraction columns.

The columns used in the cobalt extraction process are identical in design to the columns described in Section 3.4.1.2. The cobalt extraction process requires 40 parallel columns to be used to accommodate the increased residence time over manganese extraction.

To summarize, the process uses the following conditions in the extraction columns: O:A of 1, residence time of 30 minutes, 20 vol% Cyanex-272 in kerosene, equilibrium pH of 5, Co²⁺ extraction percentage of 93%, Mn²⁺ extraction percentage of 99%, Ni²⁺ extraction percentage of 4.5%, and ambient temperature and pressure. The determination of these conditions is explored in section 3.4.2.1.

3.4.2.1 Reactions Overview

Saponified Cyanex-272, diluted in kerosene, is used to selectively extract Co²⁺ ions from the aqueous feed. Saponified Cyanex-272 refers to a Cyanex-272 molecule where the acidic hydrogen has been replaced by a sodium ion, this will also be referred to as Cyanex-Na. On contact with the aqueous phase in the extraction columns, two saponified Cyanex-272 complexes shed their sodium ions and instead complex on either side of a single cobalt ion (Cyanex-Co).

The molar percentage of Co²⁺ removed from the aqueous phase into the organic phase (extraction percentage) was conservatively set at 93% for the process, though some papers found the percentage to be even higher, with one achieving up to 99% extraction.^{29,32} However, Cyanex also extracts Mn²⁺ ions, at around 99%, so this was modeled in the process as well.³¹ It also

extracts Ni²⁺, at an extraction percentage around 4.5%, which was also modeled in the process.²⁹ Modeling was done using yield-based reactor modules in Aspen Plus.

Some papers constructed McCabe-Thiele diagrams from their experimental data, finding that 2 theoretical stages is sufficient to extract Co²⁺ completely.³³ To remain conservative in our extraction percentages, the one-stage recovery was assumed to be the percent extraction over the entire column.

The reactions in the extraction column (see Table 3.4.2.1-1) have negligible heats of reaction, so no temperature control of the column is required.

Table 3.4.2.1-1	Cobalt LLE Chemical Reactions
	$2\text{Cyanex-Na} + \text{Co}^{2+} \rightarrow 2\text{Na}^+ + \text{Cyanex-Co}$
	$2\text{Cyanex-Na} + \text{Mn}^{2+} \rightarrow 2\text{Na}^+ + \text{Cyanex-Mn}$
	$2\text{Cyanex-Na} + \text{Ni}^{2+} \rightarrow 2\text{Na}^+ + \text{Cyanex-Ni}$

Cobalt extraction was modeled in ASPEN with two blocks, an RSTOIC block that performs the reaction and a SEP block that separates the organic and aqueous phases. This decision was based on the ASPEN Technology modeling of solvent extraction for Co (Section 2). The phase separation is assumed to be perfect. Both blocks run adiabatically at a constant pressure of 1 atm.

3.4.2.2 Cobalt Liquid-Liquid Extraction Column Design

The cobalt extraction occurs in columns identical to the extraction column design as described in Section 3.4.1. However, the contact time is larger in cobalt extraction, thus it requires 40 parallel extraction columns.

3.5 Stripping Column

For the products to be isolated and precipitated, the metal ions need to be removed from the organic phase and redissolved in the aqueous phase. This is done through stripping which redissolves the metal-ions in the aqueous phase by contacting the organic with an acid stream with no metal-ions. Additionally, the remaining organic is protonated by the aqueous acid, regenerating the organic to be reused. This allows the entire process of extraction, scrubbing, and stripping to be entirely circular for the organic phase. The metal-ions are redissolved in the aqueous phase so they can be precipitated into products that can be sold.

Stripping operations are the last of the three liquid-liquid operations in the manganese and cobalt blocks, taking place after extraction and after scrubbing.

Table 3.5-1 Stripping Column Tag Legend	
Tag Number	Brief Description
STRP-301	Manganese-Loaded Organic Stripping Column
STRP-401	Cobalt-Loaded Organic Stripping Column

3.5.1 Manganese Stripping Column

After scrubbing, the remaining organic solution is sent to a stripping column which removes the metals from the organic and dissolves them in H₂SO₄ (STRP-301). Section 4.3

details the streams and compositions around the stripping column. The variables for the stripping column are also contact time, acid concentration, and O:A. The optimized parameters are an O:A of 8:1, 1M H₂SO₄ and 10 min of contact time. This results in 100% of all metals stripped from the organic phase and dissolved in the aqueous phase (309-AQTE).²³ This reaction has no heat of reaction so it requires no heating or cooling. Because the conditions are similar to that of extraction, the process has the same mechanical design and uses the same column as extraction.

Table 3.5.1-1 Manganese Stripping Column Reaction Equations
$Mn-D2EHPA + 2H_2SO_4 \rightarrow 2D2EHPA + Mn^{2+} + SO_4^{2-}$
$Co-D2EHPA + 2H_2SO_4 \rightarrow 2D2EHPA + Co^{2+} + SO_4^{2-}$
$Cu-D2EHPA + 2H_2SO_4 \rightarrow 2D2EHPA + Cu^{2+} + SO_4^{2-}$
$Ca-D2EHPA + 2H_2SO_4 \rightarrow 2D2EHPA + Ca^{2+} + SO_4^{2-}$
$2Fe-D2EHPA + 3H_2SO_4 \rightarrow 6D2EHPA + 2Fe^{3+} + 3SO_4^{2-}$
$2Al-D2EHPA + 3H_2SO_4 \rightarrow 6D2EHPA + 2Al^{3+} + 3SO_4^{2-}$

Manganese stripping was modeled in ASPEN with two blocks, an RSTOIC block that performs the reaction and a SEP block that separates the organic and aqueous phases. This decision was based on the ASPEN Technology modeling of solvent extraction for Mn (Section 2). The phase separation is assumed to be perfect. Both blocks run adiabatically at a constant pressure of 1 atm.

3.5.2 Cobalt Stripping Column

Cobalt stripping occurs after the cobalt scrubbing step. After scrubbing, the remaining organic solution (the primary component of interest being Cyanex-Co) is sent (via stream 413-ORSE) to an array of parallel stripping columns (40 in total) which removes the metals from

the organic Cyanex-metal complexes and dissolves them in aqueous H₂SO₄ (via stream 414-AQTF). The outlet organic phase (stream 405-RECY) is recycled into the saponification reactor of the cobalt block and the outlet aqueous phase (415-AQTE) goes to cobalt precipitation.

The variables for the stripping column are also contact time, acid concentration, and O:A volume ratio. The optimized parameters for cobalt stripping are an O:A of 1:1,^{29,35} 2M H₂SO₄³³ and 30 min of contact time.³⁵ This results in 100% of all metals stripped from the organic phase and dissolved in the aqueous phase. Stripping percentages (mol % of metal ions stripped from organic phase) were high across sources, with some using low contact times and/or low acid concentrations and still achieving more than 91%⁶ stripping, one with 99%⁴, and one of 100%⁷. Since our process uses the most conservative conditions, a stripping percentage of 100% was assumed for Co²⁺, Ni²⁺, and Mn²⁺.

These reactions have no heat of reaction so the stripping column requires no heating or cooling. Because the conditions are similar to that of extraction, the process has the same mechanical design and uses the same column as extraction.

Table 3.5.2-1 Cobalt Stripping Column Reaction Equations
$H_2SO_4 + \text{Cyanex-Co} \rightarrow Co^{2+} + SO_4^{2-} + 2\text{Cyanex-272}$
$H_2SO_4 + \text{Cyanex-Mn} \rightarrow Co^{2+} + SO_4^{2-} + 2\text{Cyanex-272}$
$H_2SO_4 + \text{Cyanex-Ni} \rightarrow Co^{2+} + SO_4^{2-} + 2\text{Cyanex-272}$

Cobalt stripping was modeled in ASPEN with two blocks, an RSTOIC block that performs the reaction and a SEP block that separates the organic and aqueous phases. This decision was based on the ASPEN Technology modeling of solvent extraction for Co (Section

2). The phase separation is assumed to be perfect. Both blocks run adiabatically at a constant pressure of 1 atm.

3.6 Scrubbing Column

Scrubbing is the process of removing unwanted co-extracted species from the organic phase. The process is a form of LLE where a loaded organic phase is contacted with an aqueous phase rich in the metal ion looking to replace the unwanted co-extracted species. Scrubbing occurs in the manganese and cobalt extraction blocks in between the liquid-liquid extraction and stripping steps. In the manganese block, scrubbing is used to remove cobalt impurities in the organic phase. In the cobalt block, scrubbing removes the nickel impurities in the organic phase.

Table 3.6-1 Scrubbing Column Tag Legend	
Tag Number	Brief Description
SCRB-301	Manganese-Loaded Organic Scrubbing Column
SCRB-401	Cobalt-Loaded Scrubbing Column

3.6.1 Manganese Scrubbing Column

The idea of scrubbing the organic phase is to increase the purity of the main compound once the metal ions are stripped from the organic phase. Section 4.3 details the streams and compositions around the scrubbing column (SCRB-301). For manganese, the unwanted co-extracted species that can be scrubbed, due to D2EHPA's weak metal ion affinity towards it, is Co. For reference, 2,000 kg/hr of Co-D2EHPA enters the scrubbing columns with 19,600 kg/hr of Mn-D2EHPA. To scrub the organic phase of cobalt, the stream is contacted with an aqueous

phase of a 4 g/L Mn solution ($\text{MnSO}_4 \cdot \text{H}_2\text{O}$) for 10 mins at a 10:1 O:A (308-MNSF). This results in 80% of the Co in the organic phase being replaced with Mn (309-ORSE) (Reaction 3.6.1-1).⁸ Since all metals have a greater affinity than cobalt to be in the organic phase, none of the impurities (Al, Cu, Ca, and Fe) are scrubbed out. There is no noticeable heat of reaction so no heating or cooling required. Due to the similarities between this process and LLE, the mechanical design is the same and uses the same column design. It is important to note that the aqueous phase leaving the scrubbing column was considered waste that contains 131.2 kg/hr of Co and 189.9 kg/hr of Mn (310-AQSE).



Manganese scrubbing was modeled in ASPEN with two blocks, an RSTOIC block that performs the reaction and a SEP block that separates the organic and aqueous phases. The phase separation is assumed to be perfect. Both blocks run adiabatically at a constant pressure of 1 atm.

3.6.2 Cobalt Scrubbing Column

The cobalt block's scrubbing columns follow the extraction columns and precede the stripping columns. The inputs are the organic phase from extraction plus an aqueous scrubbing phase. The outputs are a Cyanex-Co-rich organic phase and a nickel sulfate aqueous waste phase.

For the cobalt block, the main impurity component that must be scrubbed out of the organic phase before stripping is nickel. The organic stream leaving the extraction column and going into the scrubbing column (stream 408-OREE) contains (in addition to the bulk kerosene and other trace metals) 15300 kg/hr Cyanex-Co and 1270 kg/hr Cyanex-Ni; if this organic phase were sent straight to stripping and precipitation, the nickel would be recovered with the cobalt and contaminate the precipitate. By scrubbing the organic phase with aqueous CoSO_4 (stream

411-AQSF), the effluent organic phase (stream 413-ORSE) contains 16500 kg/hr Cyanex-Co and just 12.7 kg/hr Cyanex-Ni.

To accomplish this, the organic phase is contacted with an aqueous phase of a 2 g/L Co^{2+} solution (CoSO_4 in H_2O) for 30 mins³⁶ at a 1:1 O:A.^{36,37} This results in 99%³⁷ of the Ni^{2+} in the organic phase being replaced with Co^{2+} (Reaction 3.6.2-2). These conditions are the average between two sources that performed cobalt scrubbing experiments, as one source found 100% of the nickel to be scrubbed out using only 1 g/L Co^{2+} solution,³⁶ while a second source found 99% extraction using a higher concentration of 8.7 g/L.³⁷ This presents an issue, because scrubbing with 8.7 g/L of cobalt (II) ion results in more cobalt going into the process for scrubbing than is produced for sale. However, the 8.7 g/L source had half as much contact time, so the 2 g/L of Co^{2+} solution was assumed to be sufficient to scrub 99% of nickel.

There is no noticeable heat of reaction so no heating or cooling required. Due to the similarities between this process and other LLE, the mechanical design is the same and uses the same column design.



Cobalt scrubbing was modeled in ASPEN with two blocks, an RSTOIC block that performs the reaction and a SEP block that separates the organic and aqueous phases. This decision was based on the ASPEN Technology modeling of solvent extraction for Co (Section 2) The phase separation is assumed to be perfect. Both blocks run adiabatically at a constant pressure of 1 atm.

3.7 Waste Stream Gas Scrubber

The following section details the design process around the packed bed gas scrubber (GS). This includes the design assumptions and associated equations.

Table 3.7-1 Waste Stream Gas Scrubber Tag Legend	
Tag Number	Brief Description
GS-101	Waste Stream Gas Scrubber

3.7.1 Waste Stream Gas Scrubber Design

During the leaching and impurity removal step, the exothermic reactions generate large amounts of vapor that need to be removed from the system. Within this vapor is a trace amount of hydrofluoric acid (HF), which is a hazardous material that can not be directly vented to the atmosphere in large quantities without further processing. Based on the Taconite Iron Processing Industry HF release standard, the maximum HF released is 0.147 mg HF per kg of product.³⁸ The current contaminated streams release about 49 mg HF per kg of product. To meet the standard, the HF within the gaseous stream will flow counter currently with a liquid caustic solution of 10% NaOH in a packed bed gas scrubber, as seen in Figure 3.7.1-1.

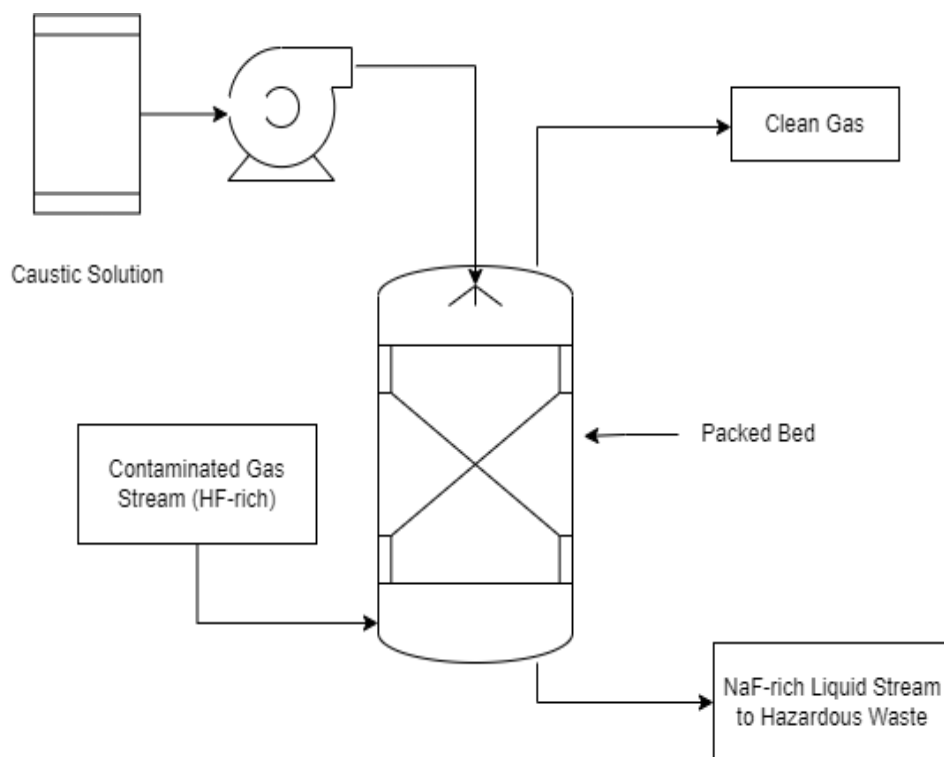


Figure 3.7.1-1 Caustic packed bed gas scrubber schematic

The phases will go through a packed bed made up of 50mm-diameter Carbon Raschig Rings, where the NaOH will react with the HF in a neutralization reaction to form NaF in the liquid phase, which will be collected and removed as hazardous waste (Reaction 3.7.1-1).³⁹



To determine the necessary diameter required for the gas scrubber, a material balance was completed using the RADFRAC block in Aspen. The RADFRAC block was run at 1 atm with the same inlet temperature of the gas streams from the leaching block and the gas stream from the impurity removal block (PRCP-201). Using the Onda correlation to calculate $H_{o,G}$ and $N_{o,G}$, along with the estimated diameter from Aspen and the industry HF release standard, the packing height can be determined. The calculation process will be shown next.⁴⁰

The first key value to calculate is the minimum liquid flow rate using the following equations (Equation 3.7.1-1 through Equation 3.7.1-3).

$$H = \frac{C}{K_{sp}}$$

Equation 3.7.1-1 Formula for Henry's Constant of HF in Caustic Solution⁴⁰

H, Henry's Constant
 C, Molar Density of H₂O mol/m³
 K_{sp}, Solubility Coefficient of HF mol HF/m³Pa

$$K = \frac{H}{P}$$

Equation 3.7.1-2 Formula for distribution coefficient⁴⁰

K, Distribution Coefficient
 H, Henry's Constant of HF
 P, Operating Pressure atm

$$\left(\frac{L}{G}\right)_{min} = \frac{y_{A,1} - y_{A,2}}{\frac{y_{A,1}}{K} - x_{A,2}}$$

Equation 3.7.1-3 Formula for minimum liquid flow rate⁴⁰

$\left(\frac{L}{G}\right)_{min}$, Minimum Liquid Flow Rate mol/hr
 y_{A,1}, Initial HF conc. mol%
 y_{A,2}, Target HF conc. mol%

After calculating the minimum liquid flow rate, to make sure the process reduces the amount of HF significantly below the standard to compensate for fluctuations in the process, the $\left(\frac{L}{G}\right)_{min}$ was increased by a factor of 1.3, becoming the actual liquid flow rate $\left(\frac{L}{G}\right)$.

The next key variable to calculate is N_{o,G} using the following equations (Equation 3.7.1-4 and 3.7.1-5).

$$\gamma = \frac{K}{L/G}$$

Equation 3.7.1-4 Formula for stripping factor⁴⁰

γ , Stripping Factor
 $(\frac{L}{G})$, Actual Liquid Flow Rate mol/hr

$$N_{o,G} = \frac{1}{1-\gamma} \ln \left[(1-\gamma) \frac{y_{A,1} - Kx_{A,2}}{y_{A,2} - Kx_{A,2}} + \gamma \right]$$

Equation 3.7.1-5 Formula for $N_{o,G}$ ⁴⁰

$x_{A,2}$, Conc. of HF in liquid outlet mol%

The final key variable required is $H_{o,G}$, which was estimated using the Onda Correlation as shown in Equation 3.7.1-6 through 3.7.1-10. The diffusivity of HF in caustic solution was estimated to be 6.71E-9 m²/s using ASPEN, from which the size of the gas scrubber was calculated.

$$a = a_p \left\{ 1 - \exp \left[- 1.45 \left(\frac{\sigma_c}{\sigma_L} \right)^{0.75} \left(\frac{L'}{a_p \mu_L} \right)^{0.1} \left(\frac{L'^2 a_p}{\rho_L g} \right)^{-0.05} \left(\frac{L'^2}{\rho_L \sigma_L a_p} \right)^{0.2} \right] \right\}$$

Equation 3.7.1-6 Formula for $N_{o,G}$ ⁴⁰

a , Interfacial Area m²/m³
 a_p , Area Density m²/m³
 L' , Liquid Mass Velocity kg/m²s
 σ_c , Surface Pressure of Packed Bed N/m
 σ_L , Surface Tension of Liquid Stream N/m
 μ_L , Viscosity of Liquid Stream Pa*s
 ρ_L , Mass Density of Liquid Stream kg/m³
 g , Gravitational constant m/s²

$$k_y = 5.23(a_p C_G D_G) \left(\frac{G'}{a_p \mu_G}\right)^{0.7} (Sc_G)^{1/3} (a_p d_p)^{-2}$$

Equation 3.7.1-7 Formula for k_y ⁴⁰

C_G ,	Molar Density of Gas	mol/m ³
D_G ,	Diffusivity of Gas Stream	m ² /s
G' ,	Gas Stream Mass Velocity	kg/m ² s
μ_G ,	Viscosity of Gas Stream	Pa*s
Sc_G	Schmidt Number for Gas Stream	
d_p	Estimated Diameter of Column	m

$$k_x = 0.0051 \left[\frac{\mu_L g(C_L)^3}{\rho_L} \right]^{1/3} \left(\frac{L'}{a \mu_L}\right)^{2/3} (Sc_L)^{-1/2} (a_p d_p)^{0.4}$$

Equation 3.7.1-8 Formula for k_x ⁴⁰

C_L ,	Molar Density of Liquid	mol/m ³
Sc_L ,	Schmidt Number for Liquid Stream	
d_p ,	Estimated Diameter of Column	m

$$H_G = \frac{G}{ak_y} \quad H_L = \frac{L}{ak_x}$$

Equation 3.7.1-9 Formulas for H_G and H_L ⁴⁰

G ,	Molar Velocity of Gas Stream	mol/m ² s
L ,	Molar Velocity of Liquid Stream	mol/m ² s

$$H_{o,G} = H_G + \gamma H_L$$

Equation 3.7.1-10 Formula for $H_{o,G}$ ⁴⁰

From there the packing height (Z) can be calculated by using the following formula, Equation 3.7.1-11. To determine the height equivalent of the theoretical plate (HETP), Equation 3.7.1-12 can be utilized to determine the minimum height required for the gas scrubbing column by dividing the calculated packing height by the number of theoretical stages used in the Aspen model.

$$Z = H_{o,G} N_{o,G}$$

Equation 3.7.1-11 Formula for Packing Height (Z)⁴⁰

$$HETP = Z/N$$

Equation 3.7.1-12 Formula for HETP⁴⁰

N, Number of Theoretical Stages in Aspen Model

Based on the calculations and modeling, there were 5 theoretical stages modeled in Aspen, each with a diameter of 1 m and height of 7.47 m. To increase reliability of the process and accommodate for the large volume of vapor that needs to be processed, the height was rounded up to 8 m. A material balance around a single scrubber is shown in Figure 3.7.1-2. An example calculation detailing the entire process following the Aspen modeling can be found below in Table 4.1.2-4.

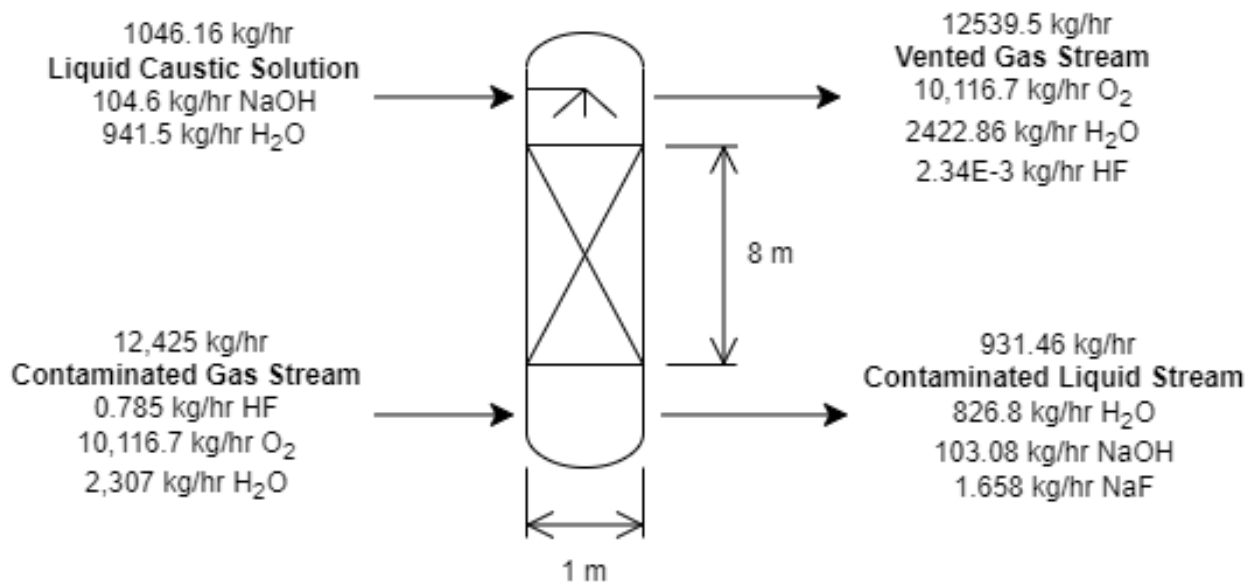


Figure 3.7.1-2 Gas scrubber material balance for a single processing unit

3.8 Saponification Reactor

In the cobalt extraction block, to facilitate the efficient liquid-liquid extraction of cobalt from the aqueous phase, Cyanex-272 is used as an extractant. Several papers have noted increasing extraction efficiency of cobalt with increasing saponification (reaction with base) percentage of Cyanex.^{23,28} However, too much saponification (more than about 60%) results in the Cyanex forming a gel, which is undesirable for the liquid-liquid extraction operations after saponification. The literature recommends saponification percentages of 40-50%,^{8,28} but Rodrigues et al. found the co-extraction of Ni²⁺ to rise quickly when increasing saponification from 40 to 50% while Co²⁺ extraction remained relatively constant;²⁹ to increase cobalt product purity, 40% saponification of Cyanex was chosen for the process.

Saponification of Cyanex-272 occurs in the cobalt block, providing fresh extractant to the extraction columns (via stream 406-OREF) and recovering regenerated extractant from the stripping columns (via stream 405-RECY), forming a recycle loop.

Table 3.8-1 Saponification Reactor Tag Legend	
Tag Number	Brief Description
SAP-401	Cobalt Saponification Reactor

3.8.1 Reaction Overview

The saponification of Cyanex-272 refers to the acid-base reaction it undergoes with NaOH. Cyanex-272 is a phosphinic acid. In the saponification reactors, 20 vol% Cyanex-272 in kerosene is contacted with aqueous NaOH in stoichiometric proportion to achieve 40% molar

saponification of Cyanex-272. The resultant species is referred to as Cyanex-Na and is the primary extractant of cobalt.

3.8.2 Cobalt Saponification Reactor Design

The saponification of Cyanex-272 occurs in 8 parallel standard reactors, as described in Section 3.1.2. The feeds to the reactors are added at ambient temperature (25°C). The heat generated by the reaction does not significantly raise the temperature of the effluent, thus, no temperature control is required. Negligible power (on the order of 10 W) is required to mix the reactor.

3.9 Rotary Vacuum Drum Filter

The following section details the design process around the rotary vacuum drum filters (RVDF). This includes the design assumptions and associated equations. These unit operations were mentioned in the ASPEN file above in Section 2: Prior Works, but this modeling was not done.

Table 3.9-1		RVDF Tag Legend
Tag Number	Brief Description	
FIL-101	Leaching RVDF	
FIL-201	Impurity Removal RVDF	
FIL-301	Manganese Carbonate RVDF	
FIL-401	Cobalt Hydroxide RVDF	
FIL-501	Nickel Hydroxide RVDF	

3.9.1 Rotary Vacuum Drum Filter Design

The process utilizes solid washers to separate the liquid stream from either the unreacted solids or the extracted metals. The specific type of solid washer is a rotary drum vacuum filter (RVDF).

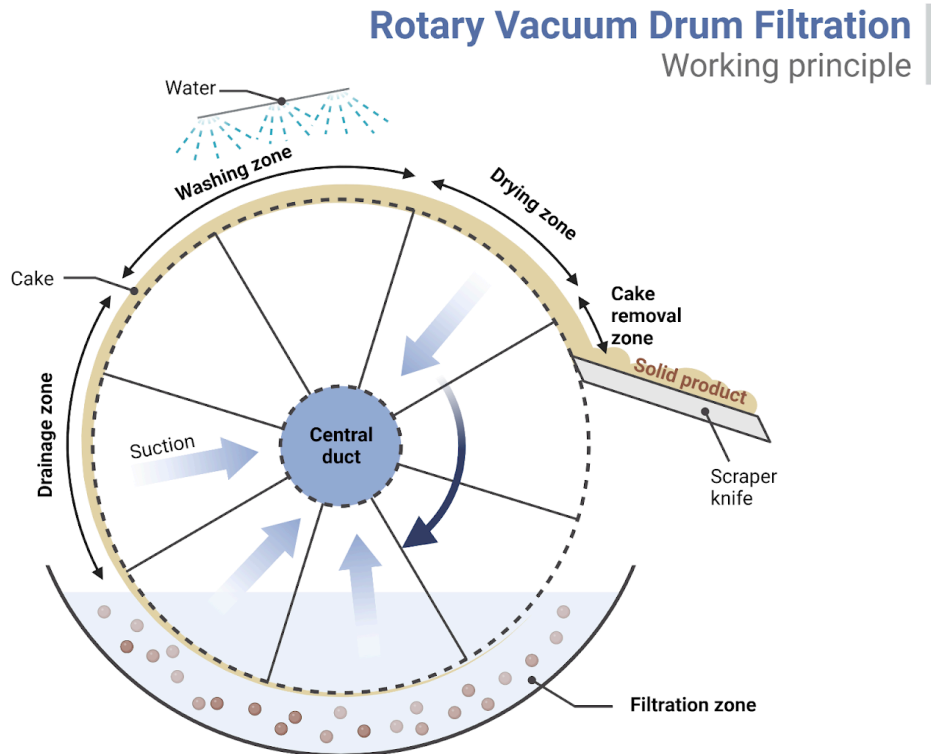


Figure 3.9.1-1 Rotary Vacuum Drum Filter Schematic⁴¹

Modeling of the filter was done using the FILTER block in Aspen. 100% recovery of the solid was assumed with 30 wt% liquid filtering out with it. The FILTER block was run at 1 atm with no change in temperature. These parameters were chosen based on the most reasonable results for wet cake exiting an RVDF as well as information based on an example found in literature.⁴² The resulting flow rates were used to calculate the necessary filter area.

The key variables used to determine the sizing of our RVDFs was slurry concentration (solid to liquid ratio), density of the incoming stream, volume of the incoming stream, and the ratio of cake to solid. Other variables, such as viscosity, rotary submergence, vacuum pressure, and filter cycle time, cannot be known without experimental data. The dimensions for our RVDF were approximated by inserting experimental data from example 30.3 in Unit Operations of Chemical Engineering, in which a slurry of calcium carbonate is being filtered.⁴² The constants for the RVDF design based on this example are in Table 3.9.1-1 below.

Table 3.9.1-1 RVDF Assumptions	
Rotary Submergence (%)	30%
Pressure Drop - Δp (atm)	0.5
Moisture % (filter cake)	30%
Filter Cycle Time (s)	300
Filter-Medium Resistance (negligible)	0
Specific Cake Resistance - α_0 (lb/ft ²)	2.90E+10
Viscosity (lb/ft-s)	0.000672

It was assumed that the RVDF has 100% solid filtration. The next step in the design process was to determine the filter area required in m². This is the key design factor needed to determine capital cost. The following equations (Equation 3.9.1-1 through Equation 3.9.1-3) detail this process.

$$C = \frac{c_F}{1 - [(m_F/m_c) - 1]c_s/\rho}$$

Equation 3.9.1-1 Formula for mass of particles deposited in filter per unit of volume

c_F ,	solid concentration	
c_S ,	concentration at surface	
m_F ,	mass of wet cake	kg
m_C ,	mass of dry cake	kg
ρ ,	density	kg/m ³

$$\dot{m} = SFR \left(\frac{1}{(c_F/\rho)+1} \right) c_F$$

Equation 3.9.1-2 Solids Production Rate

SFR, Slurry Flow Rate kg/hr

$$A_T = \dot{m}_c \left(\frac{\alpha_0 \mu}{2c\Delta p^{1-s} g_c f n} \right)^{1/2}$$

Equation 3.9.1-3 Filter Area

f , fraction of filter cycle available
 n , drum speed s

Based on these formulas and the assumptions stated above, most of the RVDF filter area requirements are above the reasonable area available for purchase in industry (Table 3.9.1-2). Based on Chemical Engineering Design⁴³, the reasonable unit size range is from 10 m² to 180 m². Table 3.9.1-2 below provides an overview of the RVDFs, detailing their total input, solid input, and required filter area. Table 3.9.1-3 details the RVDF size for each process step as well as the quantity required.

Table 3.9.1-2 RVDF Designs			
RDVF	Input (kg/hr)	Solids in Input (kg/hr)	Filter Area (m²)
FIL-101	371719	4092	346.24
FIL-201	406737	9522	543.65
FIL-301	117988	3948	184.98
FIL-401	450911	2412	295.45
FIL-501	399959	3932	353.05

Table 3.9.1-3 Individual RVDF Designs		
RDVF	Filter Area (m²)	Quantity
FIL-101	28.55	12
FIL-201	45.30	12
FIL-301	46.24	4
FIL-401	36.93	8
FIL-501	29.42	12

An example calculation detailing the entire process can be found below in Appendix A.

3.10 Rotary Drum Dryer

This section details the design process and assumptions made when designing our rotary drum dryers.

Table 3.10-1 Rotary Drum Dryer Tag Legend	
Tag Number	Brief Description
D-301	Manganese Carbonate Dryer
D-401	Cobalt Hydroxide Dryer
D-501	Nickel Hydroxide Dryer

3.10.1 Rotary Drum Dryer Design

The wet cake from the RVDFs goes to rotary drum dryers. In these dryers, the wet cake is fed continuously while hot air is pumped throughout to aid the drying process. The remaining liquid is evaporated and vented off of the dryer. An example schematic of this dryer is shown below.

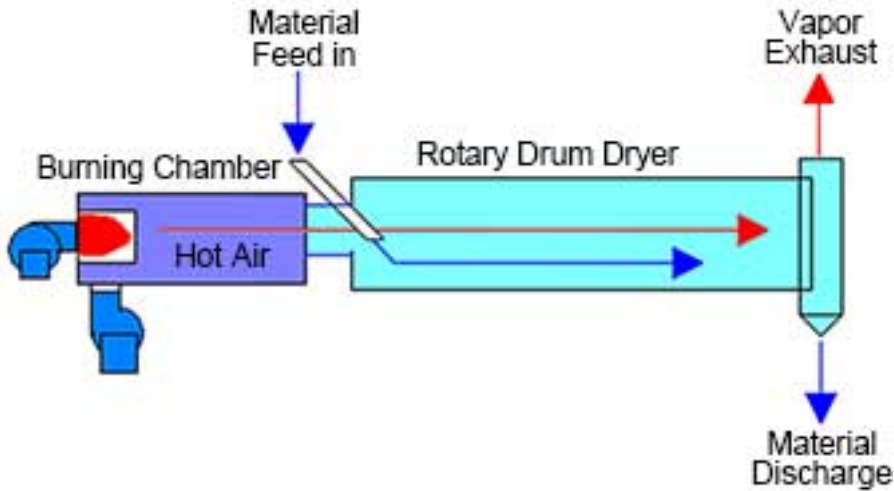


Figure 3.10.1-1 Rotary Drum Dryer Schematic⁴⁴

To accurately price this equipment, we assumed a single stage dryer and that the working dryer area and the necessary air flow rate to dry the product completely were needed. To model this dryer in Aspen, the FLASH2 block was utilized. The air inlet was set to 150 °C and a sensitivity analysis was used to vary the flow rate until the air outlet temperature was 110 °C.

This outlet temperature achieved a final dryness of nearly 100%. The dryer area was calculated to determine capital cost. This was done using a few assumptions found in literature.¹⁴ The first is that rotary dryers are usually operated with 10-15% of their volume filled with material, 15% was chosen. The second assumption is that the length/diameter ratio found to be most efficient in commercial dryers is between 4 and 10, 5 was chosen. Equations 3.10.1-1 through 3.10.1-3 detailing this process can be found below.

$$V_N = \frac{1}{0.15V}$$

Equation 3.10.1-1 Dryer Volume Needed

V_N ,	Dryer volume needed	kg/m^3
V ,	volume coming in	kg/m^3

$$D = \left(\frac{4V_N}{5\pi} \right)^{1/3}$$

$$L = 5D$$

Equation 3.10.1-2 Dryer Diameter and Length

$$A = 2\pi\left(\frac{D}{2}\right)L + 2\pi\left(\frac{D}{2}\right)^2$$

Equation 3.10.1-3 Dryer Area

Based on these formulas and the assumptions listed above the area needed for each dryer was accurately calculated. The quantity of dryers mirrors the number of parallel streams to improve reliability in the process. One limitation to the drying process is the Na^+ ions present in

the dryer feeds. This combined with the SO_4^{2-} ions results in Na_2SO_4 forming within the final product. This lowers the purity of the final product where the value is affected heavily. To reach the final purity set within the process, a washing step would be needed before the RVDF to remove the large amount of sodium present (Section 7.2). Table 3.10.1 below provides an overview of all of the rotary drum dryers, detailing their total input, solid output, required filter area, quantity and inlet air flow rate.

Table 3.10.1-1 Rotary Drum Dryer Designs					
Rotary Drum Dryer	Input (kg/hr)	Solids Output (kg/hr)	Dryer Area (m ²)	Quantity	Air Flowrate (kg/hr)
D-301	1362	987	11.32	4	23400
D-401	431	330	4.32	8	5800
D-501	469	358	3.83	12	7200

An example calculation detailing the entire process can be found below in Appendix A.

3.11 Ancillary Equipment

This section details the design process and assumptions made when designing ancillary equipment including pumps, heat exchangers, and storage tanks.

3.11.1 Mass Transport Design

This section details the design process and assumptions made when designing ancillary equipment associated with mass transport, including pumps, bucket elevators, and belt

conveyors. Each piece of equipment is uniquely tagged based on its location in the plant and its stage in the process.

Table 3.11.1-1 Mass Transport Tag Legend	
Tag Number	Brief Description
BE-101	Black mass bucket elevator into PLEACH-101
P-101	Piranha solution pump into PLEACH-101
P-102	Effluent pump into FIL-101
P-103	Effluent pump into PRCP-201
P-201	Effluent pump into FIL-201
BE-201	NaOH bucket elevator into PRCP-201
P-202	Effluent pump into PBR-201
P-203	Effluent pump into EXT-301
P-301	H ₂ SO ₄ pump into EXT-301
P-302	Effluent pump into EXT-302
P-303	Effluent pump into EXT-401 feed stream
P-304	Organic from EXT-301 pump into SCRB-301
P-305	Organic from EXT-302 pump into SCRB-301
P-306	Waste pump from SCRB-301
P-307	Effluent pump into STRP-301
P-308	Mn Loaded stream pump into SCRB-301
P-309	H ₂ SO ₄ pump into STRP-301
P-310	Effluent pump into PRCP-301
P-311	Organic pump into EXT-301

Table 3.11.1-1 Mass Transport Tag Legend	
P-312	Organic pump into EXT-302
BE-301	Base feed bucket elevator into PRCP-301
BE-302	Na ₂ CO ₃ bucket elevator into PRCP-301
P-313	Effluent into FIL-301
CB-301	Wet Cake Conveyor Belt to D-301
CB-302	MnCO ₃ Conveyor Belt from D-301
BLW-301	Dry air blower into D-301
BE-401	Base feed bucket elevator into PRCP-401 feed stream
P-401	Feed stream pump into EXT-401
P-402	Organic pump into EXT-401
P-403	Effluent pump into PRCP-501
P-404	Organic pump into SCRB-401
P-405	H ₂ SO ₄ pump into SCRB-401
P-406	Waste pump from SCRB-401
P-407	Effluent pump into STRP-401
P-408	H ₂ SO ₄ pump into STRP-401
P-409	Effluent pump into SAP-401
P-410	Co(OH) ₂ pump into SCRB-401
P-411	NaOH pump into SAP-401
P-412	Effluent pump into PRCP-401
P-413	Effluent pump into FIL-401
P-414	Waste pump from FIL-401
CB-401	Wet cake Conveyor Belt to D-401
CB-402	Co(OH) ₂ Conveyor Belt from D-401

Table 3.11.1-1 Mass Transport Tag Legend	
BLW-401	Dry air blower into D-401
BE-501	NaOH bucket elevator into PRCP-501
P-501	Effluent pump into FIL-501
P-502	Effluent pump into Lithium Extraction
CB-501	Wet cake conveyor belt to D-501
CB-502	NiCO ₃ conveyor belt from D-502
BLW-501	Dry air blower into D-502

3.11.1.1 Pump Design

Centrifugal pumps are used for the transport of slurries, aqueous solutions, and organic solutions within the plant. Their large volumetric throughput is desirable for the scale of the plant. Assuming that frictional losses in parallel streams are equal, only one pump is used between unit operations, with pipes converging and splitting as necessary. This design, although likely to complicate piping layout, allows one pump to supply power to all parallel streams instead of multiple smaller pumps. This saves significantly on both initial and future costs, as the corrosive nature of battery leaching will likely require frequent replacement. As a precautionary measure, back up pumps are also included in initial capital costs.

3.11.1.2 Blower Design

For the transport of gases, multistage centrifugal fans are used due to their low operating pressure and large continuous flow. Assuming a maximum pressure differential of 0.2 atm, one multistage centrifugal blower can supply enough driving power to support gas transport through all parallel streams. Because of the large volumetric flow rate, these fans are the largest consumers of power out of all transport equipment.

3.11.1.3 Bucket Elevator Design

Bucket elevators are the primary equipment used for solid loading in reactors due to their affordability over conveyor belts. Although screw feeders can also be considered, bucket elevators are more reliable for both performing at scale and determining cost estimates. The height of each bucket elevator is 10 m, which is twice as high as each standard reactor. This allows the use of potential energy to facilitate solid flow into the reactors. Through diverter systems, one bucket elevator can be used for each group of reactors that share reactor schedules.

3.11.1.4 Conveyor Belt Design

Where bucket elevators are not feasible, such as transport of wet cake from drum filters, conveyor belts must be used. It is challenging to estimate the distances between solid filters and downstream reactors. Instead, a length of 50 m is used for cost estimation, and a conveyor belt width of 0.5 m is used.

3.11.1.5 Transport Power Requirements

The shaft power associated with each pump is determined by the pressure differential between destinations as well as the volumetric flow rate of the fluid.

$$P = \frac{Q\Delta P}{\eta}$$

Equation 3.11.1.5-1 Shaft Power for Centrifugal Pump

P ,	shaft power	W
Q ,	flow rate	m^3/s
ΔP ,	pressure difference	Pa
η ,	pump efficiency	

The majority of unit operations are run at atmospheric pressure. As a result, pressure differences between unit operations mainly result from friction losses in pipes as well as changes

in height. To simplify shaft power calculations, it is assumed that the average friction loss between unit operations is approximately 1 atm (0.5 atm from pipe roughness and 0.5 atm from control valves). When applicable, gravity head (ρgh) is also accounted for to estimate any extra power required.

For multistage centrifugal blowers, determining power uses the same equation above. For gases, volumetric flow rate is higher and pressure differential is lower. The assumed maximum pressure differential for the blower, obtained from Towler and Sinnott, is 0.2 bar.⁴³ The density of gases is several orders of magnitude lower than liquid or solid, which results in much higher power requirements for the blowers compared to pumps.

Table 3.11.1-2 Pump and Blower Power Requirements		
Tag Number	Volumetric Flow Rate (L/s)	Power Required (kW)
P-101	88.1	21.7
P-102	94.2	13.3
P-103	94.0	14.9
P-104	93.2	22.7
P-201	90.5	14.4
P-202	89.0	14.1
P-203	87.3	33.6
P-301	1.2	0.4
P-302	89.2	34.1
P-303	89.1	14.1
P-304	121.6	19.3
P-305	120.3	19.1

Table 3.11.1-2 Pump and Blower Power Requirements		
P-306	24.2	3.8
P-307	239.6	71.3
P-308	24.1	3.8
P-309	28.3	10.1
P-310	28.7	6.9
P-311	118.2	35.3
P-312	118.2	35.3
P-313	28.7	4.6
BLW-301	31,325.3	626.5
P-401	87.6	34.0
P-402	94.9	28.3
P-403	89.9	22.7
P-404	95.1	28.1
P-405	0.1	0.1
P-406	95.6	15.2
P-407	94.0	27.9
P-408	100.8	36.9
P-409	92.7	14.7
P-410	95.6	33.0
P-411	1.3	0.2
P-412	101.3	24.9
P-413	108.0	17.1
P-414	105.5	16.7
BLW-401	19,544.8	390.9

Table 3.11.1-2 Pump and Blower Power Requirements		
P-501	90.5	14.4
P-502	89.8	14.3
BLW-501	28,915.7	578.3

3.11.2 Heat Exchanger Design

A shell-and-tube heat exchanger is required to cool the aqueous stream leaving the cobalt extraction block that feeds the nickel extraction block (stream 407-AQEE/501-EFF). The cooling occurs in 8 parallel streams, thus requiring 8 parallel heat exchangers. Each parallel stream is initially at 48°C and must be cooled to 35°C, requiring 590 kW of heat to be removed. Using Equation 3.1.2.3-1, 28.2 kg/s of CW (per exchanger) flowing in at 30°C and exiting at 35°C is required. Towler and Sinnott's Chemical Engineering Design recommends that the tubes (containing the hot stream) are 2 inch diameter tubes and that their wall thickness be 3.4 mm.⁴³ Using this information, the convective heat transfer coefficient in the hot fluid was calculated using The Gnielinski Correlation (Equation 3.1.2.3-3).¹³ The convective heat transfer coefficient of the CW in the shell is difficult to calculate, so a conservative value of 1000 W/m²K was used from Giorgio Carta's Heat and Mass Transfer table 7.1.⁴⁰ Assuming a material of construction of Stainless Steel 316, the overall heat transfer coefficient was calculated using Equation 3.1.2.3-2. This allows for calculation of the required heat transfer area in the heat exchanger using Equation 3.1.2.3-5, which is 89.2 m². The LMTD calculated by Equation 3.1.2.3-6 would need to be altered to the form represented below in Equation 3.11.2-1 below since both the hot stream and cold stream are changing temperature. A countercurrent flow configuration was assumed.

$$LMTD = \frac{(T_{hot\ stream,\ in} - T_{CW,\ out}) - (T_{hot\ stream,\ out} - T_{CW,\ in})}{\ln\left(\frac{T_{hot\ stream,\ in} - T_{CW,\ out}}{T_{hot\ stream,\ out} - T_{CW,\ in}}\right)}$$

Equation 3.11.2-1

LMTD Calculation

Table 3.11.2-1 Heat Exchanger Tag Legend	
Tag Number	Brief Description
HE-401	Shell-and-Tube Heat Exchanger

3.11.3 Storage Equipment

Table 3.12.3-1 Storage Equipment Tag Legend	
Tag Number	Brief Description
TK-BM	Black Mass Storage Silo
TK-H2O2	H ₂ O ₂ Storage Tank
TK-H2SO4	H ₂ SO ₄ Storage Tank
TK-NAOH	NaOH Storage Silo
TK-CAOH	CaOH Storage Silo
TK-NA2CO3	Na ₂ CO ₃ Storage Silo
TK-MNPD	MnCO ₃ Product Storage Silo
TK-COPD	Co(OH) ₂ Product Storage Silo
TK-NIPD	Ni(OH) ₂ Storage Silo

Storage equipment is used in this process to hold both raw materials and final products on site. The aqueous materials are held in tanks, while the solid materials are held in silos. The size

of the storage equipment depends on the amount of material. The general rule of thumb used in this plant is a two-week supply of both raw materials and final products. The volume of this storage equipment was calculated using the mass and density of each material in Eq 3.11.3-1.

$$V = \frac{m}{D}$$

Equation 3.11.3-1

V, volume	m ³
m, mass	kg
D, density	kg/m ³

Table 3.11.3-2 below details the storage equipment sizes and blocks where the material is either used or produced. According to Towler and Sinnott, floating roof tanks can range in volume from 100 to 10,000 m³.⁴³ However, the solid materials need to be stored in silos. According to CST Industries, industrial silos can reach sizes upward of 200,000 ft³ (5,600 m³). Table 3.11.3-2 lists the size and quantity of storage equipment that will be purchased. Each silo/tank was designed with extra headspace in case excess material needs to be held.⁴⁵

A key to this follows: Leaching - 1, Impurity Removal - 2, Manganese Extraction - 3, Cobalt Extraction - 4, Nickel Extraction - 5.

Table 3.11.3-2 Storage Equipment Sizes					
Equipment Tag	Total Material for 2 Weeks (kg)	Size Requirement (m ³)	Silo/Tank Size (m ³)	Quantity	Locations
TK-BM	4,257,792	1,359	1500	1	1
TK-H2O2	8,455,854	5,832	6,000	1	1
TK-H2SO4	25,643,912	13,937	7,000	2	1,3,4
TK-NAOH	23,327,932	10,952	5500	2	2,4,5
TK-CAOH	114,441	49	60	1	2
TK-NA2CO3	1,080,912	426	460	1	3
TK-MNPD	957,264	268	300	1	3
TK-COPD	449,904	147	180	1	4
TK-NIPD	1,321,488	394	425	1	5

3.11.4 Air Heaters

The air supplied to the air dryers via the blowers must be heated before it is ready to dry the product. This is done by blowing the air through a furnace where it is heated by the combustion of natural gas. The efficiency of the heating (the percent of heat released by the combustion of natural gas that raises the temperature of the air) was assumed to be 90%.⁴⁶ The combustion reaction was assumed to go to completion (i.e. no production of carbon monoxide). The heat released by combustion of one mole of natural gas (methane) is 890 kJ.⁴⁷ The combustion reaction is presented in table 3.11.4-1 below

Table 3.11.4-1	Combustion Reaction of Natural Gas
$\text{CH}_4 + 2\text{O}_2 \rightarrow 2\text{H}_2\text{O} + \text{CO}_2$	

The total flow of drying air into all blocks of the process is 226,400 kg/hr. This air begins at ambient temperature (25°C) and is heated to 150°C. Taking the specific heat capacity of air to be 1.012 kJ/kg,⁴⁰ this requires 7,960 kW of energy in total. With 90% heating efficiency, purchasing the equivalent of 8,840 kW of natural gas would be required. Natural gas is sold by its energy content in MMBtu (1,000,000 Btu); the process requires 30.2 MMBtu/hr of natural gas.

Section 4: Final Design

4.1 Leaching Block

This section details the process of leaching metals out of black mass and separating and removing the gas and solid streams from the aqueous metals. This includes all unit operations, parallel streams, batch schedules, and material balances. To process the total mass flow per hour, this block runs with 12 parallel streams. Figure 4.1-1 displays a detailed overview of the Leaching Block. Table 4.1-1 and Table 4.1-2 supplement Figure 4.1-1 by providing the stream numbers, tag numbers, and a brief description.

LEACHING BLOCK

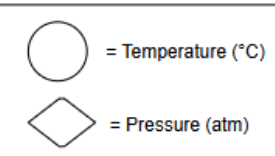
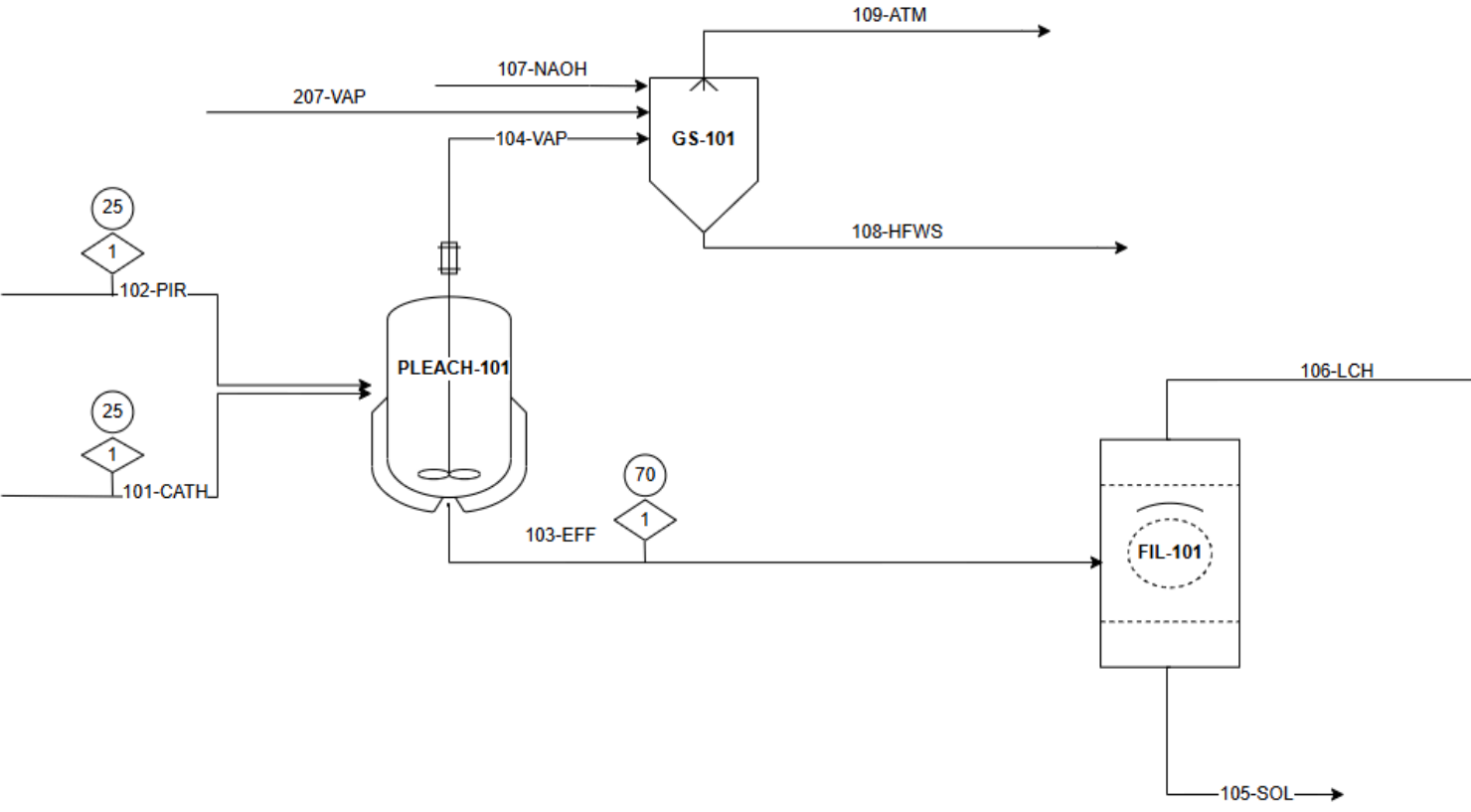


Figure 4.1-1 Leaching Block PFD

Table 4.1-1 Unit Operation Tag Legend	
Tag Number	Brief Description
PLEACH-101	Leaching Reactor
FIL-101	Leaching RVDF
GS-101	Waste Stream Gas Scrubber

Table 4.1-2 Stream Label Legend	
Stream Number	Stream Description
101-CATH	Black Mass stream entering PLEACH-101
102-PIR	Piranha Solution stream entering PLEACH-101
103-EFF	Leachate stream leaving PLEACH-101
104-VAP	Vapor Stream leaving PLEACH-101
105-SOL	Solid Stream leaving FIL-101
106-LCH	Leachate stream leaving FIL-101
107-NAOH	NaOH stream entering GS-101
207-VAP	Vapor stream leaving PBR-201
108-HFWS	HF waste stream leaving GS-101
109-ATM	Clean waste stream venting to atmosphere from GS-101

4.1.1 Final Design Description

The process block begins by leaching 12,678 kg/hr of black mass (101-CATH) fed by BE-101 from TK-BM in 359,517.6 kg/hr of piranha solution (102-PIR) pumped through P-101 from TK-H2O2 and TK-H2SO4 which contains 64,723.2 kg/hr of H₂SO₄, 25,166.2 kg/hr of H₂O₂, and the rest water in PLEACH-101. The reaction occurs in a batch reactor with a residence time of 2 hours and is stirred at 60 RPM to ensure solid suspension. Assuming each reactor takes approximately 30 minutes to be loaded and unloaded, reactor scheduling is staggered such that equal amounts of reactors will be loaded and unloaded in any given 30 minute window to simulate continuous flow. Based on the capacity of each standard reactor, a batch schedule (Table 4.1.1-1) is designed where 6 groups of 6 reactors (36 reactors total), are loading and unloading during separate 30 minute windows. This allows for the reactors with a total reaction time of 3 hours (2 hour residence time, 1 hour loading and unloading), to behave continuously.

Table 4.1.1-1 Leaching Reactor Schedule							
	Group	1	2	3	4	5	6
Time							
0:00		loading	1/4 reacted	1/2 reacted	3/4 reacted	reacted	unloading
0:30		1/4 reacted	1/2 reacted	3/4 reacted	reacted	unloading	loading
1:00		1/2 reacted	3/4 reacted	reacted	unloading	loading	1/4 reacted
1:30		3/4 reacted	reacted	unloading	loading	1/4 reacted	1/2 reacted
2:00		reacted	unloading	loading	1/4 reacted	1/2 reacted	3/4 reacted
2:30		unloading	loading	1/4 reacted	1/2 reacted	3/4 reacted	reacted
3:00		loading	1/4 reacted	1/2 reacted	3/4 reacted	reacted	unloading

The reactors operate at a constant temperature using a cooling jacket to ensure the exiting streams are at 70 °C.. The 477.42 kg/hr of vapor (104-VAP) is sent to a gas scrubber (GS-101) to remove the 0.78 kg/hr of HF to allow safe ventilation to the atmosphere. The remaining

371,719.1 kg/hr liquid-solid slurry (103-EFF) flows to a solid washer (FIL-101) using P-102 that removes graphite and other components of black mass not dissolved in PLEACH-101. 5,852.7 kg/hr of solids (105-SOL) containing 70 wt% graphite and the remaining water and unleached metals are removed from 103-EFF. Leaving the leaching block is 365,866.3 kg/hr of aqueous metals (106-LCH) by P-103.

GS-101 cleans the vapor streams 104-VAP and 207-VAP. This unit operation is the same as the one detailed in Section 4.1.1 so more information on GS-101 can be found there and Section 3.8. Additionally, Section 4.2.2 below lists the material balances around each unit operation in this process block.

4.1.2 Material Balances

Table 4.1.2-1 Leaching Block: PLEACH-101				
Name	101-CATH	102-PIR	103-EFF	104-VAP
Flowrate	kg/hr	kg/hr	kg/hr	kg/hr
Total	12,678.9	359,517.6	372,196.5	477.4
C (s)	4,092.8	0	4,092.8	0
Co (s)	1,660.9	0	0	0
Fe (s)	102.8	0	0	0
Cu (s)	219.4	0	0	0
Ni (s)	2,650.0	0	0	0
Al (s)	129.3	0	0	0
Li ₂ O (s)	1,071.4	0	0	0
CoLiO ₂ (s)	77.3	0	0	0
LiNiO ₂ (s)	77.3	0	0	0
LiMn ₂ O ₄ (s)	77.3	0	0	0
Mn ₃ O ₄ (s)	2,326.6	0	0	0
O ₂	0	0	3.0	393.5
H ₂ O	0	269,638.2	267,768.6	82.3
H ₂ O ₂	0	25,166.2	21,767.6	0.9
H ₂ SO ₄	0	64,713.2	0	0
HF	0	0	104.9	0.8
LiF(s)	193.9	0	0	0
F ⁻	0	0	42.4	0
SO ₄ ²⁻	0	0	1,800.6	0
HSO ₄ ⁻	0	0	62,229.0	0
H ₃ O ⁺	0	0	6,852.6	0
Al ³⁺	0	0	129.3	0
Co ²⁺	0	0	1,707.4	0
Mn ²⁺	0	0	1,722.8	0
Cu ²⁺	0	0	219.4	0
Li ⁺	0	0	563.5	0
Ni ²⁺	0	0	2,696.4	0
Fe ³⁺	0	0	102.8	0

Table 4.1.2-2 Leaching Block: FIL-101			
Name	103-EFF	105-SOL	106-LCH
Flowrate	kg/hr	kg/hr	kg/hr
Total	371,719.1	5,852.7	365866.4
C	4,092.8	4,092.8	0
O ₂	3.0	0	3.0
H ₂ O	267,687.0	1,281.5	266,405.5
H ₂ O ₂	21,766.7	104.2	21,662.5
HF	104.2	0.5	103.7
F ⁻	42.4	0.2	42.1
SO ₄ ²⁻	1,797.1	8.6	1,788.5
HSO ₄ ⁻	62,232.6	297.9	61,934.6
H ₃ O ⁺	6,851.9	32.8	6,819.0
Al ³⁺	129.3	0.6	128.6
Co ²⁺	1,707.4	8.2	1,699.2
Mn ²⁺	1,722.8	8.2	1,714.5
Cu ²⁺	219.4	1.1	218.4
Li ⁺	563.5	2.7	560.8
Ni ²⁺	2,696.4	12.9	2,683.5
Fe ³⁺	102.8	0.5	102.3

Table 4.1.2-3 Leaching Block: GS-101					
Name	104-VAP	207-VAP	107-NAOH	108-HFWS	109-ATM
Flowrate	kg/hr	kg/hr	kg/hr	kg/hr	kg/hr
Total	477.4	12,384.4	1046.16	931.46	12539.5
O ₂	393.5	10,083.9	0	0.01	10,116.7
H ₂ O	82.3	2,300.5	941.5	826.8	2422.86
HF	0.785	0	0	0	0.00234
NaF	0	0	0	1.658	0
NaOH	0	0	104.6	103.08	0

4.2 Impurity Removal Block

This section details the process of removing impurities from the aqueous phase moving forward. This includes all unit operations, parallel streams, batch schedules, and material balances. To process the total mass flow per hour, this block runs with 12 parallel streams. Figure 4.2-1 displays a detailed overview of the Impurity Removal Block. Table 4.2-1 and Table 4.2-2 supplements Figure 4.2-1 by providing the stream numbers, tag numbers, and a brief description.

IMPURITY REMOVAL BLOCK

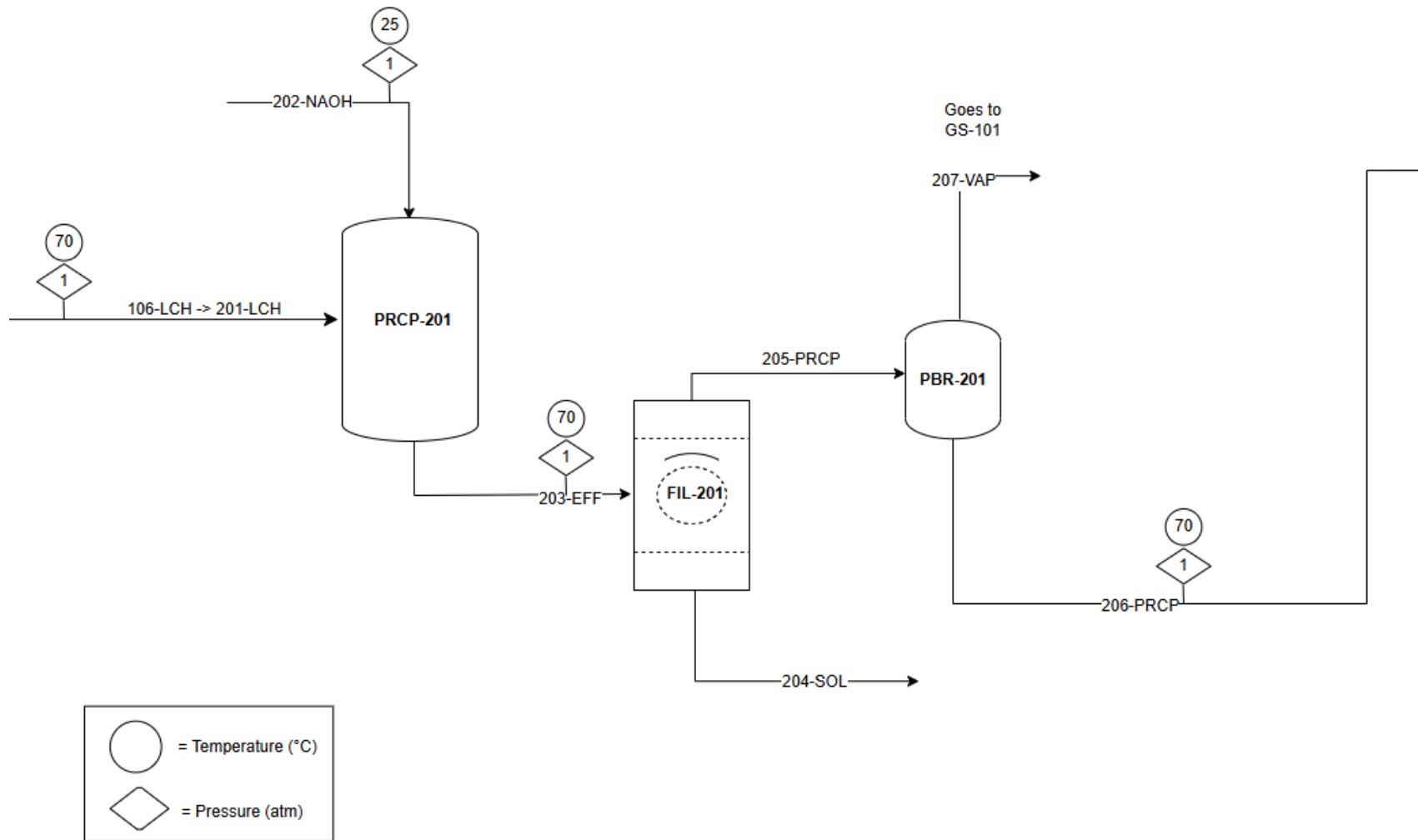


Figure 4.2-1

Impurity Removal Block PFD

Table 4.2-1 Unit Operation Tag Legend	
Tag Number	Brief Description
PRCP-201	Impurity Removal Precipitator
FIL-201	Impurity Removal RVDF
PBR-201	H ₂ O ₂ Decomposition Packed Bed Reactor
GS-101	Waste Stream Gas Scrubber

Table 4.2-2 Stream Label Legend	
Stream Number	Stream Description
201-LCH	Leachate stream entering PRCP-201
202-NAOH	NaOH entering PRCP-201
203-EFF	Precipitate leaving PRCP-201
204-SOL	Impurities leaving FIL-201
205-PRCP	Aqueous stream leaving FIL-201
206-PRCP	Aqueous stream leaving PBR-201
207-VAP	Vapor stream entering GS-101

4.2.1 Final Design Description

This process block begins with 365,866 kg/hr (201-LCH) entering PRCP-201 using P-104. It is important to note that 107-LCH and 201-LCH are the same stream. 40,872 kg/hr of NaOH (202-NAOH) is added in using BE-201 from TK-NAOH to bring the reactor pH up to 5.9. PRCP-201 operates with a residence time of 6 hours with a half hour for both loading and unloading. A cooling jacket is used on this reactor to keep the reaction temperature steady at 70

°C. This temperature remains consistent throughout the remainder of this process block. The batch schedule in Table 4.2.1-1 was used to achieve pseudo-continuous flow. This results in a total of 84 standard reactors (14 groups of 6). The resulting precipitate (203-EFF), approximately 406,738 kg/hr, is pumped into FIL-201 using P-201.

Table 4.2.1-1 PRCP-201 Batch Schedule															
	Group	1	2	3	4	5	6	7	8	9	10	11	12	13	14
Time															
0:00	Loading														
0:30	Reacting														
1:00	Reacting														
1:30	Reacting														
2:00	Reacting														
2:30	Reacting														
3:00	Reacting														
3:30	Reacting														
4:00	Reacting														
4:30	Reacting														
5:00	Reacting														
5:30	Reacting														
6:00	Reacting														
6:30	Unloading														
7:00	Loading														

FIL-201 separates the solid impurities from the aqueous phase moving forward. Leaving FIL-201 is 13,617 kg/hr of solid impurities (204-SOL), and an aqueous stream of 393,121 kg/hr (205-PRCP). This unit operation is carried out through 12 RVDFs. The impurities are sent to waste management while the aqueous stream using P-202 is sent to PBR-201.

PBR-201 breaks down the H₂O₂ unreacted in 205-PRCP into H₂O and O₂. Leaving this block is 380,736 kg/hr of effluent (206-PRCP) and 12,384 kg/hr of vapor (207-VAP). 12 packed bed reactors (PBR-201) are required, one for each parallel stream. The effluent is sent to

EXT-301 and the vapor is sent to GS-101. GS-101 scrubs the vapor streams 104-VAP and 207-VAP. Additionally, Section 4.2.2 below lists the material balances around each unit operation in this process block.

4.2.2 Material Balances

Table 4.2.2-1 Impurity Removal Extraction Block: PRCP-201			
Name	201-LCH	202-NAOH	203-EFF
Flowrate	kg/hr	kg/hr	kg/hr
Total	365,866.4	40,871.6	406,738.0
O ₂	3.0	0	3.0
H ₂ O	266,405.5	0	289,172.8
H ₂ O ₂	21,662.5	0	21,662.5
HF	103.7	0	0
NaOH	0	36,784.5	0
CaF ₂ (s)	0	0	247.1
Ca(OH) ₂	0	4,087.2	0
CaSO ₄ ²⁻	0	0	8,295.9
Fe(OH) ₃ (s)	0	0	195.8
Al(OH) ₃ (s)	0	0	371.9
Cu(OH) ₂ (s)	0	0	333.0
Ni(OH) ₂ (s)	0	0	78.9
F ⁻	42.1	0	20.4
SO ₄ ²⁻	1,788.5	0	58,451.0
HSO ₄ ⁻	61,934.6	0	0.6
H ₃ O ⁺	6,819.0	0	0
Na ⁺	0	0	21,142.7
Al ³⁺	128.6	0	0

Table 4.2.2-1 Impurity Removal Extraction Block: PRCP-201 CONTINUED			
Name	201-LCH	202-NAOH	203-EFF
Flowrate	kg/hr	kg/hr	kg/hr
Co ²⁺	1,699.2	0	1,699.2
Mn ²⁺	1,714.5	0	1,714.5
Cu ²⁺	218.4	0	1.5
Li ⁺	560.8	0	560.8
Ca ²⁺	0	0	152.9
Ni ²⁺	2,683.5	0	2,633.
NiOH ⁺	0	0	0.1
Fe ³⁺	102.3	0	0

Table 4.2.2-2 Impurity Removal Extraction Block: FIL-201

Name	203-EFF	204-SOL	205-PRCP
Flowrate	kg/hr	kg/hr	kg/hr
Total	406,738.0	13,617.4	393,120.5
O ₂	3.0	0	2.9
H ₂ O	289,172.8	2,981.0	286,191.8
H ₂ O ₂	21,662.5	223.3	21,439.2
CaF ₂ (s)	247.1	247.1	0
CaSO ₄ ²⁻	8,295.9	8,295.9	0.1
Fe(OH) ₃ (s)	195.8	195.8	0
Al(OH) ₃ (s)	371.9	371.9	0
Cu(OH) ₂ (s)	333.0	333.0	0
Ni(OH) ₂ (s)	78.9	78.9	0
F ⁻	20.4	0.2	20.1
SO ₄ ²⁻	58,451.0	602.6	57,848.4
HSO ₄ ⁻	0.6	0	0.6
Na ⁺	21,142.7	218.0	20,924.7
Co ²⁺	1,699.2	17.5	1,681.7
Mn ²⁺	1,714.5	17.7	1,696.8
Cu ²⁺	1.5	0	1.4
Li ⁺	560.8	5.8	555.0
Ca ²⁺	152.9	1.6	151.3
Ni ²⁺	2,633.4	27.1	2,606.3
NiOH ⁺	0.1	0	0.1

Table 4.2.2-3 Impurity Removal Extraction Block: PBR-201			
Name	205-PRCP	206-PRCP	207-VAP
Flowrate	kg/hr	kg/hr	kg/hr
Total	393,120.5	380,736.1	12,384.4
O ₂	2.9	3.3	10,083.9
H ₂ O	286,191.8	295,246.1	2,300.5
H ₂ O ₂	21,439.2	0	0
CaSO ₄ ²⁻	0.1	0	0
F ⁻	20.1	20.1	0
SO ₄ ²⁻	57,848.4	57,848.4	0
HSO ₄ ⁻	0.6	0.6	0
Na ⁺	20,924.7	20,924.7	0
Co ²⁺	1,681.7	1,681.7	0
Mn ²⁺	1,696.8	1,696.8	0
Cu ²⁺	1.4	1.4	0
Li ⁺	555.0	555.0	0
Ca ²⁺	151.3	151.3	0
Ni ²⁺	2,606.3	2,606.3	0
NiOH ⁺	0.1	0.1	0

4.3 Manganese Extraction Block

This section details the process of extracting, purifying, and precipitating the manganese out of the total aqueous metals stream. This includes all unit operations, parallel streams, batch schedules, and material balances. To process the total mass flow per hour, this block runs with 24 parallel streams up to the precipitation reactor in which it then operates with 4 parallel streams. Figure 4.3-1 displays a detailed overview of the Manganese Extraction Block. Table 4.3-1 and

Table 4.3-2 supplement Figure 4.3-1 by providing the stream numbers, tag numbers, and a brief description.

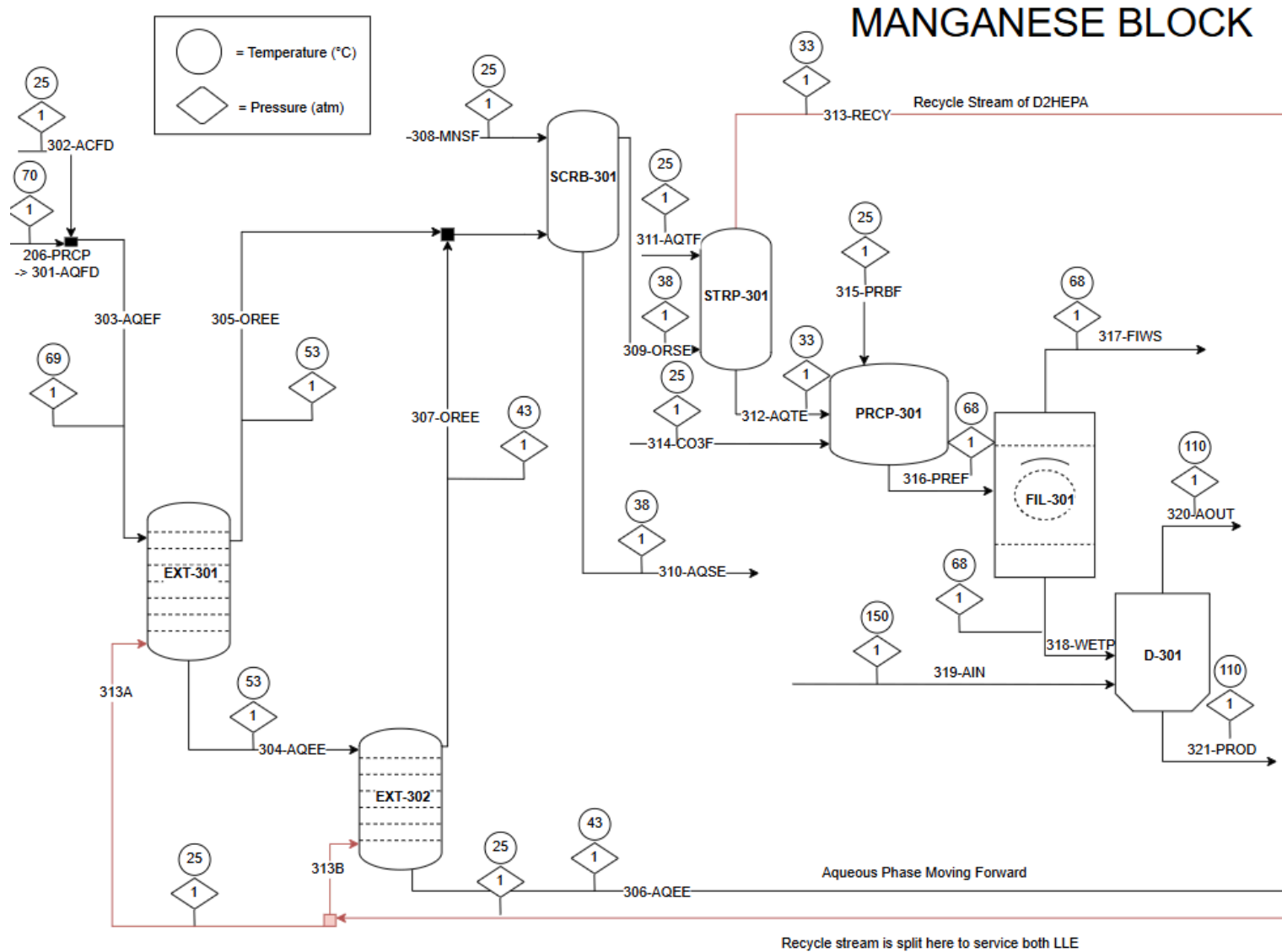


Figure 4.3-1

Manganese Extraction Block PFD

Table 4.3-1 Unit Operation Tag Legend	
Tag Number	Brief Description
EXT-301	Manganese Extraction Column
EXT-302	Manganese Extraction Column
SCRB-301	Manganese-Loaded Organic Scrubbing Column
STRP-301	Manganese-Loaded Organic Stripping Column
PRCP-301	Manganese Carbonate Precipitator
FIL-301	Manganese Carbonate RVDF
D-301	Manganese Carbonate Dryer

Table 4.3-2 Stream Label Legend	
Stream Number	Stream Description
301-AQFD	Aqueous Metals into Manganese Extraction Block
302-ACFD	H ₂ SO ₄ stream into EXT-301 feed stream
303-AQEF	Aqueous Metals stream into EXT-301
304-AQEE	Aqueous Metals stream into EXT-302
305-OREE	Loaded Organic D2EHPA stream leaving EXT-301
306-AQEE	Aqueous Metals stream leaving EXT-302
307-OREE	Loaded Organic D2EHPA stream leaving EXT-302
308-MNSF	Aqueous MnSO ₄ stream into SCRB-301
309-ORSE	Loaded Organic D2EHPA stream into STRP-301
310-AQSE	Aqueous Waste leaving SCRB-301
311-AQTF	H ₂ SO ₄ stream into STRP-301

Table 4.3-2 Stream Label Legend	
312-AQTE	Redissolved Aqueous Metals stream leaving STRP-301
313-RECY	Recycle D2HEPA stream leaving STRP-301
313A	Organic D2EHPA stream into EXT-301
313B	Organic D2EHPA stream into EXT-302
314-CO3F	Na ₂ CO ₃ stream into PRCP-301
315-PRBF	NaOH stream into PRCP-301
316-PREF	Aqueous stream into FIL-301
317-FIWS	Aqueous waste leaving FIL-301
318-WETP	Wet MnCO ₃ into D-301
319-AIN	Dry air into D-301
320-AOUT	Saturated air out of D-301
321-PROD	Final MnCO ₃ Product out of D-301

4.3.1 Final Design Description

The block begins by contacting 380,736 kg/hr of aqueous metals (301-AQFD/206-PRCP) through P-204 with 4,800 kg/hr of 2M H₂SO₄ (302-ACFD) using P-301 from TK-H2SO4 to bring the pH to 3. Additionally, this aids in converting MnOH⁺, generated by adding base in the impurity removal, back to Mn²⁺. The 385,536 kg/hr mixture (303-AQEF) is fed into the top of EXT-301 and contacted with 319,502.4 kg/hr of 0.5M D2EHPA in kerosene (313A) via P-311 fed in through the bottom. The differences in density allow for them to flow countercurrently where sufficient mixing and phase separation occurs. All unit operations run adiabatically at constant pressure as the process is insensitive to temperature. The aqueous product (304-AQEE) then flows to an identical RDC column (EXT-302) via P-302 where it undergoes the same

process and is contacted with pure 0.5M D2EHPA in kerosene (313B) using P-312. The remaining 383,745 kg/hr of aqueous product (306-AQEE) is sent to the cobalt block using P-303.

Both loaded organic products coming from EXT-301 (305-OREE) and EXT-302 (307-OREE) are mixed and sent to SCRB-301 using P-304 and P-305 to remove co-extracted cobalt. 640,792 kg/hr of loaded-organic are contacted with 87,454 kg/hr of a 4 g/L Mn solution ($\text{MnSO}_4 \cdot \text{H}_2\text{O}$) (308-MNSF) in SCRB-301 using P-308. The 87,463 kg/hr aqueous stream leaving SCRB-301 (310-AQSE) is waste and the remaining 640,786 kg/hr organic stream (309-ORSE) is sent to STRP-301 using P-307.

To strip all metals out of the organic and into the aqueous, 309-ORSE is contacted with 107,856 kg/hr of 1M H_2SO_4 (311-AQTF) in STRP-301 using P-309 from TK- H_2SO_4 . The aqueous solution (312-AQTE) is then sent to PRCP-301 using P-310 to be precipitated. The organic phase (313-RECY), now protonated by the H_2SO_4 stream, is recycled and split into 313A and 313B to be used in extraction.

The precipitate (312-AQTE) goes into PRCP-301 using P-310 along with 3,218 kg/hr of Na_2CO_3 (314-CO3F) from TK- Na_2CO_3 using BE-302 and 5,142 kg/hr of NaOH (315-PRBF) from TK-NAOH using BE-301. PRCP-301 operates with a residence time of 3 hours with a half hour for both loading and unloading. No cooling jacket is used on this reactor since the temperature does not affect the future unit operations within this process block. The batch schedule in Table 4.3.1-1 was used to achieve pseudo-continuous flow. This results in a total of 16 standard reactors (8 groups of 2). The resulting precipitate (316-PREF), approximately 117,988 kg/hr, is pumped into FIL-301 using P-313.

Table 4.3.1-1 PRCP-301 Reactor Schedule									
	Group	1	2	3	4	5	6	7	8
Time									
0:00	Loading								
0:30	Reacting								
1:00	Reacting								
1:30	Reacting								
2:00	Reacting								
2:30	Reacting								
3:00	Reacting								
3:30	Unloading								
4:00	Loading								

FIL-301 separates the formed product from the aqueous waste. Leaving FIL-301 is 5,454 kg/hr MnCO₃ (318-WETP) and the waste aqueous stream (317-FIWS) of 112,535 kg/hr. This unit operation is carried out through 4 RVDFs. The aqueous stream is sent to waste management while the wet solid is sent to D-301 using CB-301.

D-301 takes the MnCO₃ solid and uses hot dry air (319-AIN), approximately 23,400 kg/hr at 150 °C to evaporate and remove remaining liquid. This saturated air (320-AOUT) comes out at 110 °C with nearly 100% of the aqueous phase removed. The final product of this block (321-PROD) is 3,943 kg/hr which is moved using CB-302 into TK-COPD. This stream is not 100% pure MnCO₃ due to impurities including Ca, Al, Fe, and Cu. Additionally, Section 4.3.2 details the material balances around each unit operation discussed above.

4.3.2 Material Balances

Table 4.3.2-1 Manganese Extraction Block: EXT-301					
Name	302-ACFD	303-AQEF	313A	304-AQEE	305-OREE
Flowrate	kg/hr	kg/hr	kg/hr	kg/hr	kg/hr
Total	4800	385,536.5	319,502.4	384,166.3	320,872.4
O ₂	0	3.3	0	3.3	0
H ₂ O	3874.9	299,265.3	0	299,183.7	0
HF	0	0.2	0	0.7	0
F ⁻	0	20.0	0	19.5	0
SO ₄ ²⁻	85.5	57,166.4	0	52,447.0	0
HSO ⁴⁺	673.7	1,450.3	0	6,219.1	0
H ₃ O ⁺	165.9	13.2	0	99.8	0
Na ⁺	0	20,924.6	0	20,924.6	0
Co ²⁺	0	1,681.7	0	1,597.6	0
Mn ²⁺	0	1,696.8	0	509.0	0
Cu ²⁺	0	1.7	0	0.5	0
Li ⁺	0	555.1	0	555.1	0
Ca ²⁺	0	151.3	0	0	0
Ni ²⁺	0	2,606.3	0	2606.3	0
C12	0	0	281,162.1	0	281,162.1
D2EHPA	0	0	38,340.3	0	21,032.1
D2EHP-Mn	0	0	0	0	15,086.1
D2EHP-Co	0	0	0	0	1,001.3
D2EHP-Cu	0	0	0	0	13.1
D2EHP-Ca	0	0	0	0	2,577.7

Table 4.3.2-2 Manganese Extraction Block: EXT-302			
Name	313B	306-AQEE	307-OREE
Flowrate	kg/hr	kg/hr	kg/hr
Total	319,502.4	383,745.5	319,923.1
O ₂	0	3.3	0
H ₂ O	0	299,125.0	0
HF	0	0.74	0
F ⁻	0	19.4	0
SO ₄ ²⁻	0	51,252.4	0
HSO ⁴⁺	0	7,426.3	0
H ₃ O ⁺	0	161.7	0
Na ⁺	0	20,924.6	0
Co ²⁺	0	1,517.7	0
Mn ²⁺	0	152.7	0
Cu ²⁺	0	0.2	0
Li ⁺	0	555.1	0
Ni ²⁺	0	2,606.3	0
C12	281,162.1	0	281,162.1
D2EHPA	38,340.3	0	33,280.1
D2EHP-Mn	0	0	4,525.8
D2EHP-Co	0	0	951.2
D2EHP-Cu	0	0	3.9

Table 4.3.2-3 Manganese Extraction Block: SCRB-301			
Name	308-MNSF	309-ORSE	310-AQSE
Flowrate	kg/hr	kg/hr	kg/hr
Total	87,454.5	640,786.6	87,463.3
H ₂ O	86,596.3	0	86,596.3
SO ₄ ²⁻	546.0	0	546.0
Co ²⁺	0	0	131.2
Mn ²⁺	312.2	0	189.9
C12	0	562,324.2	0
D2EHPA	0	54,312.2	0
D2EHP-Mn	0	21,165.0	0
D2EHP-Co	0	390.5	0
D2EHP-Cu	0	17.0	0
D2EHP-Ca	0	2577.7	0

Table 4.3.2-4 Manganese Extraction Block: STRP-301		
Name	311-AQTF	312-AQTE
Flowrate	kg/hr	kg/hr
Total	107,846.8	109,628.7
H ₂ O	98,140.6	97,187.8
H ₂ SO ₄	9,706.2	0
SO ₄ ²⁻	0	2,237.8
HSO ⁴⁻	0	7,345.2
H ₃ O ⁺	0	1,006.0
Co ²⁺	0	32.8
Mn ²⁺	0	1,666.4
Cu ²⁺	0	1.5
Ca ²⁺	0	151.3

Table 4.3.2-5 Manganese Extraction Block: PRCP-301

Name	312-AQTE	314-CO3F	315-PRBF	316-PREF
Flowrate	kg/hr	kg/hr	kg/hr	kg/hr
Total	109,628.7	3,217.8	5,142.0	117,988.5
H ₂ O	97,186.8	0	0	100,387.0
NaOH	0	0	5,142.0	0
Na ₂ CO ₃ (s)	0	3,217.8	0	0
CaSO ₄ ²⁻	0	0	0	327.2
Cu(OH) ₂ (s)	0	0	0	2.4
MnCO ₃ (s)	0	0	0	3,484.2
OH ⁺	0	0	0	0.1
CO ₃ ²⁻	0	0	0	0.2
HCO ₃ ⁻	0	0	0	2.7
SO ₄ ²⁻	2,242.9	0	0	9,324.2
HSO ₄ ⁻	7,340.0	0	0	0
H ₃ O ⁺	1,007.0	0	0	0
Na ⁺	0	0	0	4,351.4
Co ²⁺	32.8	0	0	32.8
Mn ²⁺	1,666.3	0	0	1.1
Cu ²⁺	1.6	0	0	0
Ca ²⁺	151.3	0	0	75.2

Table 4.3.2-6 Manganese Extraction Block: FIL-301			
Name	316-PREF	317-FIWS	318-WETP
Flowrate	kg/hr	kg/hr	kg/hr
Total	117,988.5	112,534.7	5,453.8
H ₂ O	100,387.0	98,945.1	1,441.9
CaSO ₄ ²⁻	327.2	0	327.3
Cu(OH) ₂ (s)	2.4	0	2.4
MnCO ₃ (s)	3,484.2	0	3,484.2
OH ⁺	0.1	0.1	0
CO ₃ ²⁻	0.2	0.2	0
HCO ₃ ⁻	2.7	2.7	0
SO ₄ ²⁻	9,324.2	9,190.3	133.9
Na ⁺	4,351.4	4,288.9	62.5
Co ²⁺	32.8	32.3	0.5
Mn ²⁺	1.1	1.1	0
Ca ²⁺	75.2	74.1	1.1

Table 4.3.2-7 Manganese Extraction Block: D-301				
Name	318-WETP	319-AIN	320-AOUT	321-PROD
Flowrate	kg/hr	kg/hr	kg/hr	kg/hr
Total	5,453.8	93,600.0	95,110.4	3943.4
O ₂	0	19,656.0	19,656.0	0
H ₂ O	1,441.9	0	1,510.4	0
CaSO ₄ ²⁻	327.3	0	0	0
Cu(OH) ₂ (s)	2.4	0	0	2.4
MnCO ₃ (s)	3,484.2	0	0	3484.2
Na ₂ SO ₄ (s)	0	0	0	193.1
CaSO ₄ (s)	0	0	0	262.43
SO ₄ ²⁻	133.9	0	0	0
Na ⁺	62.5	0	0	0
Co ²⁺	0.5	0	0	0
Ca ²⁺	1.1	0	0	0
N ₂	0	73,944.0	73,944.0	0

4.4 Cobalt Extraction Block

This section details the process of extracting, purifying, and precipitating the Cobalt out of the total aqueous metals stream. This includes all unit operations, parallel streams, batch schedules, and material balances. To process the total mass flow per hour, this block runs with 8 parallel streams. Figure 4.4-1 displays a detailed overview of the Cobalt Extraction Block. Table 4.4-1 and Table 4.4-2 supplements Figure 4.4-1 by providing the stream numbers, tag numbers, and a brief description. Note that pumps are not included in Figure 4.4-1. Note that there is also a heat exchanger not pictured in Figure 4.4-1 that exists on stream 407-AQEE/501-EFF.

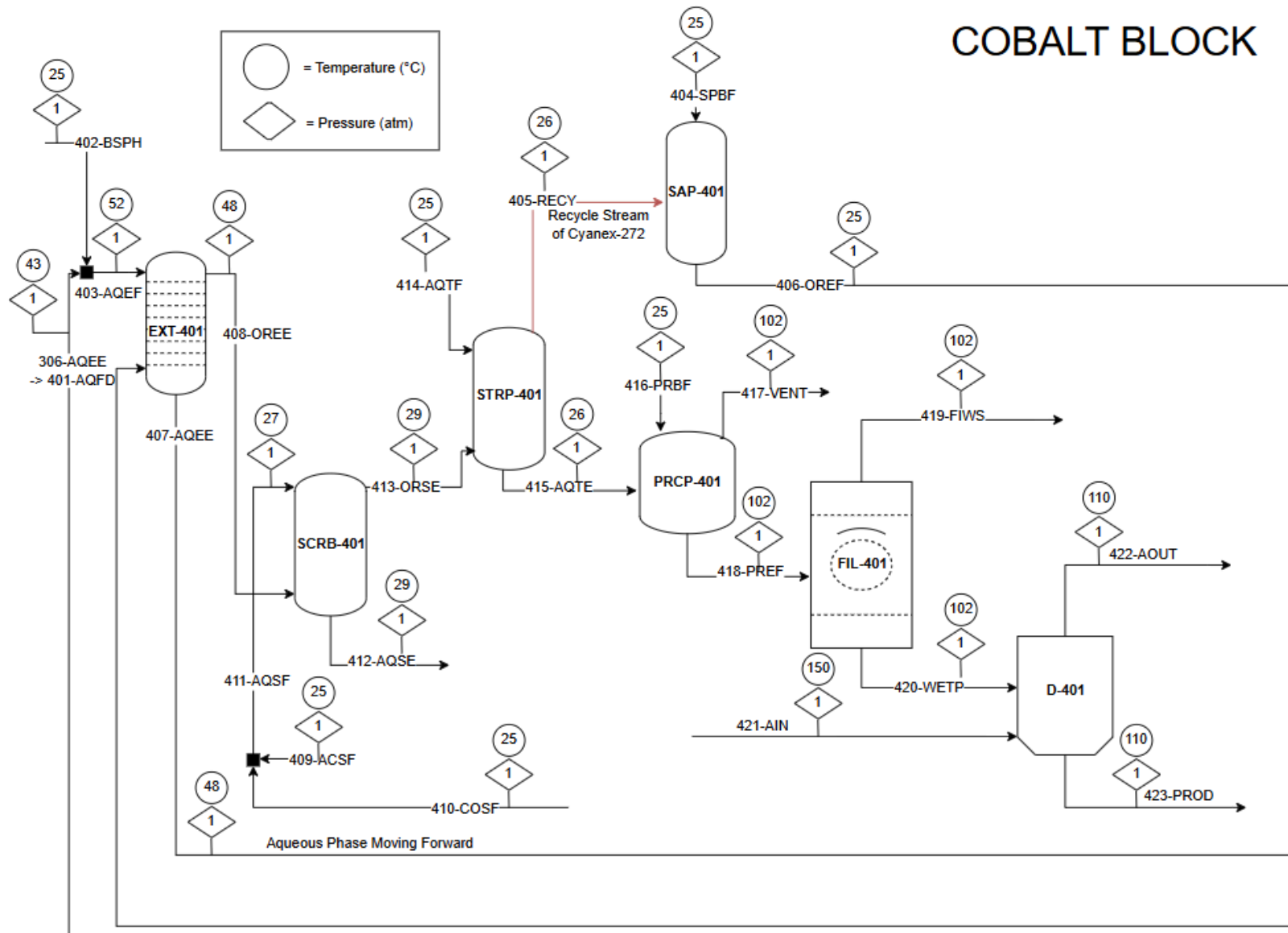


Figure 4.4-1

Cobalt Extraction Block PFD

Table 4.4-1 Unit Operation Tag Legend	
Tag Number	Brief Description
EXT-401	Cobalt Extraction Column
SCRB-401	Cobalt-Loaded Organic Scrubbing Column
STRP-401	Cobalt-Loaded Organic Stripping Column
SAP-401	Cobalt Saponification Reactor
PRCP-401	Cobalt Hydroxide Precipitator
FIL-401	Cobalt Hydroxide RVDF
D-401	Cobalt Hydroxide Dryer
HE-401	Aqueous Stream Shell-and-Tube Heat Exchanger

Table 4.4-2 Stream Label Legend	
Stream Number	Stream Description
401-AQFD	Aqueous Feed into EXT-401
402-BSPH	NaOH Pellets Mixing with 401-AQFD for pH Balance
403-AQEF	Aqueous Feed to EXT-401, Combined 401-AQFD and 402-BSPH
404-SPBF	Base Feed to SAP-401
405-ORSF	Organic Feed to SAP-401, Recycle Organic from STRP-401
406-OREF	Organic Effluent from SAP-401, Feed to EXT-401
407-AQEE	Aqueous EXT-401 Effluent, Sent Forward to Nickel Extraction Block
408-OREE	Organic EXT-401 Effluent, Sent to SCRB-401
409-ACSF	Anhydrous H ₂ SO ₄ Feed to Mixing Point Before SCRB-401
410-COSF	Aqueous Co(OH) ₂ Feed to Mixing Point Before SCRB-401

Table 4.4-2 Stream Label Legend	
411-AQSF	Aqueous Feed of Cobalt Sulfate to SCRB-401
412-AQSE	Aqueous SCRB-401 Effluent, Waste
413-ORSE	Organic SCRB-401 Effluent, Sent to STRP-401
414-AQTF	Aqueous H ₂ SO ₄ Feed to STRP-401
415-AQTE	Aqueous STRP-401 Effluent, Sent to PRCP-401
416-PRBF	Base Feed to PRCP-401
417-VENT	Steam Vent from PRCP-401
418-PREF	PRCP-401 Effluent, Sent to FIL-401
419-FIWS	FIL-401 Waste Stream
420-WETP	Wet Co(OH) ₂ into D-401
421-AIN	Dry Air into D-401
422-AOUT	Saturated Air out of D-401
423-PROD	Final Co(OH) ₂ Product out of D-401

4.4.1 Final Design Description

The cobalt extraction block begins with 383,746 kg/hr of aqueous feed (401-AQFD/306-AQEE) coming in from the manganese extraction block using P-303. This stream is combined with NaOH pellets (402-BSPH) dissolved in water from TK-NAOH, at 3,397 kg/hr such that the equilibrium pH in the EXT-401 columns reaches 5. Streams 401-AQFD and 402-BSFD combine to form the aqueous feed 403-AQEF (387,143 kg/hr) to the top of the EXT-401 extraction columns (of which there are 40 in parallel) using P-401.

The extractant Cyanex-272 (20 vol% in kerosene) is fed to the SAP-401 (of which there are 8) via stream 405-RECY (249,212 kg/hr) using P-409. SAP-401 combines the Cyanex-272

with aqueous NaOH from 404-SPBF (6,423 kg/hr) using P-411, to reach 40% saponification of Cyanex-272. The effluent stream from SAP-401 is 406-OREF (255,635 kg/hr), which feeds into the bottom of EXT-401 using P-402.

Two phases exit each EXT-401 extractor, totaling 391,440 kg/hr in the aqueous stream 407-AQEE (which moves on to the nickel block as feed) using P-403, and 251,337 kg/hr in the organic stream 408-OREE, which goes to SCRB-401 (of which there are 40) using P-404. 407-AQEE passes through HE-401 to reduce its temperature from 48°C to 35°C before it is sent to the Nickel Extraction block. 408-OREE contains the metals Ni, Co, and Mn extracted in the form of their respective Cyanex-272 complexes. The aqueous feed to SCRB-401 is stream 411-AQSF (344,792 kg/hr), pumped using P-405 and P-410, which is the product of mixing aqueous $\text{Co}(\text{OH})_2$ from 410-COSF (343,652 kg/hr) with anhydrous H_2SO_4 from 409-ACSF (1,140 kg/hr) to form 2 g/L Co^{2+} scrubbing solution. In SCRB-401, 99% of the nickel is scrubbed out, which leaves as a NiSO_4 waste stream in 412-AQSE (344,791 kg/hr) pumped using P-406. The remaining organic phase, 413-ORSE (251,338 kg/hr) feeds to STRP-401 (of which there are 40) through P-407. This stream is contacted with 403,793 kg/hr of 2M H_2SO_4 (414-AQTF) using P-408, causing the complete regeneration of Cyanex-272 (which is sent back to SAP-401 in 405-RECY) and also causing all of the remaining cobalt, manganese, and nickel ions to move into 415-AQTE (405,918 kg/hr). This aqueous effluent feeds into the precipitation reactors, PRCP-401 using P-412, where it mixes with 416-PRBF (56,347 kg/hr of solid NaOH pellets) added in using BE-401 from TK-NAOH.

NaOH is added until the total pH of the precipitator is raised to 11. The PRCP-401 reactors operate with a 1 hour residence time with a half hour for loading and unloading. No cooling jackets were used on this reactor since solubility is not temperature-dependent. The batch

schedule visualized in Table 4.4.1-1 below was used to achieve pseudo-continuous flow. This results in a total of 16 standard reactors (4 groups of 4). Out of PRCP-401 is a pure steam vent stream, 417-VENT (11,353 kg/hr), and a resulting precipitate (401-PREF), approximately 450,912 kg/hr is sent to FIL-401 using P-413.

Table 4.4.1-1 PRCP-401 Reactor Schedule					
	Group	1	2	3	4
Time					
0:00		Loading			
0:30		Reacting			
1:00		Reacting			
1:30		Unloading			
2:00		Loading			

FIL-401 washes the precipitate so that the wet solid (420-WETP) can be separated from the aqueous waste stream 419-FIWS (447,463 kg/hr). The wet solid is moved using CB-401 through a solids washer, which has not been designed and is outside the scope of this project; the solids washer would use pure water with some aqueous $\text{Co}(\text{OH})_2$ to dissolve the precipitated Na_2SO_4 without dissolving the $\text{Co}(\text{OH})_2$ product (this residual Na_2SO_4 is reported in the final product stream 423-PROD but is assumed to come out as a completely separate product). The washed, wet product is moved out of the solids washer by CB-401 to D-401. 46,400 kg/hr of hot air at 150°C (421-AIN) is blown into D-401 using BLW-401 to remove 99.99% of the water, coming out in 422-AOUT (47,207 kg/hr). The final dried solid product stream out of D-401 (423-PROD), 2,420 kg/hr of 99.6 wt% $\text{Co}(\text{OH})_2$ (neglecting any amount of Na_2SO_4 , since that is assumed to be removed in the theoretical solids washer), is moved with CB-402 into storage tank TK-COPD. Some of the wet $\text{Co}(\text{OH})_2$ produced is diverted (1080 kg/hr) to the scrubbing column in stream 410-COSF. An unknown amount of $\text{Co}(\text{OH})_2$ produced would need to be diverted to

the theoretical solids washer, though this is currently outside the scope of this project.

Subtracting only the product diverted to the scrubbing column, a net 1,339 kg/hr of $\text{Co}(\text{OH})_2$ is produced.

4.4.2 Material Balances

The material balances presented in this section summarize the significant components in the streams around every process block catalogued in Table 4.4-1. For complete stream tables listing every component in every stream, see Appendix B.

Table 4.4.2-1 Cobalt Extraction Block: EXT-401				
Name	403-AQEF	406-OREF	407-AQEE	408-OREE
Flowrate	kg/hr	kg/hr	kg/hr	kg/hr
Total	387,143	255,635	391,440	251,337
O ₂	3.3	0	3.3	0
H ₂ O	300,808	4,658	305,466	0
NaOH	0	0.1	0	0
F ⁻	20.1	0	20.1	0
SO ₄ ²⁻	58,593	0	58,593	0
HSO ₄ ⁻	9.0	0	8.8	0
H ₃ O ⁺	0.1	0	0.1	0
Na ⁺	22,877	0	24,197	0
Co ²⁺	1,520	0	106.0	0
Mn ²⁺	153	0	1.53	0
Cu ²⁺	0.2	0	0.2	0
Li ⁺	555.1	0	555.1	0
Ni ²⁺	2,610	0	2,490	0
C ₁₂	0	190,918	0	190,918
Cyanex	0	34,976	0	34,976
Cyanex-Na	0	25,082	0	7,149
Cyanex-Co	0	0	0	15,275
Cyanex-Ni	0	0	0	1,274
Cyanex-Mn	0	0	0	1,744

Table 4.4.2-2 Cobalt Extraction Block: SAP-401			
Name	404-SPBF	405-RECY	406-OREF
Flowrate	kg/hr	kg/hr	kg/hr
Total	6,423	249,212	255,635
H ₂ O	3,211	0	4,658
NAOH	3,211	0	0.1
C ₁₂	0	190,918	190,918
Cyanex	0	58,294	34,976
Cyanex-Na	0	0	25,082

Table 4.4.2-3 Cobalt Extraction Block: SCRB-401				
Name	408-OREE	411-AQSF	412-AQSE	413-ORSE
Flowrate	kg/hr	kg/hr	kg/hr	kg/hr
Total	251,337	344,792	344,791	251,338
H ₂ O	0	342,990	342,990	0
SO ₄ ²⁻	0	1,117	1,117	0
Co ²⁺	0	685	569	0
Ni ²⁺	0	0	116	0
C ₁₂	190,918	0	0	190,918
Cyanex	34,976	0	0	34,976
Cyanex-Na	7,149	0	0	7,149
Cyanex-Co	15,275	0	0	16,537
Cyanex-Ni	1,274	0	0	12.7
Cyanex-Mn	1,744	0	0	1,744

Table 4.4.2-4 Cobalt Extraction Block: STRP-401				
Name	413-ORSE	414-AQTF	405-RECY	415-AQTE
Flowrate	kg/hr	kg/hr	kg/hr	kg/hr
Total	251,338	403,793	249,212	405,918
H ₂ O	0	337,408	0	325,310
H ₂ SO ₄	0	66,400	0	0
SO ₄ ²⁻	0	0	0	7,210
HSO ₄ ⁻	0	0	0	58,400
H ₃ O ⁺	0	0	0	12,800
Na ⁺	0	0	0	526.0
Co ²⁺	0	0	0	1,528
Mn ²⁺	0	0	0	151.0
Ni ²⁺	0	0	0	1.2
C ₁₂	190,918	0	190,918	0
Cyanex	34,976	0	58,294	0
Cyanex-Na	7,149	0	0	0
Cyanex-Co	16,537	0	0	0
Cyanex-Ni	12.70	0	0	0
Cyanex-Mn	1,744	0	0	0

Table 4.4.2-5 Cobalt Extraction Block: PRCP-401				
Name	415-AQTE	416-PRBF	417-VENT	418-PREF
Flowrate	kg/hr	kg/hr	kg/hr	kg/hr
Total	405,918	56,347	11,353	450,912
H ₂ O	325,310	0	11,353	348,995
NaOH	0	56,347	0	0
Co(OH) ₂	0	0	0	2,410
Ni(OH) ₂	0	0	0	1.85
OH ⁻	0	0	0	1,415
SO ₄ ²⁻	7,205	0	0	65,021
HSO ₄ ⁻	58,422	0	0	trace
H ₃ O ⁺	12,775	0	0	trace
Na ⁺	526.1	0	0	32,913
Co ²⁺	1,528	0	0	trace
Mn ²⁺	151.2	0	0	135.0
MnOH ⁺	trace	0	0	21.23
Ni ²⁺	1.17	0	0	trace

Table 4.4.2-6 Cobalt Extraction Block: FIL-401			
Name	418-PREF	419-FIWS	420-WETP
Flowrate	kg/hr	kg/hr	kg/hr
Total	450,912	447,463	3,449
H ₂ O	348,995	348,188	807.0
Co(OH) ₂ (s)	2,410	0	2,410
Ni(OH) ₂ (s)	1.85	0	1.85
OH ⁻	1,415	1,411	3.27
SO ₄ ²⁻	65,021	64,870	150.4
Na ⁺	32,913	32,836	76.11
Mn ²⁺	135.0	134.7	0
MnOH ⁺	21.23	21.18	0

Table 4.4.2-7 Cobalt Extraction Block: D-401				
Name	420-WETP	421-AIN	422-AOUT	423-PROD
Flowrate	kg/hr	kg/hr	kg/hr	kg/hr
Total	3,449	46,400	47,207	2,642
O ₂	0	9,744	9,744	0
H ₂ O	807	0	806.9	0.1
NaOH	0	0	0	6.5
Na ₂ SO ₄ (S)	0	0	0	222.3
Co(OH) ₂ (s)	2,410	0	0	2,410
Ni(OH) ₂ (s)	1.9	0	0	1.9
OH ⁻	3.3	0	0	0.4
SO ₄ ²⁻	150.0	0	0	0
Na ⁺	76.1	0	0	0.4
Mn ²⁺	0.3	0	0	0
MnOH ⁺ (s)	0	0	0	0.5
N ₂	0	36,656	36,656	0

4.5 Nickel Extraction Block

This section details the process of extracting, purifying, and precipitating the Nickel out of the total aqueous metals stream. This includes the necessary unit operations, parallel streams, batch schedules, and material balances. In order to handle the total mass flow per hour, this process block runs with 12 parallel streams. Figure 4.5-1 displays a detailed overview of the Nickel Extraction Block. Table 4.5-1 and Table 4.5-2 supplements Figure 4.5-1 by providing the stream numbers, tag numbers, and a brief description.

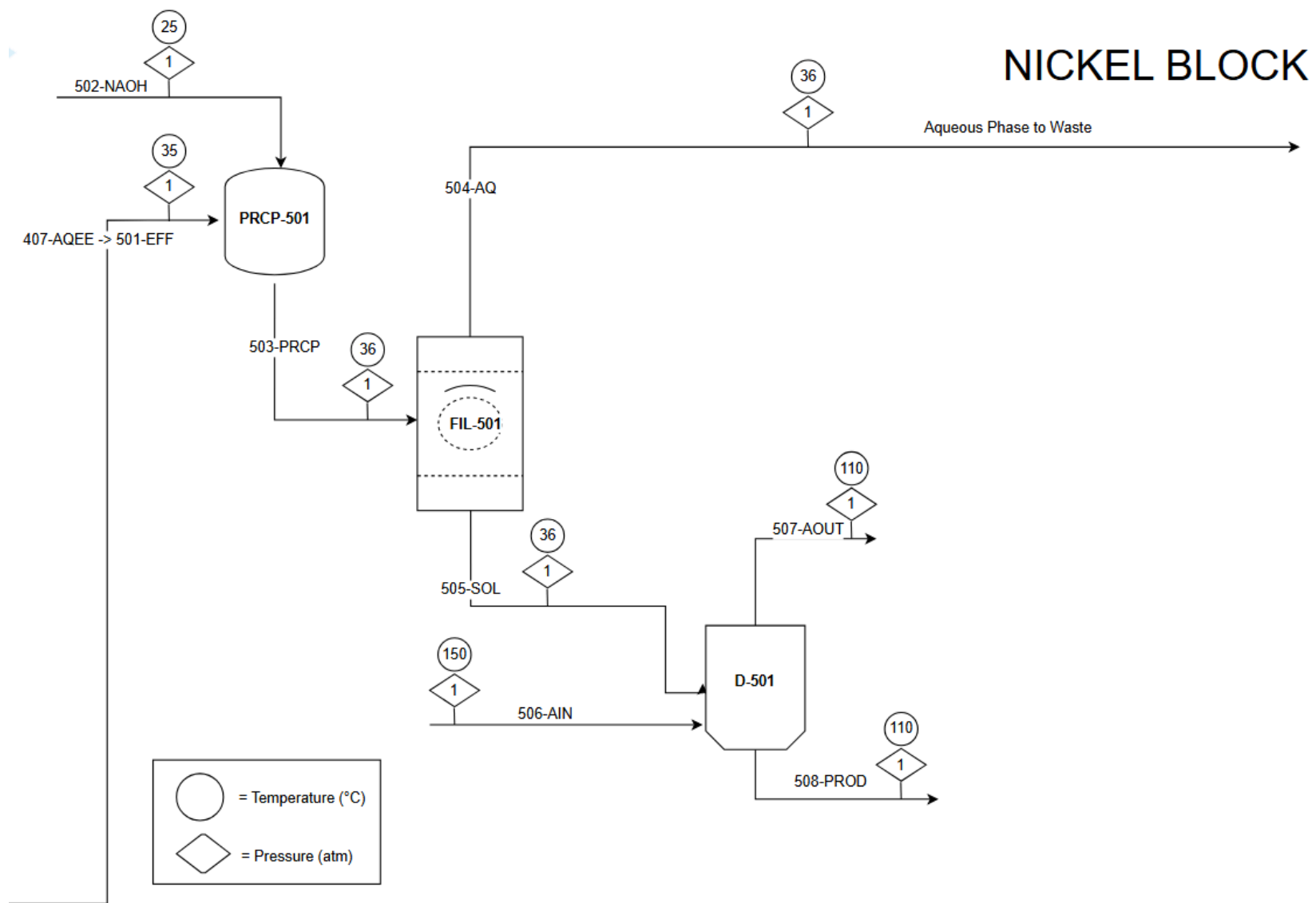


Figure 4.5-1

Nickel Extraction Block PFD

Table 4.5-1 Unit Operation Tag Legend	
Tag Number	Brief Description
PRCP-501	Nickel Hydroxide Precipitator
FIL-501	Nickel Hydroxide RVDF
D-501	Nickel Hydroxide Dryer

Table 4.5-2 Stream Label Legend	
Stream Number	Stream Description
501-EFF	Effluent into Nickel Extraction
502-NAOH	NaOH stream into PRCP-501
503-PRCP	Ni(OH) ₂ stream leaving PRCP-501
504-AQ	Aqueous waste leaving FIL-501
505-SOL	Wet Ni(OH) ₂ into PRCP-502
506-AIN	Dry air into D-501
507-AOUT	Saturated air out of D-501
508-PROD	Final Ni(OH) ₂ Product out of D-501

4.5.1 Final Design Description

The process block begins with 391,440 kg/hr of effluent (501-EFF) using P-403 into PRCP-501 with 8,518 kg/hr of NaOH (502-NAOH) from TK-NAOH using BE-501. 12 parallel streams are used to achieve this total flow rate. NaOH is added until the total pH of the precipitator is raised to 10 so that precipitation of the nickel ions into Ni(OH)₂ is favored.

PRCP-501 operates with a residence time of 4 hours with a half hour both for loading and unloading. No cooling jackets were used on this reactor since heat generation is negligible. The batch schedule in Table 4.5.1-1 was used to achieve pseudo-continuous flow. This results in a total of 60 standard reactors (10 groups of 6). The resulting precipitate (503-PRCP), approximately 399,958 kg/hr, is sent to FIL-501 using P-501.

Table 4.5.1-1 PRCP-501 Reactor Schedule											
	Group	1	2	3	4	5	6	7	8	9	10
Time											
0:00		Loading									
0:30		Reacting									
1:00		Reacting									
1:30		Reacting									
2:00		Reacting									
2:30		Reacting									
3:00		Reacting									
3:30		Reacting									
4:00		Reacting									
4:30		Unloading									
5:00		Loading									

FIL-501 washes the precipitate so that the wet solid (505-SOL) can be separated from the remaining aqueous solution (504-AQ). The wet solid is moved using CB-501 to D-501. The aqueous phase is sent to lithium extraction through P-502. This unit operation is carried out through 12 RVDFs.

The Ni(OH)₂ solid (505-SOL), at 4,297 kg/hr, is sent to D-501. D-501 takes the Ni(OH)₂ solid and uses hot dry air (506-AIN), approximately 7,200 kg/hr at 150 °C to evaporate and remove the remaining liquid. This saturated air (507-AOUT) comes out at 110 °C with nearly 100% of the aqueous phase removed. The final product of this block (508-PROD) is 4,297 kg/hr

which is moved using CB-502 into TK-NIPD. This stream is not 100% Ni(OH)₂ due to impurities including Na (Section 7.2.5). Additionally, Section 4.5.2 details the material balances around each unit operation discussed above.

4.5.2 Material Balances

Table 4.5.2-1 Nickel Extraction Block: PRCP-501			
Name	501-EFF	502-NAOH	503-PRCP
Flowrate	kg/hr	kg/hr	kg/hr
Total	391,440.4	3,408.6	394,849.0
O ₂	3.3	0	3.3
H ₂ O	305,466.0	0	305,467.9
NaOH	0	3,408.6	0
Cu(OH) ₂ (s)	0	0	0.2
Ni(OH) ₂ (s)	0	0	3,931.7
OH ⁻	0	0	5.0
F ⁻	20.1	0	20.1
SO ₄ ²⁻	58,593.2	0	58,601.6
HSO ₄ ⁻	8.5	0	0
H ₃ O ⁺	0.2	0	0
Na ⁺	24,197.0	0	26,156.2
Co ²⁺	106.2	0	106.2
Mn ²⁺	1.5	0	1.5
Cu ²⁺	0.2	0	0
Li ⁺	555.1	0	555.1
Ni ²⁺	2,489.1	0	0

Table 4.5.2-2 Nickel Extraction Block: FIL-501			
Name	503-PRCP	504-AQ	505-SOL
Flowrate	kg/hr	kg/hr	kg/hr
Total	394,849.0	389,226.4	5,622.6
O ₂	3.3	3.3	0
H ₂ O	305,467.9	304,146.8	1,321.2
Cu(OH) ₂ (s)	0.2	0	0.2
Ni(OH) ₂ (s)	3,931.7	0	3,931.7
OH ⁻	5.0	5.0	0
F ⁻	20.1	20.1	0.1
SO ₄ ²⁻	58,601.6	58,348.2	253.5
Na ⁺	26,156.2	26,043.0	113.1
Co ²⁺	106.2	105.8	0.5
Mn ²⁺	1.5	1.5	0
Li ⁺	555.1	552.7	2.4

Table 4.5.2-3 Nickel Extraction Block: D-501				
Name	505-SOL	506-AIN	507-AOUT	508-PROD
Flowrate	kg/hr	kg/hr	kg/hr	kg/hr
Total	5,622.6	86,400.0	87,721.2	4,301.5
O ₂	0.0	18,144.0	18144.0	0
H ₂ O	1,321.2	0	1,321.1	0
Na ₂ SO ₄ (s)	0	0	0	349.5
LiF(s)	0	0	0	0.1
Li ₂ SO ₄ (s)	0	0	0	18.7
Cu(OH) ₂ (s)	0.2	0	0	0.2
Ni(OH) ₂ (s)	3,931.7	0	0	3,931.7
F ⁻	0.1	0	0	0
SO ₄ ²⁻	253.5	0	0	0.7
Na ⁺	113.1	0	0	0
Co ²⁺	0.5	0	0	0.5
Li ⁺	2.4	0	0	0
N ₂	0	68,256.0	68,256.0	0

4.6 Lithium Extraction Block

Due to the large presence of sodium ions in the aqueous metals stream leaving the nickel block (507-AOUT), lithium carbonate (Li₂CO₃) can not be successfully isolated. As such the aqueous metals stream leaving the nickel block will be treated as hazardous waste (507-AOUT). Section 5.2.3 discusses how the waste is treated and how that affects the economics.

Section 5: Economics

5.1 Capital Costs

This section covers capital costs of all plant equipment. The majority of capital costs are estimated from the following equation obtained from Towler and Sinnott.

$$C_e = a + bS^n$$

Equation 5.1.-1 Purchased Equipment Cost

C_e ,	cost	USD
S ,	size parameter	
a, b ,	constants	m^2/s

Here, S is a sizing parameter, the units of which depend on the equipment used.

Table 5.1-1 Sizing Parameters of Various Plant Equipment	
Equipment Piece	Sizing Parameter S
Exchangers	area, m^2
Rotary Vacuum Drum Filters	area, m^2
Pumps	flow, L/s
Reactors/precipitators	volume, m^3
Tanks	capacity, m^3
Blowers	driver power, kW
Conveyors	length, m
Dryers	area, m^2
Pressure Vessels	shell mass, kg
Packings	m^3
Trays	diameter, m

Equipment cost will vary depending on the materials of construction. Unless specified otherwise, Equation 5.1.-1 assumes carbon steel as the base material of construction for capital cost estimation. Although capital costs of different materials will scale differently than carbon steel, they can be reasonably approximated by multiplying through a cost factor f_m . After accounting for inflation using the Chemical Engineering Plant Cost Index (CEPCI), a complete equation for capital cost estimation is obtained.

$$C = f_m C_e \left(\frac{CEPCI_c}{CEPCI_L} \right)$$

Equation 5.1.-2 Purchased Equipment Cost Revised

C , final cost USD
 f_m , cost factor
 $CEPCI_c$, current CEPCI (800)
 $CEPCI_L$, listed CEPCI (478.6)

For complex equipment such as rotary disk contactors, gas scrubbers, and packed bed reactors, costs are estimated from a database created by Townsend and Faber.⁴⁸ The database draws from multiple sources, including Towler and Sinnott, *Rules of Thumbs in Engineering Practice* by Donald Woods⁴⁹, and *Product and Process Design Principles: Synthesis, Analysis and Evaluation* by Seider et al.⁵⁰ To adapt all sources to the database, the equation for capital cost estimation is slightly altered.

$$C_e = C_{min} \left(\frac{S}{S_{min}} \right)^n$$

Equation 5.1.-3 Purchased Equipment Cost for Columns and Packed Bed Reactors

C_{min} , cost of minimum equipment size USD
 S_{min} , minimum equipment size (Height (ft))(Diameter (ft))^{1.5}

Here, the values of C_{min} , S_{min} , and n are obtained from the sources mentioned above, and the final cost C is obtained from Equation 5.1-2. This adapted equation can lead to more variations in final cost estimates, therefore it is only used when direct access to the source is unavailable.

5.1.1 Leaching Block

The leaching block requires a variety of equipment and materials to dissolve the metal ions into the aqueous stream. The necessary equipment includes leaching reactors, rotary vacuum drum filters, pumps, cooling jackets, and bucket elevators. The capital costs presented in Table 5.1.1-1 are categorized based on each individual piece of equipment. It should be noted that cost estimates associated with PLEACH-101 and all future reactors include reactor bodies and cooling jackets.

Table 5.1.1-1 Breakdown of Capital Cost for Leaching Block			
Equipment Tag	Quantity	Cost Per Unit (USD)	Total Cost (USD)
PLEACH-101	36	\$1,676,741	\$60,362,680
GS-101	1	\$36,403	\$36,403
FIL-101	12	\$234,821	\$2,817,853
Impellers	36	\$27,437	\$987,744
Pumps	4	\$76,946	\$307,782
Bucket Elevators	6	\$47,599	\$285,595
		Total Cost	\$64,798,058

5.1.2 Impurity Removal Block

The capital costs presented in Table 5.1.2-1 are categorized based on each individual piece of equipment, which includes precipitation reactors, rotary drum vacuum filters, pumps, cooling jackets, and bucket elevators.. Although the geometry and mechanical design of PBR-201 are unknown, it is still important to approximate the costs associated with the equipment. As a rough estimation of PBR-201's capital costs, it is assumed that translation between mass throughput and mechanical design is similar to that of the columns used in manganese and cobalt extraction. The mass flow rate entering PBR-201 is approximately 60% of the mass flow rate entering manganese extraction. Again, it is a crude estimate, but this results in 15 packed bed reactors, the dimensions of which are 1 m in diameter and 12 m in height and are used for the cost estimation for PBR-201. The parameters used to estimate cost of the packed bed reactor are different from rotary disc contactors and are retrieved from the Townsend and Faber Capital Equipment Cost Database. In the database, the cost estimates associated with packed columns are adapted from *Rules of Thumbs in Engineering Practice* by Donald Woods.

Table 5.1.2-1 Breakdown of Capital Cost for Impurity Removal Block			
Equipment Tag	Quantity	Cost Per Unit (USD)	Total Cost (USD)
PRCP-201	84	\$1,676,741	\$140,846,254
FIL-201	12	\$284,228	\$3,410,733
PBR-201	15	\$314,267	\$4,714,004
Impellers	84	\$27,437	\$2,304,735
Pumps	6	\$38,473	\$230,837
Bucket Elevators	6	\$47,599	\$285,595
		Total Cost	\$151,792,159

5.1.3 Manganese Extraction Block

The capital costs presented in Table 5.1.3-1 are categorized based on each individual piece of equipment, which includes precipitation reactors, scrubbers, strippers, extraction columns, rotary drum vacuum filters, pumps, cooling jackets, bucket elevators, conveyor belts, and blowers. Townsend and Faber drew from Seider et al. to determine the sizing parameters surrounding rotary disc contactors. These parameters are used to estimate costs for extractors, scrubbers, and strippers.

Table 5.1.3-1 Breakdown of Capital Cost for Manganese Extraction Block			
Equipment Tag	Quantity	Cost Per Unit (USD)	Total Cost (USD)
EXT-301	24	\$16,190	\$388,566
EXT-302	24	\$16,190	\$388,566
SCRB-301	24	\$16,190	\$388,566
STRP-301	24	\$16,190	\$388,566
PRCP-301	20	\$435,953	\$8,719,054
FIL-301	4	\$286,589	\$1,146,355
D-301	4	\$52,206	\$208,825
Impellers	20	\$27,437	\$548,747
Pumps	26	\$33,591	\$873,354
Bucket Elevators	4	\$47,599	\$190,397
Conveyor Belts	2	\$95,766	\$191,532
Blowers	1	\$176,829	\$176,829
		Total Cost	\$13,609,358

5.1.4 Cobalt Extraction Block

The capital costs presented in Table 5.1.4-1 are categorized based on each individual piece of equipment, which includes precipitation reactors, scrubbers, strippers, extraction columns, saponification reactors, rotary drum vacuum filters, pumps, cooling jackets, bucket elevators, conveyor belts, and blowers.

Table 5.1.4-1 Breakdown of Capital Cost for Cobalt Extraction Block			
Equipment Tag	Quantity	Cost Per Unit (USD)	Total Cost (USD)
EXT-401	40	\$16,190	\$647,611
SCRB-401	40	\$16,190	\$647,611
STRP-401	40	\$16,190	\$647,611
SAP-401	8	\$435,953	\$3,487,622
PRCP-401	16	\$435,953	\$6,975,243
FIL-401	8	\$261,519	\$2,092,153
D-401	8	\$14,766	\$118,131
HE-401	8	\$29,836	\$238,691
Impellers	24	\$27,437	\$658,496
Pumps	28	\$35,232	\$986,489
Bucket Elevators	8	\$95,198	\$761,587
Conveyor Belts	2	\$95,766	\$191,532
Blowers	1	\$241,770	\$241,770
		Total Cost	\$17,694,545

5.1.5 Nickel Extraction Block

The capital costs presented in Table 5.1.5-1 are categorized based on each individual piece of equipment, which includes precipitation reactors, rotary drum vacuum filters, pumps, cooling jackets, bucket elevators, conveyor belts, and blowers .

Table 5.1.5-1 Breakdown of Capital Cost for Nickel Extraction Block			
Equipment Tag	Quantity	Cost Per Unit (USD)	Total Cost (USD)
PRCP-501	60	\$435,953	\$26,157,162
FIL-501	12	\$237,830	\$2,853,959
D-501	12	\$11,980	\$143,758
Impellers	60	\$27,437	\$1,646,240
Pumps	4	\$38,473	\$153,891
Bucket Elevators	6	\$47,599	\$285,595
Conveyor Belts	2	\$95,766	\$191,532
Blowers	1	\$169,195	\$169,195
		Total Cost	\$31,601,331

5.1.6 General Costs

This section discusses capital costs that are not directly related to a specific block and are not applicable to energy or operating costs. Table 5.1.6-1 outlines general capital costs such as piping, storage tanks, permitting, and approval surrounding the plant. Additionally, one time purchases of kerosene, D2EHPA, and Cyanex-272 are made to be continually recycled through the process.

Table 5.1.6-1 Breakdown of General Capital Costs			
Equipment Tag/Item	Quantity	Cost Per Unit (USD)	Total Cost (USD)
TK-BM	1	\$205,178	\$205,178
TK-H2O2	1	\$830,276	\$830,276
TK-H2SO4	2	\$902,148	\$1,804,295
TK-NAOH	2	\$495,341	\$990,682
TK-CAOH	1	\$30,083	\$30,083
TK-MNPD	1	\$95,063	\$95,063
TK-COPD	1	\$72,944	\$72,944
TK-NIPD	1	\$53,879	\$53,879
TK-NA2CO3	1	\$90,454	\$90,454
kerosene	950,130 (kg)	\$0.78	\$741,101
D2EHPA	64,177 (kg)	\$0.97	\$62,252
Cyanex-272	154,557 (kg)	\$0.75	\$115,918
		Total Cost	\$5,092,125

5.1.7 Fixed Capital Investment and Lang Factor

The capital costs presented in Table 5.1.7-1 are categorized based on each previous capital cost section and represent the total fixed capital investment for this process. To account for other costs associated with equipment such as construction and installation, the fixed capital investment is multiplied by a Lang factor. Towler and Sinnott propose a Lang factor of 3.63 for solids and fluids processing.

Table 5.1.7-1 Breakdown of Fixed Capital Investment	
Section	Cost
Leaching	\$64,798,058
Impurity Removal	\$151,792,159
Manganese	\$13,609,358
Cobalt	\$17,694,545
Nickel	\$31,601,331
General	\$5,092,125
Total	\$284,587,576
Total with Lang Factor	\$1,033,052,901

5.1.8 Working Capital

Should access to raw materials become unavailable, it is important to establish an amount of working capital to keep on site. A 2 week supply of raw materials is deemed sufficient to serve as insurance in the event of a plant shutdown, and it is used as the amount for working capital that needs to be purchased. Table 5.1.8-1 outlines the costs associated with working capital, including black mass, reactants, and water.

Table 5.1.8-1 Raw Material Working Capital			
Raw Material	2 week supply (kg)	Price (USD/kg)	Cost (USD)
Black Mass	4,257,789	\$5.76	\$24,524,864
H ₂ O ₂	8,455,854	\$0.35	\$2,959,549
H ₂ SO ₄	25,643,912	\$0.12	\$3,077,270
NaOH	23,327,933	\$0.32	\$7,464,939
CaOH	114,450	\$0.15	\$17,168
Na ₂ CO ₃	1,080,912	\$0.21	\$226,992
H ₂ O	233,369,977	\$0.0008	\$186,696
		Total	\$38,457,476

5.2 Operating Cash Flow

5.2.1 Raw Materials

The entirety of the battery recycling process requires an extensive variety of raw materials, including black mass, water, salts, acids, and unconventional organic fluids. The cost of materials is determined on a yearly basis, extrapolating hourly mass flow rates into expected hours of annual operation. The prices of each chemical is estimated from online vendors and are outlined in Table 5.2.1-1. Price estimates for process water are obtained from a study conducted in 2017 by the Department of Energy⁵¹ on price escalation rates for water and waste water in select cities. Using the rate for water in Chesterfield, VA and accounting for inflation, a price estimate of \$0.0008/kg is used for cost estimates of feed water. The remainder of chemical prices

were obtained from a variety of online market sources to determine the most competitive pricing.⁵²⁻⁵⁵

Table 5.2.1-1 Annual Raw Material Costs			
Raw Material	Annual Feedrate (kg/year)	Price (USD/kg)	Cost (USD/Year)
Black Mass	100,000,000	\$5.76	\$576,000,000
H ₂ O ₂	198,597,307	\$0.35	\$69,509,057
H ₂ SO ₄	602,282,392	\$0.12	\$72,273,887
NaOH	547,888,442	\$0.32	\$175,324,301
CaOH	2,688,015	\$0.15	\$403,202
Na ₂ CO ₃	25,386,698	\$0.21	\$5,331,207
H ₂ O	5,481,013,416	\$0.0008	\$4,384,811
		Total Cost	\$903,226,465

5.2.2 Utility Costs

Energy is required for various processes within the plan, such as mixing, mass transport, heat transfer, drying, and more. Table 5.2.2-1 Outlines the various energy requirements to operate the plant and their associated cost. Here energy costs are drawn from the average electricity cost in Virginia⁵⁶ as well as the costs associated with natural gas heating for dryers.⁵⁷

Table 5.2.2-1 Annual Energy Costs			
Energy Requirement	Annual Energy Required (kWh/year)	Cost (USD/kWh)	Cost (USD/Year)
Electricity Consumption			
Pumps/Compressors	12,451,872	\$0.15	\$1,867,781
Reactors/Columns	8,838,390	\$0.15	\$1,325,759
Filters	13,570,401	\$0.15	\$2,035,560
Natural Gas Consumption			
Dryers	10,093,565	\$0.093	\$942,241
		Total Cost	\$6,171,340

5.2.3 Waste Disposal

Due to the presence of heavy metals, hazardous waste from the plant must be treated by a waste disposal facility. Using a price of \$0.145/kg for hazardous waste disposal obtained from Table 6-14 in Peters and Timmerhaus,⁵⁸ it is estimated that the plant will need to spend \$1,158,219,055 annually on waste disposal. Table 5.2.3-1 outlines each waste stream, flow rate, and associated annual cost.

Table 5.2.3-1 Waste Disposal Requirements			
Stream Label	Annual Waste Amount (kg/year)	Hazardous Waste Cost (USD/kg)	Cost (USD/Year)
108-HFWS	4,229,576	\$0.145	\$613,289
105-SOL	46,178,132	\$0.145	\$6,695,829
204-SOL	107,451,747	\$0.145	\$15,580,503
310-AQSE	690,170,533	\$0.145	\$100,074,727
317-FIWS	888,011,318	\$0.145	\$128,761,641
412-AQSE	2,720,745,781	\$0.145	\$394,508,138
419-FIWS	3,530,930,533	\$0.145	\$511,984,927
504-AQ	3,071,385,522	\$0.145	\$445,350,901
	Total		\$1,603,569,956

5.2.4 Labor and Maintenance

Excluding lithium extraction, the process is split into four major blocks. The costs associated with labor and maintenance is dependent on the amount shift workers, engineers, and plant managers. The following equation obtained from Alkhayat and Gerrard is used to estimate the amount of workers needed for plant operation.

$$N_{OL} = (6.20 + 31.7P^2 + 0.23N_{np})^{0.5}$$

Equation 5.2.3-1 Estimation of Operators Needed for Process⁵⁹

N_{OL} , number of operators
 P , number of solid handling steps
 N_{np} , number of non-solid handling steps

Counting 72 solid handling steps and 130 non-solid handling steps, approximately 405 operators are needed for continuous processing of the plant. Using a median operator salary of \$64,000/year and multiplying by a factor of 1.2 to represent additional supervising labor, a final cost estimate of \$31,104,000 / yr is used for labor costs.

Estimates surrounding maintenance, insurance, and licensing can be obtained through a model that correlates the costs through a percentage of fixed capital investment. With a fixed capital investment of \$283,668,304 and costs associated with maintenance, insurance, and licensing at 6% of FCI, it is estimated that \$17,020,098 is needed.

5.3 Process Viability

The price summaries from Trade Economics are used as a basis for product pricing.⁶³ For materials that are only listed on the forum in their pure form (e.g. cobalt instead of cobalt (II) hydroxide), the prices are assumed to be similar on a per mole metal basis. Table 5.3-1 outlines the revenue obtained from the battery grade products as of March 2025. The bottom of the table shows the potential revenue should all of the lithium be recovered from the nickel extraction block and precipitated. Assuming all 552.7 kg/hr of lithium ions from 504-AQ are converted into lithium carbonate, the lithium extraction block has the potential to produce 23,217,217 kg of lithium carbonate per year, leading to an overall revenue of \$993,625,362.

Table 5.3-1 Product Revenue			
Product	Annual Production (kg/yr)	Price as of March 2025 (USD/kg)	Revenue (USD/yr)
MnCO ₃	27,773,016	\$0.98	\$27,256,298
Co(OH) ₂	19,213,615	\$21.31	\$409,445,493
Ni(OH) ₂	31,336,111	\$10.20	\$319,575,382
		Total Revenue	\$756,277,173
Li ₂ CO ₃	23,217,217	\$10.22	\$237,348,189

Taking this in consideration with operating costs, Table 5.3-2 evaluates the operating cash flow of the plant on an annual basis.

Table 5.3-2 Operating Cash Flow	
Raw Materials	-\$903,226,465
Energy	-\$6,171,340
Labor and Maintenance	-\$48,134,098
Waste Disposal	-\$1,603,569,956
Product Revenue	\$756,277,173
Operating Profit	-\$1,804,824,686

Because operating profit is in the negative, evaluating the process using return on investment, cumulative cash flow over time, and net present value is irrelevant. Currently this process is not a worthwhile investment and should not be pursued without considerable changes that are addressed in Section 7.2.

Section 6: Environmental, Social, and Safety Considerations

6.1 Environmental Considerations

A commercial-scale battery recycling plant utilizing large quantities of sulfuric acid (H_2SO_4), hydrogen peroxide (H_2O_2), sodium carbonate (Na_2CO_3) and sodium hydroxide (NaOH) must implement stringent environmental controls to mitigate the impact of its operations. One of the primary concerns is the generation of hazardous byproducts, including hydrogen fluoride (HF), which is a highly toxic and corrosive gas. To prevent its release into the atmosphere, a caustic solution packed bed scrubber was employed to neutralize HF emissions and ensure compliance with regulatory limits, including those set by the Environmental Protection Agency (EPA) and industry-specific standards. Additionally, the process generates significant quantities of metal hydroxide and sulfate waste products, including aluminum(II) hydroxide ($\text{Al}(\text{OH})_3$), iron(II) hydroxide ($\text{Fe}(\text{OH})_3$), copper(II) hydroxide ($\text{Cu}(\text{OH})_2$), and calcium(II) sulfate (CaSO_4), which require proper handling and disposal. These solid wastes must be characterized for potential hazardous components and either treated for safe landfill disposal or processed for potential reuse in other industrial applications to minimize environmental impact. Even the non-hazardous chemical byproducts are classified as hazardous as they are produced in such high quantities and concentrations that they would destabilize local environments and can't be disposed of in traditional landfills. Table 6.1-1. breaks down what each waste stream contains and how they are generally disposed of.

Table 6.1-1 — Hazardous Waste Stream Breakdown		
Stream Name	Hazardous Chemicals Present	Proper Disposal Method
108-HFWS (Liquid)	NaF	Convert to CaF ₂ ; Send to Public Landfill; Sell to Steel Manufacturers
105-SOL (Solid)	H ₂ O ₂ , H ₂ SO ₄	Incineration; Hazardous Waste Landfill
204-SOL (Solid)	Cu(OH) ₂	Hazardous Waste Landfill; Copper Recovery via Electroplating
310-AQSE (Liquid)	MnSO ₄ , CoSO ₄	Hazardous Waste Landfill; Recycle Back into Process
317-FIWS (Liquid)	MnSO ₄ , CoSO ₄ , Na ₂ SO ₄	Hazardous Waste Landfill
412-AQSE (Liquid)	CoSO ₄ , NiSO ₄	Electrowinning; Hazardous Waste Landfill
419-FIWS (Liquid)	MnSO ₄ , Mn(OH) ₂	Hazardous Waste Landfill

Water consumption is another critical environmental factor, as the plant is expected to use hundreds of thousands of kilograms of water per hour for chemical reactions, cooling, and washing processes. To reduce freshwater demand and minimize wastewater discharge, the facility should implement water recycling and treatment systems, such as reverse osmosis or evaporative recovery, to reclaim and reuse processed water. Effluent streams containing heavy metals and acidic or alkaline residues must undergo rigorous treatment to remove contaminants before discharge, ensuring compliance with water quality regulations. Given the presence of rare and valuable metals such as lithium (Li), cobalt (Co), nickel (Ni), and manganese (Mn), specialized recovery processes should be integrated to maximize metal reclamation and reduce

waste generation. Implementing a closed-loop recycling approach not only minimizes environmental impact but also enhances the overall sustainability of the operation.

6.2 Societal Considerations

Although the main purpose of this plant is to take advantage of the rare and valuable metals in waste lithium-ion batteries (LIBs), the establishment of a safe and effective recycling plant has many benefits to society. On the surface, the plant would create about 500 jobs which include managing unit operations, innovating processes, and maintaining a standard level of safety. However, the main impact this plant would have is the creation of a new way to process LIB waste. Currently, many spent LIBs are trashed in landfills or improper waste handling facilities. This is a safety risk as improper disposal of LIBs leads to thermal runaway, which generates fires. These fires release toxic vapors including HF to the surrounding environment. This plant would eliminate those risks and allow for a consistently safe disposal facility.

The recycling of valuable metals back into the LIB market would reduce the cost to manufacture LIBs for vehicles, phones, and other energy storage devices. This would improve the mission to go from gas to electric as technologies with LIBs would be less expensive.

6.3 Safety Considerations

The battery recycling process involves the use of sulfuric acid, hydrogen peroxide, and battery metals, generating significant amounts of hydrogen fluoride (HF) as a byproduct and operating at temperatures exceeding 100°C due to exothermic reactions. Adequate ventilation and gas scrubbing systems are required to mitigate HF emissions and prevent occupational exposure. Temperature control mechanisms and controlled reagent dosing are critical to minimizing the risk of thermal runaway. The selection of corrosion-resistant materials for

equipment and containment structures is essential to ensure process integrity and longevity. Additionally, comprehensive personal protective equipment (PPE), including acid-resistant clothing, gloves, and respiratory protection, must be mandated for personnel working in proximity to hazardous chemicals. Emergency response protocols, such as neutralization stations and spill containment measures, should be established to address accidental releases. The following sections will provide a detailed assessment of specific safety considerations for each major chemical, including handling, reaction control, gas management, and waste treatment.

6.3.1 Piranha Solution

The leaching block of the battery recycling process utilizes large quantities of piranha solution, a highly reactive mixture of sulfuric acid (H_2SO_4) and hydrogen peroxide (H_2O_2), to dissolve metals from the black mass. This solution presents significant safety challenges due to its extreme oxidizing properties, highly exothermic reactions, and potential for rapid gas evolution. To mitigate these risks, all process equipment exposed to high temperatures and aggressive acidic conditions is constructed from Grade 7 titanium, which offers superior corrosion resistance under such harsh operating conditions. Polypropylene is used selectively for low-temperature piping, where its chemical resistance provides adequate protection without being subjected to excessive thermal stress. Strict temperature and reactant dosing controls are implemented to prevent uncontrolled heat generation and maintain process stability.

To further enhance safety, a hydrogen peroxide decomposition unit is integrated downstream to eliminate residual H_2O_2 before subsequent processing. This unit utilizes a manganese oxide catalyst to efficiently break down unreacted H_2O_2 into water and oxygen, preventing unintended oxidative reactions that could pose safety risks.

Following the leaching step, sodium hydroxide (NaOH) is added to gradually raise the pH, reducing the solution's acidity and facilitating the controlled precipitation of target metal hydroxides. However, a significant concentration of sulfate ions (SO_4^{2-}) remains in solution throughout the process, requiring proper disposal or potential treatment to prevent environmental contamination. These sulfate-rich effluents must be managed in compliance with environmental regulations, potentially through controlled discharge, neutralization, or industrial reuse. By employing corrosion-resistant materials, decomposition safeguards, and pH stabilization strategies, the leaching block is designed to minimize operational hazards while ensuring process efficiency and environmental compliance.

6.3.2 Hydrofluoric acid

Hydrofluoric acid (HF) is a highly toxic and corrosive substance that presents significant safety risks within the battery recycling process. In our system, HF is generated in the leaching reactor as a byproduct of lithium fluoride (LiF) decomposition from black mass, producing approximately 0.8 kg of HF per hour. Given HF's ability to cause severe chemical burns, respiratory damage, and systemic toxicity through skin contact or inhalation, strict handling and containment measures are necessary to protect both personnel and equipment. HF vapors can corrode standard materials, requiring process components exposed to HF to be constructed from corrosion-resistant materials, such as fluoropolymer-lined piping and specialized alloys, such as Grade 7 Titanium. Additionally, stringent leak prevention protocols and ventilation controls are enforced to minimize exposure risks.

Emissions control is a critical aspect of HF safety management. The current HF emission rate from the process is approximately 4.93×10^{-5} kg of HF per kg of final product, significantly

exceeding the regulatory limit set by the Taconite Iron Processing Industry and EPA regulations of 1.47×10^{-7} kg of HF per kg of final product. To meet these stringent standards, a caustic packed bed gas scrubber was designed Section 3.7. This system neutralizes HF vapors by reacting them with an alkaline sodium hydroxide (NaOH) solution, converting HF into sodium fluoride (NaF), which remains in the liquid phase. Over time, NaF accumulates in the scrubber solution, leading to saturation, at which point the spent liquid stream is collected and sent for hazardous waste disposal in accordance with environmental regulations. Continuous monitoring of HF concentrations in both gas and liquid effluent streams ensures that the system operates safely and remains compliant with regulatory requirements. The integration of proper containment, neutralization, and waste management strategies ensures that HF risks are effectively controlled throughout the battery recycling process.

A release of HF is also one of the more credible release scenarios. Modeling was attempted on ALOHA for a pump seal failure release, however, due to the presence of water in the system ALOHA cannot model this release due to limitations within the program. If this modeling were possible, the release would have been modeled at night, in December, with a wind speed of 5.5 mph and a temperature of 33 F.⁶⁰ The high wind and dry conditions result in a stability class E environment. This means that any potential release in a stable environment could lead to a catastrophic event, but the high wind speed does help to fight this.

6.3.3 Organic Solvents

The battery recycling process utilizes significant amounts of organic solvents, including D2EHPA and CYANEX-272, in liquid-liquid extraction (LLE) operations for metal separation. These solvents are essential for selectively extracting manganese, cobalt, and nickel, but their use

introduces several safety concerns, including flammability, chemical reactivity, and environmental hazards. Organic solvents such as D2HEPA and CYANEX-272 are combustible and can form flammable vapors, necessitating strict control measures to prevent ignition sources in areas where they are stored or used. Adequate ventilation, explosion-proof equipment, and fire suppression systems must be implemented to mitigate the risk of solvent fires or vapor explosions. Additionally, solvent spills pose both environmental and health hazards, requiring secondary containment systems and proper personal protective equipment (PPE) for workers handling these chemicals.

A critical safety concern is the potential interaction between residual, unreacted hydrogen peroxide (H_2O_2) and organic solvents within the process stream. H_2O_2 is a strong oxidizer that can violently react with organic compounds, leading to exothermic decomposition, gas evolution, and even potential runaway reactions if not properly managed. To eliminate this risk, a hydrogen peroxide decomposition unit is integrated into the process before any solvent extraction steps. This unit employs a manganese oxide catalyst to fully decompose residual H_2O_2 into water (H_2O) and oxygen (O_2), ensuring that no reactive oxidizers enter the organic solvent phase. Failure to effectively remove H_2O_2 before solvent contact could result in dangerous solvent degradation, overpressure incidents, or unintended chemical reactions.

In the event of a solvent release, rapid containment and mitigation strategies are essential to prevent environmental contamination and worker exposure. Solvent vapors can pose inhalation hazards, and liquid spills may lead to soil and water contamination if not properly managed. Emergency response measures, including spill kits, absorbent materials, and chemical-resistant barriers, must be in place to quickly contain and neutralize any accidental releases. Additionally, solvent recovery and recycling systems should be implemented to

minimize waste generation and reduce the environmental footprint of the process. By integrating robust safety controls, chemical handling protocols, and emergency preparedness measures, the risks associated with large-scale organic solvent use can be effectively managed in the battery recycling facility.

6.3.4 Kerosene

Kerosene is used in large quantities throughout the battery recycling process as the diluent for the organic phase in liquid-liquid extraction (LLE) operations. While kerosene is essential for efficient metal separation, its extensive use introduces several safety concerns, primarily related to its flammability, volatility, and potential for environmental contamination. As a combustible hydrocarbon, kerosene poses a significant fire and explosion risk, particularly in areas where it is stored or used in large volumes. Vapor accumulation in enclosed spaces can create flammable atmospheres, making it critical to implement proper ventilation, explosion-proof equipment, and strict ignition control measures. Additionally, all kerosene storage tanks, pipelines, and process vessels must be equipped with leak detection systems, grounding, and bonding to prevent static discharge-related ignition.

A kerosene release, whether through a spill, leak, or vapor loss, can have severe consequences. In addition to fire hazards, uncontrolled kerosene discharges can lead to soil and water contamination, posing long-term environmental and regulatory concerns. Spills in process areas can also create slip hazards, increasing the risk of workplace accidents. To mitigate these risks, secondary containment systems, such as bunded storage areas and spill retention basins, are required to capture any accidental releases. Additionally, all process areas handling kerosene

must be equipped with fire suppression systems, including automatic sprinklers and foam-based extinguishing agents that can effectively combat hydrocarbon fires.

To further reduce the likelihood of accidental kerosene release, strict operational controls and routine maintenance procedures must be enforced. This includes regular inspections of pipelines, storage tanks, and transfer pumps to detect potential leaks before they escalate into hazardous situations. Process automation and interlock systems should also be employed to ensure safe handling, including emergency shutdown mechanisms that can immediately isolate kerosene-containing units in the event of a system failure. Personnel working with kerosene must be provided with specialized training on spill response, fire prevention, and safe handling procedures to minimize human error and ensure rapid response to potential incidents. By implementing robust containment, fire prevention, and operational safety measures, the risks associated with large-scale kerosene usage can be effectively managed within the battery recycling facility.

6.3.5 Airborne Powders

Handling and processing fine, dry powders in the battery recycling process presents significant occupational health concerns due to the risk of airborne particulate matter acting as respiratory irritants. Several key inputs, including sodium hydroxide (NaOH) and sodium carbonate (Na₂CO₃), as well as final products such as manganese(II) carbonate (MnCO₃), nickel(II) hydroxide (Ni(OH)₂), cobalt(II) hydroxide (Co(OH)₂), and potentially lithium carbonate (Li₂CO₃), exist in powder form and can readily become airborne during drying, conveying, and packaging operations. When inhaled, these fine particulates can cause respiratory tract irritation, coughing, throat discomfort, and, with prolonged exposure, more serious

pulmonary conditions, particularly for alkaline compounds like NaOH and transition metal hydroxides, which are known to be caustic or cytotoxic to lung tissue.

To mitigate these health risks, strict process controls must be implemented to limit dust generation and exposure. Within the air dryer, where final products undergo moisture removal, flow rates must be carefully regulated to prevent excessive agitation of the material that could lead to dust entrainment. Local exhaust ventilation and dust collection systems—such as high-efficiency particulate air (HEPA) filters and cyclone separators—should be installed and maintained to capture airborne dust at the source. Additionally, enclosed transfer systems and sealed processing equipment can help minimize particulate release. Work areas must be routinely cleaned to prevent the accumulation of settled dust that could be re-entrained into the air.

Personnel must be equipped with appropriate personal protective equipment (PPE), including N95 or P100 respirators, depending on exposure levels, and be trained on safe material handling procedures and the proper use of ventilation systems. Regular air quality monitoring should also be performed to ensure compliance with occupational exposure limits for each compound. By proactively managing airborne particulate hazards, the facility can protect worker health and maintain a safe operational environment.

6.3.6 Contaminated Water

The water process stream in our battery recycling facility contains significant concentrations of dissolved metal ions, including manganese (Mn), cobalt (Co), aluminum (Al), iron (Fe), copper (Cu), lithium (Li), and nickel (Ni), as well as various salts such as sodium hydroxide (NaOH), sodium sulfate (Na₂SO₄), calcium hydroxide (Ca(OH)₂), calcium sulfate (CaSO₄), and calcium fluoride (CaF₂). These contaminants pose serious safety and

environmental risks if not properly managed. The presence of heavy metals in wastewater can lead to toxicity concerns, while high salt concentrations can disrupt aquatic ecosystems if discharged untreated. Additionally, certain metal ions and compounds can lead to scaling, corrosion, or precipitation issues within process piping and storage tanks, potentially causing equipment failures or blockages.

To ensure compliance with environmental regulations and to prevent hazardous discharges, all contaminated water streams must be sent to a hazardous waste processing facility for proper treatment. This treatment typically includes chemical precipitation, ion exchange, or membrane filtration to remove residual metal ions and salts before disposal or potential reuse. Given the caustic and acidic nature of some of the dissolved species, the pH of the wastewater must also be carefully monitored and neutralized before transport to the waste processing facility. Proper containment and leak detection systems must be in place to prevent accidental releases during storage and transport. Additionally, facility personnel must be trained in handling hazardous wastewater, ensuring safe transfer procedures and minimizing the risk of exposure. By implementing strict wastewater management protocols, the facility can safely handle and dispose of metal-laden water streams while maintaining compliance with environmental and safety regulations.

6.3.7 Natural Gas

Natural gas is used on-site to provide energy for the heat exchanger system, introducing several safety considerations related to flammability, pressure containment, and leak prevention. As a highly combustible fuel, natural gas poses fire and explosion hazards if leaks occur in confined areas or near ignition sources. To mitigate these risks, all natural gas storage tanks and

pipelines must be equipped with pressure relief valves, leak detection sensors, and automatic shutoff systems to prevent accidental releases. Proper ventilation is essential in storage and processing areas to disperse any leaked gas and prevent the formation of explosive mixtures.

Additionally, strict adherence to safety regulations is required for the handling and transfer of natural gas to the heat exchanger. Piping and connections must be routinely inspected for signs of wear, corrosion, or damage that could lead to leaks. Personnel working in areas where natural gas is stored or utilized must be trained in emergency response procedures, including evacuation protocols and fire suppression techniques. Given the potential for high-temperature operations in the heat exchanger, all ignition sources must be controlled, and explosion-proof equipment should be used in designated areas. By implementing robust containment, monitoring, and emergency response measures, the risks associated with natural gas storage and usage can be effectively managed, ensuring a safe operating environment for the facility.

A potential release of natural gas is likely the most credible event in this process. Modeling was attempted using ALOHA, but the small release amount, and high wind speed results in no generated plots for jet fires, however, an explosion was modeled for the full release run. To accurately model the potential release of natural gas to the best of our ability, two separate runs were made. The first was assuming a release based on 20% of the cross sectional area of the piping. To pipe the necessary 578 kg of natural gas, a pipe diameter of 0.93 m is required. This equates to a 20% cross section area of 0.13 m² and 114 kg of natural gas over 60 minutes. The flammable area of this run reaches less than 10 meters at a 60% LEL and no explosion was modeled. The second run was assuming a full pipe rupture with a total release of 578 kg of natural gas over 60 minutes. The flammable area of this run reaches just over 20

meters at 60% LEL and the generated plot for an explosion can be found below in Figure 6.3.7-1.

At no point does this explosion do anymore than shatter glass, so unless operators are in close proximity, this release event is not major.

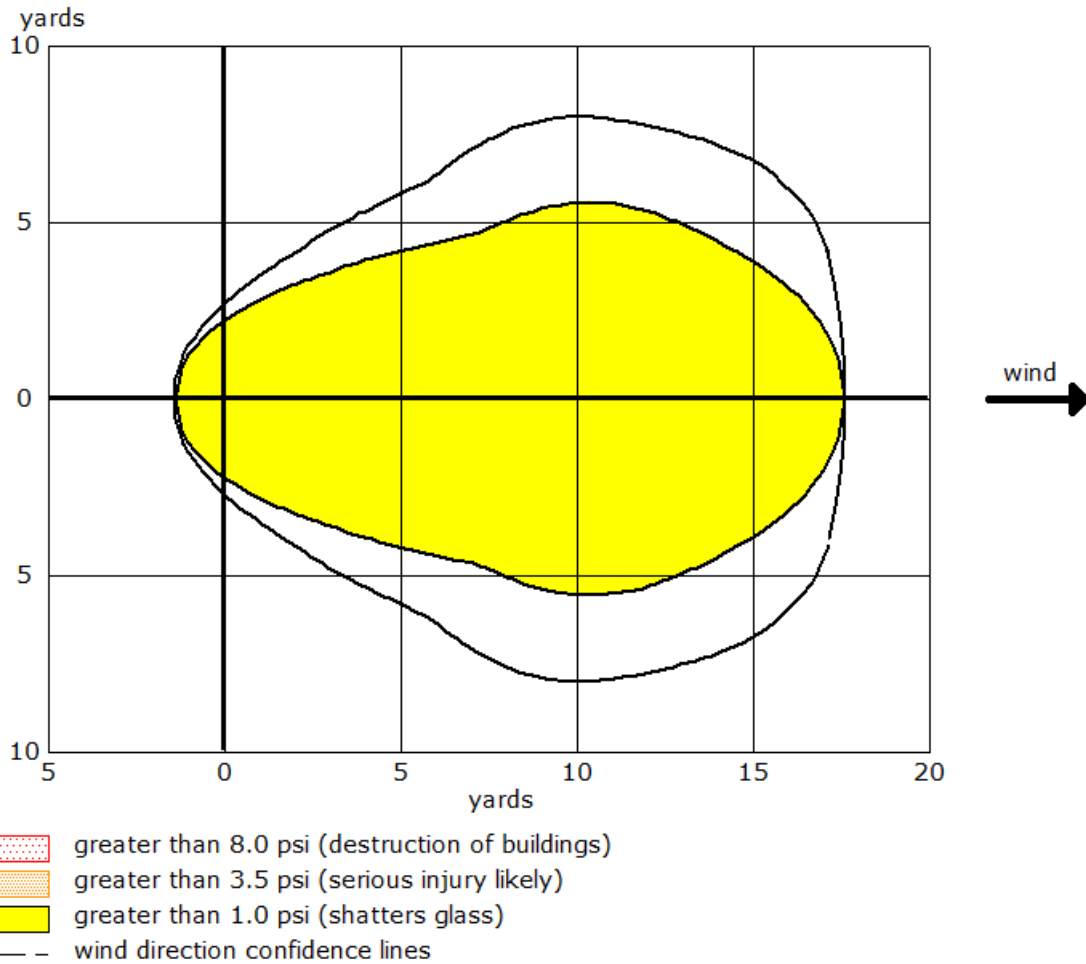


Figure 6.3.7-1 Full Release Natural Gas Explosion

Section 7: Conclusions and Recommendations

7.1 Conclusions

Overall, the process described in this report is a functional layout and design for a lithium ion battery (LIB) recycling facility. Mechanically and thermally treated black mass from LIBs are leached in sulfuric acid and hydrogen peroxide to dissolve the valuable metals. The aqueous metals are then selectively extracted using liquid-liquid extraction. Finally, the metals are precipitated out of solution as either a hydroxide or carbonate salt. All waste gas streams in the process are scrubbed to remove harmful emissions including HF. In the end, the process successfully converts 12,678 kg/hr of black mass into 3,943 kg/hr of MnCO_3 , 1,339 kg/hr of Co(OH)_2 , and 4,297 kg/hr of Ni(OH)_2 . Additionally, there is a lithium rich stream containing 552 kg/hr of Li^+ leaving the process that has not been fully maximized.

However, due to the large operational cost, capital cost, and resource cost, this process is not economically viable. The main issue that prevents efficiency is the large amount of water added and generated in the leaching reaction. This large amount of water creates a need for many unit operations to be at their maximum design specifications and run in parallel. Additionally, the process does a poor job of minimizing waste so a large operational cost goes into waste remediation which tanks any economic growth.

7.2 Future Work Recommendations

The sections below detail future work recommendations around each process block. These are suggestions that future groups could use to improve upon our proposed design.

The first recommendation for this project is the reduction of water present in the initial feed. The full basis of the plant requires 269,628 kg/hr of water in the leaching reactor alone. Not only is this an expensive situation, but due to the sheer volume of the process, everything is sized much larger and with a larger quantity in order to operate on a continuous basis. Finding better research on a reliable recipe to complete the leaching process would result in high savings. To meet the same goals in terms of breakdown and dissolution, a higher molar concentration of H_2O_2 or more H_2SO_4 may be needed. This in turn could result in an estimated nearly 50% savings of both capital cost and yearly operation if the overall volume is reduced to half. This is due to less volume within each reactor and less bases needed to raise the pH.

The second recommendation is with regard to the liquid-liquid extraction processes in the manganese and cobalt removal blocks. In both blocks, the extraction, scrubbing, and stripping columns were designed by scale-up of laboratory-scale reports, maintaining the O/A phase ratio and concentration of extractant stream/scrubbing stream/acid stream. The extraction efficiencies obtained from these experiments are also on the basis of those single-stage lab-scale experiments; all columns in this project were designed as if they operated using the single-stage lab-scale efficiencies. It is likely that these columns, given that they have eight stages each, result in more robust separation than predicted. It is also possible that less concentrated extraction, scrubbing, and stripping streams are required to achieve high degrees of separation. Future works should investigate the mass transfer in these columns more closely, perhaps through experiments to determine the mass transport coefficients of metal ions in the organic phases (kerosene mixed

with either Cyanex-272 or D2EHPA), so that higher product purities can be achieved without using as much acid in the stripping streams or rerouting as much salable product into the scrubbing streams.

The third recommendation within this project is to improve the purity of the final products. The large amount of Na^+ and SO_4^{2-} present in the wet solids result in the formation of Na_2SO_4 which lowers the final purity dramatically. Finding a replacement for NaOH as a base or removing the SO_4^{2-} ions could potentially solve this problem. By replacing the NaOH with something like LiOH, you would still be able to generate the final product but potentially have less impurities generated in product drying. The Li^+ from LiOH would also likely be recovered again in the lithium extraction step. More research is needed to determine the actual effects of formation rate and purity with using these replacements. Another way to manage the formation of Na_2SO_4 could be the use of solids washers between the precipitation and drying steps; these solids washers should rinse the solid product with pure water with some pure product dissolved, which would cause some of the Na_2SO_4 to dissolve into the water stream while leaving the desired product as a solid.

The last major recommendation to improve this process is the recovery of lithium. By removing most of the sodium ions present in the aqueous phase, the result would be consequential yields of lithium carbonate from the process. If the amount of sodium cannot be reduced, then the second recommendation would be to find an alternative process for lithium extraction. This process will likely be similar to how lithium extraction is traditionally done with brine, and as such will require much more involved unit operations than the process currently proposed. Hypothetically if the lithium from stream 504-AQ were to be recovered,

approximately \$237,348,189 in additional revenue would be generated and significantly improve operating profit.

Acknowledgments

We would like to acknowledge the following persons and groups for their contributions to this project.

We would like to acknowledge Eric Anderson, our technical advisor, for supporting us from start to finish, giving us direction, and important industry insight without which this project would not have been possible.

We would also like to acknowledge Ron Unnerstall for his recommendations with respect to the safety analysis portion of our project.

We would also like to acknowledge Aspen Technology for the Aspen Plus file published alongside their report, “Li-ion Battery Recycling Process with TEA and LCA Analysis.” This file was instrumental in identifying the interplay of unit operations of this hydrometallurgical process, and was the jumping-off point for this project.

References

- (1) *Cobalt Life Cycle* | Cobalt Institute.
<https://www.cobaltinstitute.org/about-cobalt/cobalt-life-cycle/cobalt-mining/> (accessed 2025-03-23).
- (2) *What Exactly is Lithium Battery 'Black Mass'?* AquaMetals.
<https://aquametals.com/recyclopedia/what-exactly-is-black-mass/> (accessed 2025-03-23).
- (3) Gaines, L. The Future of Automotive Lithium-Ion Battery Recycling: Charting a Sustainable Course. *ResearchGate* **2024**. <https://doi.org/10.1016/j.susmat.2014.10.001>.
- (4) Zeng, X.; Li, Jinhui; and Singh, N. Recycling of Spent Lithium-Ion Battery: A Critical Review. *Crit. Rev. Environ. Sci. Technol.* **2014**, *44* (10), 1129–1165.
<https://doi.org/10.1080/10643389.2013.763578>.
- (5) Zhou, Z.; Lai, Y.; Peng, Q.; Li, J. Comparative Life Cycle Assessment of Merging Recycling Methods for Spent Lithium Ion Batteries. *Energies* **2021**, *14* (19), 6263.
<https://doi.org/10.3390/en14196263>.
- (6) Wang, X.; Gaustad, G.; Babbitt, C. W.; Bailey, C.; Ganter, M. J.; Landi, B. J. Economic and Environmental Characterization of an Evolving Li-Ion Battery Waste Stream. *J. Environ. Manage.* **2014**, *135*, 126–134. <https://doi.org/10.1016/j.jenvman.2014.01.021>.
- (7) Yang, J.; Harper, G. D.; Anderson, P. Hydrometallurgical Process Optimization for Lithium-Ion Battery Recycling. *J. Ind. Ecol.* **2022**, 654–669.
- (8) Vieceli, N.; Benjamasutin, P.; Promphan, R.; Hellstrom, P.; Paulsson, M.; Petranikova, M. Recycling of Lithium-Ion Batteries: Effect of Hydrogen Peroxide and a Dosing Method on the Leaching of LCO, NMC Oxides, and Industrial Black Mass | ACS Sustainable Chemistry & Engineering. *ACS Sustain. Chem. Eng.* **2023**, *11* (26). <https://doi.org/10.1021>.
- (9) Nayl, A. A.; Elkhashab, R. A.; Badawy, S. M.; El-Khateeb, M. A. Acid Leaching of Mixed Spent Li-Ion Batteries. *Arab. J. Chem.* **2017**, *10*, S3632–S3639.
<https://doi.org/10.1016/j.arabjc.2014.04.001>.
- (10) He, L.-P.; Sun, S.-Y.; Song, X.-F.; Yu, J.-G. Leaching Process for Recovering Valuable Metals from the LiNi_{1/3}Co_{1/3}Mn_{1/3}O₂ Cathode of Lithium-Ion Batteries. *Waste Manag.* **2017**, *64*, 171–181. <https://doi.org/10.1016/j.wasman.2017.02.011>.
- (11) Fan, X.; Song, C.; Lu, X.; Shi, Y.; Shenglong, Y.; Zheng, F.; Huang, Y.; Liu, K.; Hongqiang, W.; Qingyu, L. Separation and Recovery of Valuable Metals from Spent Lithium-Ion Batteries via Concentrated Sulfuric Acid Leaching and Regeneration of LiNi_{1/3}Co_{1/3}Mn_{1/3}O₂ - ScienceDirect. *Journal Alloys Compd.* **2021**, 863.
<https://doi.org/10.1016/j.jallcom.2021.158775>.
- (12) Granata, G. Lithium Ion Battery Recycling - Techno-Economic Assessment and Process Optimization with SuperPro Designer. *ResearchGate* **2020**.
<https://doi.org/10.13140/RG.2.2.24648.88321>.
- (13) Gnielinski, V. *New Equations for Heat and Mass Transfer in Turbulent Pipe and Channel Flow*; International Chemical Engineering, 1976; Vol. 16.
- (14) Green, D. W.; Southard, M. Z. *Perry's Chemical Engineers' Handbook*; McGraw-Hill Education: New York, 2019.
- (15) Chernyaev, A.; Wilson, B. P.; Lundström, M. Study on Valuable Metal Incorporation in the Fe–Al Precipitate during Neutralization of LIB Leach Solution. *Sci. Rep.* **2021**, *11* (1), 23283. <https://doi.org/10.1038/s41598-021-02019-2>.
- (16) Aoudj, S.; Drouiche, N.; Hecini, M.; Ouslimane, T.; Palaouane, B. Coagulation as a

- Post-Treatment Method for the Defluoridation of Photovoltaic Cell Manufacturing Wastewater. *Procedia Eng.* **2012**, *33*, 111–120.
<https://doi.org/10.1016/j.proeng.2012.01.1183>.
- (17) Silva, A. M.; Cunha, E. C.; Silva, F. D. R.; Leão, V. A. Treatment of High-Manganese Mine Water with Limestone and Sodium Carbonate. *J. Clean. Prod.* **2012**, *29–30*, 11–19.
<https://doi.org/10.1016/j.jclepro.2012.01.032>.
- (18) Yüzer, H.; Kara, M.; Sabah, E.; Çelik, M. S. Contribution of Cobalt Ion Precipitation to Adsorption in Ion Exchange Dominant Systems. *J. Hazard. Mater.* **2008**, *151* (1), 33–37.
<https://doi.org/10.1016/j.jhazmat.2007.05.052>.
- (19) Harvey, R.; Hannah, R.; Vaughan, J. Selective Precipitation of Mixed Nickel–Cobalt Hydroxide. *Hydrometallurgy* **2011**, *105* (3), 222–228.
<https://doi.org/10.1016/j.hydromet.2010.10.003>.
- (20) Wanta, K. C.; Tanujaya, F. H.; Putra. SYNTHESIS AND CHARACTERIZATION OF NICKEL HYDROXIDE FROM EXTRACTION SOLUTION OF SPENT CATALYST. *ResearchGate*.
- (21) De Laat, J. Catalytic Decomposition of Hydrogen Peroxide by Fe(III) in Homogeneous Aqueous Solution: Mechanism and Kinetic Modeling | Environmental Science & Technology. *ACS EST Eng.* **1999**, *33* (16). <https://doi.org/10.1021/es981171v>.
- (22) Do, S.-H.; Batchelor, B.; Lee, H.-K.; Kong, S.-H. Hydrogen Peroxide Decomposition on Manganese Oxide (Pyrolusite): Kinetics, Intermediates, and Mechanism. *Chemosphere* **2009**, *75* (1), 8–12. <https://doi.org/10.1016/j.chemosphere.2008.11.075>.
- (23) Vieceli, N.; Reinhardt, N.; Ekberg, C. Optimization of Manganese Recovery from a Solution Based on Lithium-Ion Batteries by Solvent Extraction with D2EHPA. *MDPI Met.* **2020**, *11* (1). <https://doi.org/10.3390/met11010054>.
- (24) Nadimi, H.; Karazmoudeh, N. J. Selective Separation and Purification of Mn from Co and Ni in Waste Mobile Phone Lithium-Ion Batteries Using D2EHAP via Solvent Extraction Method. *J. Sustain. Metall.* **2021**, *7* (2), 653–663.
<https://doi.org/10.1007/s40831-021-00371-1>.
- (25) Li, Y. Improving Extraction Performance of D2EHPA for Impurities Removal from Spent Lithium-Ion Batteries Leaching Solution by TPC[4] | ACS Sustainable Chemistry & Engineering. *ACS Sustain. Chem. Eng.* **2022**, *10* (13).
- (26) Koch Modular Process Systems. Designing Liquid-Liquid Extraction Columns. <https://www.aiche.org/sites/default/files/community/160956/aiche-community-site-files/1720551/liquid-liquidextraction-koch-dec2020.pdf> (accessed 2025-04-04).
- (27) Ripperger, S.; Bart, J.; Bohle, M. Computational Fluid Dynamics Aided Design of Stirred Liquid-Liquid Extraction Columns, Technischen Universität Kaiserslautern, 2013.
https://kluedo.ub.rptu.de/frontdoor/deliver/index/docId/3633/file/_Dissertation_Bart_Final_Druck.pdf (accessed 2025-04-04).
- (28) Shakib, B.; Torkaman, R.; Torab-Mostaedi, M.; Saremi, M.; Asadollahzadeh, M. Performance Evaluation during Extraction Technique in Modified Rotating Disc Column: Experimental and Mathematical Modeling. *Chem. Eng. Process. - Process Intensif.* **2022**, *171*, 108762. <https://doi.org/10.1016/j.cep.2021.108762>.
- (29) Rodrigues, I. R.; Deferm, C.; Binnemans, K.; Riaño, S. Separation of Cobalt and Nickel via Solvent Extraction with Cyanex-272: Batch Experiments and Comparison of Mixer-Settlers and an Agitated Column as Contactors for Continuous Counter-Current Extraction. *Sep. Purif. Technol.* **2022**, *296*, 121326. <https://doi.org/10.1016/j.seppur.2022.121326>.

- (30) Peng, C.; Chang, C.; Wang, Z.; Wilson, B. P.; Liu, F.; Lundström, M. Recovery of High-Purity MnO₂ from the Acid Leaching Solution of Spent Li-Ion Batteries. *JOM* **2020**, *72* (2), 790–799. <https://doi.org/10.1007/s11837-019-03785-1>.
- (31) Lee, M. S.; Yun, S. H.; Wen, J. Separation of Co(II), Mn(II), and Ni(II) by Solvent Extraction with Cyanex 272 and D2EHPA from the Sulfuric Acid Leaching Solution of Spent Lithium-Ion Batteries. <https://doi.org/10.37190/ppmp/193742>.
- (32) Kihlblom, C. Separation of Cobalt and Nickel Using CYANEX 272 for Solvent Extraction. *New Boliden* **2021**.
- (33) Kang, J.; Senanayake, G.; Sohn, J.; Shin, S. M. Recovery of Cobalt Sulfate from Spent Lithium Ion Batteries by Reductive Leaching and Solvent Extraction with Cyanex 272. *Hydrometallurgy* **2010**, *100* (3), 168–171. <https://doi.org/10.1016/j.hydromet.2009.10.010>.
- (34) Mc, O.; C, D.; Jj, E. Extraction of Cobalt(II) and Iron(II) from Nickel(II) Solutions with Nickel Salts of Cyanex 272. **2011**.
- (35) Jing, X.; Sun, Z.; Zhao, D.; Sun, H.; Ren, J. Single-Stage Extraction and Separation of Co²⁺ from Ni²⁺ Using Ionic Liquid of [C₄H₉NH₃][Cyanex 272]. *Molecules* **2022**, *27* (15), 4806. <https://doi.org/10.3390/molecules27154806>.
- (36) Lee, M. S.; Yun, S. H.; Wen, J. Separation of Co(II), Mn(II), and Ni(II) by Solvent Extraction with Cyanex 272 and D2EHPA from the Sulfuric Acid Leaching Solution of Spent Lithium-Ion Batteries. *Physicochem. Probl. Miner. Process.* **2024**. <https://doi.org/10.37190/ppmp/193742>.
- (37) Nogueira, C.; Oliveira, P.; Pedrosa, F. Scrubbing of Cadmium and Nickel from Cyanex 272 Loaded with Cobalt. *Solvent Extr. Ion Exch.* **2003**, *21* (5), 717–734. <https://doi.org/10.1081/SEI-120024553>.
- (38) *National Emission Standards for Hazardous Air Pollutants: Taconite Iron Ore Processing*. Federal Register. <https://www.federalregister.gov/documents/2024/03/06/2024-02305/national-emission-standards-for-hazardous-air-pollutants-taconite-iron-ore-processing> (accessed 2025-04-04).
- (39) Separation Columns (Distillation, Absorption, and Extraction). In *Design of Distillation and Packed bed*; pp 587–616.
- (40) Carta, G. *Heat and Mass Transfer for Chemical Engineers: Principles and Applications*, 1st Edition.; McGraw-Hill Education, 2021.
- (41) Tucak-Smajic, A. *Rotary Vacuum Drum Filtration | BioRender Science Templates*. <https://www.biorender.com/template/rotary-vacuum-drum-filtration> (accessed 2025-03-31).
- (42) McCabe, W. L.; Smith, J. C.; Harriott, P. *Unit Operations of Chemical Engineering*, 5th ed.; McGraw-Hill Education, 1993.
- (43) Towler, G.; Sinnott, R. Chapter 1 - Introduction to Design. In *Chemical Engineering Design (Third Edition)*; Towler, G., Sinnott, R., Eds.; Butterworth-Heinemann, 2022; pp 3–24. <https://doi.org/10.1016/B978-0-12-821179-3.00001-7>.
- (44) Everflow. *Rotary drum dryer drying system, working principle and details*. Rotary Dryer. <https://briquettesolution.com/rotary-dryer/> (accessed 2025-03-31).
- (45) CST. *Mineral Mining Storage | CST Industries*. Silos for Minerals, Mining and Aggregate Storage. <https://www.cstindustries.com/minerals-mining/> (accessed 2025-03-31).
- (46) USDE. *Furnaces and Boilers*. Energy.gov. <https://www.energy.gov/energysaver/furnaces-and-boilers> (accessed 2025-03-31).
- (47) Methane | NIST Chemistry WebBook. <https://webbook.nist.gov/cgi/cbook.cgi?ID=C74828&Mask=1>.

- (48) Townsend, W.; Faber, G. Capital Cost Estimation Database, 2021.
<https://assessccus.globalco2initiative.org/wp-content/uploads/Capital-Equipment-Cost-Database.xlsx>.
- (49) Woods, D. R. *Rules of Thumb in Engineering Practice*; Wiley-VCH, 2007.
- (50) Seider, W. D.; Lewin, D. R.; Seader, J. D. *Product and Process Design Principles: Synthesis, Analysis and Evaluation*, 4th ed.; Wiley, 2016.
- (51) Federal Energy Management Program. *Water and Wastewater Annual Price Escalation Rates for Selected Cities Across the United States*. Energy.gov.
<https://www.energy.gov/femp/articles/water-and-wastewater-annual-price-escalation-rates-selected-cities-across-united> (accessed 2025-04-04).
- (52) *Critical mass: Asian demand for North American scrap sees recycler prices spike*. Benchmark Source.
https://source.benchmarkminerals.com/article/critical-mass-asian-demand-for-north-american-scrap-sees-recycler-prices-spike?utm_source=chatgpt.com (accessed 2025-04-04).
- (53) Mike. *Calcium Hydroxide price index*. businessanalytiq.
<https://businessanalytiq.com/procurementanalytics/index/calcium-hydroxide-price-index/> (accessed 2025-04-04).
- (54) *Cyanex 272 Best Quality Wholesale Price Hot Sell Acid 83411-71-6 Cyanex 272 Factory Directly Sell - Buy Cyanex 272 Liquid Factory Grade Good Sell Product on Alibaba.com*.
https://www.alibaba.com/product-detail/Cyanex-272-Best-Quality-Wholesale-Price_1600864717410.html?spm=a2700.7724857.0.0.169c445aEQVyxD (accessed 2025-04-04).
- (55) *[Hot Item] High Quality CAS 298-07-7 Di (2-ethylhexyl) Phosphoric Acid D2ehpa*. Made-in-China.com.
<https://wffondland.en.made-in-china.com/product/sdgtFPVTZcWn/China-High-Quality-CAS-298-07-7-Di-2-ethylhexyl-Phosphoric-Acid-D2ehpa.html> (accessed 2025-04-04).
- (56) *Electricity Cost in Virginia: 2025 Electric Rates*. EnergySage.
<https://www.energysage.com/local-data/electricity-cost/va/> (accessed 2025-04-04).
- (57) *Natural gas - Price - Chart - Historical Data - News*.
<https://tradingeconomics.com/commodity/natural-gas> (accessed 2025-04-04).
- (58) Peters, M. S.; Timmerhaus, K. D.; West, R. E. *Plant Design and Economics for Chemical Engineers*, 5th ed.; McGraw-Hill Education.
- (59) Verret, J.; Qiao, R.; Barghout, R. A. Cost of Operating Labour. **2020**.
- (60) *Richmond December Weather, Average Temperature (Virginia, United States) - Weather Spark*.
<https://weatherspark.com/m/20906/12/Average-Weather-in-December-in-Richmond-Virginia-United-States> (accessed 2025-04-04).

Appendix A: Design and Operating Calculations

Leaching Reactor Just Suspension Speed Calculation

$$N_{js} = Sv^{0.1} \left[\frac{g(\rho_s - \rho_l)}{\rho_l} \right]^{0.45} X^{0.13} d_p^{0.2} D^{-0.85}$$

$$v \sim 1 * 10^{-6} \text{ m}^2/\text{s}$$

$$g = 9.8 \text{ m}^2/\text{s}$$

$$\rho_s = 3133 \text{ kg/m}^3$$

$$\rho_l = 1107 \text{ kg/m}^3$$

$$X = \frac{1057 \text{ kg}}{31016 \text{ kg}} * 100 = 3.4$$

$$d_p = 1.5 * 10^{-5} \text{ m}$$

$$D = 1 \text{ m}$$

$$S = 10.42 \left(\frac{C}{T} \right)^{0.455} \left(\frac{H}{T} \right)^{-0.107} = 10.42 \left(\frac{1 \text{ m}}{3 \text{ m}} \right)^{0.455} \left(\frac{5 \text{ m}}{3 \text{ m}} \right)^{-0.107} = 5.98$$

$$N_{js} = (5.98)(1 * 10^{-6})^{0.1} \left[\frac{9.8(3133-1107)}{1107} \right]^{0.45} (3.4)^{0.13} (1.5 * 10^{-5})^{0.2} (1)^{-0.85} = 0.7 \text{ rps}$$

Leaching Reactor Impeller Power Calculations

$$N_{js} = 0.7 \text{ rps}$$

$$n_{\text{design}} = 1 \text{ rps}$$

$$P = N_p \rho n^3 D^5$$

$$N_p = 1.3$$

$$\rho = 1107 \text{ kg/m}^3$$

$$n = 1 \text{ rps}$$

$$D = 1 \text{ m}$$

$$P = (1.3)(1107)(1)^3(1)^5 = 1440 \text{ W}$$

RDC Column Power Calculation

Power = Torque x Speed

$$\text{Torque} = 0.5 * \rho * \pi * D^2 * L * C_d * \omega^2 * R$$

$$\text{Torque} = 0.5 * 1000 * \pi * 0.12 * 12 * 0.5 * (2\pi * 200/60)^2 * 0.05$$

$$\text{Torque} = 2067 \text{ N-m}$$

$$\text{Power} = 2067 * (2\pi * 200/60) = 43.3 \text{ kW}$$

Rotary Vacuum Drum Filter Calculation

$$A_T = m_c \left(\frac{\alpha_0 \mu}{2c \Delta p^{(1-s)} g_c f n} \right)^{1/2}$$

$$f = 0.3$$

$$\Delta p = 0.5 \text{ atm} = 1058 \frac{\text{lb}_f}{\text{ft}^2}$$

$$s = 0.26$$

$$n = \frac{1}{5 \text{ min}} = \frac{1}{300 \text{ s}}$$

$$\alpha_0 = 2.90 * 10^{10} \text{ ft/lb}$$

$$\mu = 0.000672 \frac{\text{lb}}{\text{ft} * \text{s}}$$

$$m_c = 4093 \frac{\text{kg}}{\text{hr}} = 2.49 \frac{\text{lbs}}{\text{s}}$$

$$c = \frac{C_F}{1 - [(m_F/m_c) - 1] C_F / \rho}$$

$$C_F = \frac{9004 \frac{\text{lbs}}{\text{hr}}}{11817 \frac{\text{ft}^3}{\text{hr}}} = 0.76 \frac{\text{lbs}}{\text{ft}^3}$$

$$\frac{m_F}{m_c} = \frac{1}{.3} = 3.33$$

$$\rho = 68.5 \frac{\text{lbs}}{\text{ft}^3}$$

$$c = \frac{0.76}{1 - [(3.33) - 1] 0.76 / 68.5} = 0.78$$

$$A_T = 2.49 \left(\frac{(2.9 * 10^{10})(0.000672)}{2(0.78)(1058)^{0.76}(32.17)(0.3)(1/300)} \right)^{1/2} = 3727 \text{ ft}^2 = 346.2 \text{ m}^2$$

Rotary Drum Dryer Area Calculation

$$V = 0.209 \text{ kg/m}^3$$

$$\text{(Eq 3.11.1-1)} V_N = \frac{1}{0.15} * 0.209 = 1.39 \text{ m}^3$$

$$\text{(Eq 3.11.1-2)} D = \left(\frac{4 * 1.39}{5 * \pi} \right)^{1/3} = 0.71 \text{ m}$$

$$\text{(Eq 3.11.1-2)} L = 5 * 0.71 = 3.54 \text{ m}$$

$$\text{(Eq 3.11.1-3)} \quad A = 2\pi\left(\frac{0.71}{2}\right)3.54 + 2\pi\left(\frac{0.71}{2}\right)^2 = 4.32 \text{ m}^2$$

Heat Exchanger Cooling Water Mass Flow Rate Calculation

This calculation demonstrates how to determine the amount of CW needed in HE-401.

$$Q = 588.9 \text{ kW} = 588,900 \text{ W}$$

$$T_{\text{CW, in}} = 30^\circ\text{C}$$

$$T_{\text{CW, out}} = 35^\circ\text{C}$$

$$C_{p, \text{CW}} = 4,181 \text{ J/kg K}$$

$$\text{(Eq. 3.1.2.3-1): } m = Q / (C_p * (T_{\text{out}} - T_{\text{in}})) = 588,900\text{W} / (4,181 \text{ J/kg K} * 5 \text{ K}) = 28.17 \text{ kg/s of CW}$$

required

Heat Exchanger Area Requirement Calculation

This calculation shows how to determine the required heat exchange area of HE-401.

$$Q = 588.9 \text{ kW} = 588900 \text{ W}$$

$$T_{\text{CW, in}} = 30^\circ\text{C}$$

$$T_{\text{CW, out}} = 35^\circ\text{C}$$

$$C_{p, \text{CW}} = 4181 \text{ J/kgK}$$

$$T_{\text{hot stream, in}} = 48^\circ\text{C}$$

$$T_{\text{hot stream, out}} = 35^\circ\text{C}$$

$$h_o = 1000 \text{ W/m}^2\text{K}$$

$$r_i = 0.022 \text{ m}$$

$$r_o = 0.0254 \text{ m}$$

$$\rho_{\text{hot stream}} = 1216 \text{ kg/m}^3$$

$$\mu_{\text{hot stream}} = 1.09\text{E-}03 \text{ Pa-s}$$

$$v_{\text{hot stream}} = \mu / \rho = 9.00\text{E-}07 \text{ m}^2/\text{s}$$

$$\alpha_{hot\ stream} = 1.53E-07\ m^2/s$$

$$m_{hot\ stream} = 48930\ kg/hr = 13.5917\ kg/s$$

$$u_{hot\ stream} = V/A_c = (m_{hs}/\rho_{hs})/(\pi r_i^2) = (13.5917\ kg/s / 1216\ kg/m^3)/(\pi*(0.022m)^2) = 7.35\ m/s$$

$$k_{hot\ stream} = 0.64\ W/mK$$

$k_{316\ Stainless\ Steel\ pipe}$

$$Re = u_{hs} * 2 * r_i / \nu_{hs} = (7.35\ m/s * 2 * 0.022m) / 9.00E-07 m^2/s = 3.60E+05$$

$$Pr = \nu_{hs} / \alpha_{hs} = 9.00E-07\ m^2/s / 1.53E-07\ m^2/s = 5.88$$

$$(f/2) = 0.125 * (0.79 * \ln(Re) - 1.64)^{-2} = 1.74E-03$$

$$(Eqn\ 3.1.2.3-3): h_i = [(k_{hs}/(2r_i)) * (f/2) * (Re - 1000) * Pr] / [1.0 + 12.7 * \sqrt{(f/2)} * (Pr^{2/3} - 1)] = [(0.64\ W/mK / (2 * 0.022m)) * 1.74E-03 * (3.60E+05 - 1000) * 5.88] / [1.0 + 12.7 * \sqrt{(1.74E-03)} * (5.88^{2/3} - 1)] = 24328\ W/m^2K$$

$$(Eqn\ 3.1.2.3-2): U = [(1/h_o) + ((r_o \ln(r_o/r_i))/k_{pipe}) + (r_o/h_i r_i)]^{-1} = [(1/1000W/m^2K) + ((0.0254m * \ln(0.0254m/0.022m))/16.3W/mK) + (0.0254m / (24328W/m^2K * 0.022m))]^{-1} = 786.5\ W/m^2K$$

$$(Eqn\ 3.12.2-1): LMTD = ((T_{hot\ stream,\ in} - T_{CW,\ out}) - (T_{hot\ stream,\ out} - T_{CW,\ in})) / \ln((T_{hot\ stream,\ in} - T_{CW,\ out}) / (T_{hot\ stream,\ out} - T_{CW,\ in})) = ((48^\circ C - 35^\circ C) - (35^\circ C - 30^\circ C)) / \ln((48^\circ C - 35^\circ C) / (35^\circ C - 30^\circ C)) = 8.37^\circ C$$

$$(Eqn\ 3.1.2.3-5): A_{required} = Q/U * LMTD = 588900W / (786.5W/m^2K * 8.37K) = \mathbf{89.4\ m^2\ required}$$

heat transfer area of heat exchanger

Hot Air Furnace Heater Natural Gas Requirement Calculation

The hot air supplied to product driers is heated in a furnace by the burning of natural gas. Natural gas is purchased based on its energy content in MMBtu (millions of Btu's).

$$m = 226400\ kg/hr = 62.89\ kg/s = \text{total mass flow of hot air needed across the plant}$$

$$T_{air,\ ambient} = 25^\circ C$$

$$T_{air,\ hot} = 150^\circ C$$

$$C_{p,\ air} = 1.012\ kJ/kgK$$

$$(Eqn\ 3.1.2.3-1): Q = m C_p (T_{air,\ hot} - T_{air,\ ambient}) = 62.89\ kg/s * 1.012\ kJ/kgK * (150^\circ C - 25^\circ C) = 7956\ kW$$

The burning of natural gas is 90% efficient in heating the air, so the energy content of natural gas is: $Q_{gas} * 0.9 = Q_{air}$, or $Q_{gas} = Q_{air} / 0.9 = 7956\ kW / 0.9 = 8840\ kW$

$$Q_{gas} = 8840\ kW = 8379\ Btu/s = \mathbf{30.16\ MMBtu/hr\ of\ gas\ needed}$$

Cooling Jacket Area Sufficiency Validation Calculation

This calculation demonstrates the math behind one single leaching reactor cooling jacket.

$$Q = 385 \text{ kW}$$

$$T_{\text{reactor}} = 70^\circ\text{C}$$

$$T_{\text{CW, in}} = 30^\circ\text{C}$$

$$T_{\text{CW, out}} = 45^\circ\text{C}$$

$$N = 1 \text{ rotation per second}$$

$$D_{\text{impeller}} = 1 \text{ m}$$

$$D_T = 3 \text{ m}$$

$$H_T = 5 \text{ m}$$

$$\text{Reactor surface area, } A_{\text{available}} = \pi D_T H_T = 47.1 \text{ m}^2$$

$$\text{Impeller constant } a = 0.53$$

$$\text{Impeller constant } b = 2/3$$

$$r_o = 1.5 \text{ m}$$

$$r_i = 1.4975 \text{ m}$$

$$\rho_{\text{tank fluid}} = 1155 \text{ kg/m}^3$$

$$\mu_{tf} = 4.71\text{E-}04 \text{ Pa-s}$$

$$v_{tf} = 4.08\text{E-}07 \text{ m}^2/\text{s}$$

$$\alpha_{tf} = 1.29\text{E-}07 \text{ m}^2/\text{s}$$

$$k_{tf} = 6.90\text{E-}01 \text{ W/mK}$$

$$\text{Re}_{tf} = ND^2/v_{tf} = (1\text{s}^{-1}*(1\text{m})^2)/4.08\text{E-}07 \text{ m}^2/\text{s} = 2.45\text{E+}06$$

$$\text{Pr} = 3.16$$

$$\text{(Eqn 3.1.2.3-4): } h_i = (k_{tf}/(2*r_i))*a*\text{Re}^b*\text{Pr}^{1/3} =$$

$$(6.90\text{E-}01\text{W/mK}/(2*1.4975\text{m}))*0.53*(2.45\text{E+}06)^{2/3}*3.16^{1/3} = 3256 \text{ W/m}^2\text{K}$$

(Eqn 3.1.2.3-3): $h_o = 3.09\text{E+}03 \text{ W/m}^2\text{K}$ (calculation skipped here because calculation of convective heat transfer coefficient for flow in a circular pipe has already been shown above in Heat Exchanger Area Requirement Calculation)

$$\text{(Eqn 3.1.2.3-2): } U = 1276 \text{ W/m}^2\text{K}$$

$$\begin{aligned} \text{(Eqn 3.1.2.3-6): LMTD} &= ((T_{\text{reactor}} - T_{\text{CW, in}}) - (T_{\text{reactor}} - T_{\text{CW, out}})) / \text{LN}((T_{\text{reactor}} - T_{\text{CW, in}}) / (T_{\text{reactor}} - T_{\text{CW, out}})) \\ &= ((70^\circ\text{C} - 30^\circ\text{C}) - (70^\circ\text{C} - 45^\circ\text{C})) / \ln((70^\circ\text{C} - 30^\circ\text{C}) / (70^\circ\text{C} - 45^\circ\text{C})) = 31.9^\circ\text{C} \end{aligned}$$

$$A_{\text{required}} = Q/U * \text{LMTD} = 385000\text{W} / (1276\text{W}/\text{m}^2\text{K} * 31.9\text{K}) = \mathbf{9.5 \text{ m}^2} < A_{\text{available}} = \mathbf{47.1 \text{ m}^2},$$

cooling jacket sufficient

Waste Stream Gas Scrubber Column Height Calculation

This calculation demonstrates the values utilized in and calculated from the equations described in Section [3.7.1 Waste Stream Gas Scrubber Design](#).

Total Product Mass (kg of Solid Final Product) = 15,916.72 kg

Maximum HF Emission Limit (kg HF/kg Final Product) = 1.47E-7 (Taconite Industry Standard)

Initial HF Mass Flow Rate = 0.78456 kg/hr HF

Maximum HF Mass Flow Rate = 1.47E-7 * 15,916.72 = 2.34E-3 kg/hr HF

Total Vapor Stream Mass Flow Rate = 1511.56 kg/hr

$y_{A,1} = 0.78456 \text{ kg/hr HF} / 1511.56 \text{ kg/hr} = 5.19\text{E-}4 \text{ kg HF/kg}$

$y_{A,2} = 2.34\text{E-}3 \text{ kg/hr HF} / 1511.56 \text{ kg/hr} = 1.55\text{E-}6 \text{ kg HF/kg}$

Solubility Coefficient HF in Caustic Solution = 6.71E-9 m²/s

Molar Density of Water = 55,600 mol/m³

H Henry's Constant = 8.18E7 Pa *Equation 3.7.1-1*

K at 1 atm = H / 101300 Pa = 807.15 *Equation 3.7.1-2*

$(\frac{L}{G})_{\text{min}} = 804.7$ *Equation 3.7.1-3*

$(\frac{L}{G}) = 1.3 * (\frac{L}{G})_{\text{min}}$, Estimation factor recommended from text⁴⁰

$\gamma = 0.7715$ *Equation 3.7.1-4*

No,G = 19.025 *Equation 3.7.1-5*

$a_p = 95 \text{ m}^2/\text{m}^3$ Table 14-13 Perry's Handbook

$$A = \frac{\pi(1\text{m column diameter})^2}{4} = 0.785 \text{ m}^2, \text{ Diameter calculated using Aspen RadFrac Block}$$

$$L_S = \frac{\text{Liquid Molar Flow Rate (mol/s)}}{A} = \frac{1.832}{0.785} = 2.332 \text{ mol/m}^2 \text{ s}$$

$$L' = \frac{\text{Liquid MW} * L_s}{1000} = \frac{18.196 \text{ kg/kmol} * 2.332 \text{ mol/m}^2 \text{ s}}{1000} = 0.0424 \text{ kg/m}^2 \text{ s}$$

$$\sigma_c = 0.061 \text{ N/m, Table 14-13 Perry's Handbook}$$

$$\sigma_L = 0.08305 \text{ N/m, Table 14-13 Perry's Handbook}$$

$$\mu_L = 0.00185 \text{ Pa} * \text{ s, Aspen Modeling}$$

$$\rho_L = 1110.2 \text{ kg/m}^3, \text{ Aspen Modeling}$$

$$g = 9.81 \text{ m/s}^2$$

$$a = 10.178, \text{ Equation 3.7.1-6}$$

$$C_G = 32.358 \text{ mol/m}^3, \text{ Aspen Modeling}$$

$$D_G = 1.66\text{E-}6 \text{ m}^2/\text{s, Aspen Modeling}$$

$$Sc_G = \frac{D_G}{10^{-6}} = 1.66$$

$$\mu_G = 2.24\text{E-}5 \text{ Pa*s, Aspen Modeling}$$

$$d_p = 0.05 \text{ m, 50mm Carbon Raschig Rings}$$

$$k_y = 0.03, \text{ Equation 3.7.1-7}$$

$$Sc_L = \frac{D_G}{10^{-6}} = 0.00168$$

$$k_x = 71.11, \text{ Equation 3.7.1-8}$$

$$G_S = \frac{\text{Gas Molar Flow Rate (mol/s)}}{A} = \frac{4.702}{0.785} = 5.987 \text{ mol/m}^2 \text{ s}$$

$$G' = \frac{\text{Gas MW} * G_s}{1000} = \frac{28.203 \text{ kg/kmol} * 5.987 \text{ mol/m}^2\text{s}}{1000} = 0.1689 \text{ kg/m}^2\text{s}$$

$$H_G = 1.96, \text{ Equation 3.7.1-9}$$

$$H_L = 0.00322, \text{ Equation 3.7.1-9}$$

$$H_{o,G} = 1.97, \text{ Equation 3.7.1-10}$$

$$Z = 37.39 \text{ m}, \text{ Equation 3.7.1-11}$$

$$HETP = \frac{Z}{\# \text{ of Theoretical Stages}} = \frac{37.38 \text{ m}}{5} = 7.48 \text{ m}$$

Pump Energy Requirements - P-101

$$\Delta P = 50,000 \text{ Pa (friction)} + 50,000 \text{ Pa (control valve)} + \rho gh$$

$$\rho = 1134 \text{ kg/m}^3 \text{ (from Aspen)}$$

$$g = 9.8 \text{ m/s}^2$$

$$h = 5 \text{ m (from tank height)}$$

$$\rho gh = 55,566 \text{ Pa}, \Delta P = 155,566 \text{ Pa}$$

$$\text{mass flow rate} = 359520 \text{ kg/hr (from Aspen)}$$

$$Q = \frac{359520 \text{ kg/hr}}{1134 \text{ kg/m}^3} = 317 \text{ m}^3/\text{hr}$$

$$\text{Power} = \frac{\Delta P Q}{\eta}$$

$$\text{Electrical Efficiency} = 0.9 \text{ (Lecture)}$$

$$\text{Mechanical Efficiency} = 0.7 \text{ (Lecture)}$$

$$\eta = (0.9)(0.7) = 0.63$$

$$\text{Power} = \frac{\Delta P Q}{\eta} = \frac{(155,566)(317)}{(0.63)} = 21746 \text{ W} = 21.75 \text{ kW}$$

Capital Cost Estimation - PLEACH-101

$$\text{Quantity} = 36$$

Material – Titanium Clad, $f_m = 5$ (Woods)

$$S = 35.3 \text{ m}^3$$

$$a = 14000, b = 15400, n = 0.7 \text{ (Towler and Sinnott)}$$

$$C_e = a + bS^n = 14,000 + 15400(35.3)^{0.7} = \$200,622$$

$$CEPCI_c \sim 800$$

$$CEPCI_L = 478.6$$

$$C = f_m C_e \left(\frac{CEPCI_c}{CEPCI_L} \right) = 5 * (200,622) \left(\frac{800}{478.6} \right) = \$1,676,741$$

$$36 * \$1,676,741 = \$60,362,680$$

Appendix B: Full Stream Tables

Leaching Block

Leaching Block Full Stream Table						
Name	101-CATH	102-PIR	103-EFF	104-VAP	105-SOL	106-LCH
Flowrate	kg/hr	kg/hr	kg/hr	kg/hr	kg/hr	kg/hr
From	TK-BM	TK-H2O2 and TK-H2SO4	PLEACH-101	PLEACH-101	FIL-101	FIL-101
To	PLEACH-101	PLEACH-101	FIL-101	GS-101	Waste	PRCP-201 (becomes 201-LCH)
Total	12678.9	359517.6	372196.5	477.4	5852.7	365866.4
C	4092.8	0.0	4092.8	0.0	4092.8	0.0
Co	1660.9	0.0	0.0	0.0	0.0	0.0
Fe	102.8	0.0	0.0	0.0	0.0	0.0
Cu	219.4	0.0	0.0	0.0	0.0	0.0
Ni	2650.0	0.0	0.0	0.0	0.0	0.0
Al	129.3	0.0	0.0	0.0	0.0	0.0
Li ₂ O	1071.4	0.0	0.0	0.0	0.0	0.0
CoLiO ₂	77.3	0.0	0.0	0.0	0.0	0.0
LiNiO ₂	77.3	0.0	0.0	0.0	0.0	0.0

Leaching Block Full Stream Table						
Name	101-CATH	102-PIR	103-EFF	104-VAP	105-SOL	106-LCH
Flowrate	kg/hr	kg/hr	kg/hr	kg/hr	kg/hr	kg/hr
From	TK-BM	TK-H2O2 and TK-H2SO4	PLEACH-101	PLEACH-101	FIL-101	FIL-101
To	PLEACH-101	PLEACH-101	FIL-101	GS-101	Waste	PRCP-201 (becomes 201-LCH)
LiMn ₂ O ₄	77.3	0.0	0.0	0.0	0.0	0.0
Mn ₃ O ₄	2326.6	0.0	0.0	0.0	0.0	0.0
O ₂	0.0	0.0	396.5	393.5	0.0	2.97E+00
H ₂ O	0.0	269638.2	267768.6	82.3	1281.5	266405.5
H ₂ O ₂	0.0	25166.2	21767.6	0.9	104.2	21662.5
H ₂ SO ₄	0	64713.2	2.58E-04	3.25E-12	1.24E-06	2.58E-04
HF	0	0	104.9	0.8	0.5	103.7
LiF(S)	193.9	0	0	0	0	0
OH ⁻	0	0	2.42E-09	0	1.16E-11	2.42E-09
F ⁻	0	0	42.4	0	0.2	42.1
SO ₄ ²⁻	0	0	1800.6	0	8.6	1788.5
HSO ₄ ⁻	0	0	62229.0	0	297.9	61934.6
H ₃ O ⁺	0	0	6852.6	0	32.8	6819.0

Leaching Block Full Stream Table						
Name	101-CATH	102-PIR	103-EFF	104-VAP	105-SOL	106-LCH
Flowrate	kg/hr	kg/hr	kg/hr	kg/hr	kg/hr	kg/hr
From	TK-BM	TK-H2O2 and TK-H2SO4	PLEACH-101	PLEACH-101	FIL-101	FIL-101
To	PLEACH-101	PLEACH-101	FIL-101	GS-101	Waste	PRCP-201 (becomes 201-LCH)
Al ³⁺	0	0	129.3	0	0.6	128.6
AlOH ²⁺	0	0	0.002	0	7.33E-06	1.52E-03
Al(OH) ²⁺	0	0	2.99E-08	0	1.44E-10	3.00E-08
Co ²⁺	0	0	1707.4	0	8.2	1699.2
Mn ²⁺	0	0	1722.8	0	8.2	1714.5
MnOH ⁺	0	0	1.19E-08	0	5.68E-11	1.18E-08
Cu ²⁺	0	0	219.4	0.0	1.1	218.4
Li ⁺	0	0	563.5	0.0	2.7	560.8
Ni ²⁺	0	0	2696.4	0.0	12.9	2683.5
NiOH ⁺	0	0	9.82E-08	0	4.70E-10	9.77E-08
Fe ³⁺	0	0	102.8	0.0	0.5	102.3
FeOH ²⁺	0	0	0.01	0.00	4.04E-05	8.40E-03
Fe(OH) ₂ ⁺	0	0	5.48E-08	0	2.62E-10	5.44E-08

Leaching Block Full Stream Table

Leaching Block Full Stream Table						
Name	101-CATH	102-PIR	103-EFF	104-VAP	105-SOL	106-LCH
Flowrate	kg/hr	kg/hr	kg/hr	kg/hr	kg/hr	kg/hr
From	TK-BM	TK-H2O2 and TK-H2SO4	PLEACH-101	PLEACH-101	FIL-101	FIL-101
To	PLEACH-101	PLEACH-101	FIL-101	GS-101	Waste	PRCP-201 (becomes 201-LCH)
Fe ₂ (OH) ₂	0	0	0.002	0	9.46E-06	1.97E-03

Impurity Removal Block

Impurity Removal Block Full Stream Table							
Name	201-LCH	202-NAOH	203-EFF	204-SOL	205-PRCP	206-PRCP	207-VAP
Flowrate	kg/hr	kg/hr	kg/hr	kg/hr	kg/hr	kg/hr	kg/hr
From	Leaching Block (was 106-LCH)	TK-NAOH	PRCP-201	FIL-201	FIL-201	PBR-201	PBR-201
To	PRCP-201	PRCP-201	FIL-201	Waste	PBR-201	Mn Extraction Block (becomes 301-AQFD)	GS-101
Total	365866.4	40871.6	406738.0	13617.4	393120.5	380736.1	12384.4
O ₂	3.0	0.0	3.0	0.0	2.9	3.3	10083.9
H ₂ O	266405.5	0.0	289172.8	2981.0	286191.8	295246.1	2300.5
H ₂ O ₂	21662.5	0.0	21662.5	223.3	21439.2	0.0	0.0
H ₂ SO ₄	2.58E-04	0	2.46E-15	2.54E-17	2.44E-15	2.08E-15	7.68E-22
HF	103.7	0	9.10E-05	9.38E-07	9.01E-05	8.25E-05	1.43E-05
NaOH	0	36784.5	0	0	0	0	0
CaF ₂ (S)	0	0	247.1	247.1	0	0	0
Ca(OH) ₂	0	4087.2	0	0	0	0	0
CaSO ₄ ²⁻	0	0	8295.9	8295.9	0.1	0	0

Impurity Removal Block Full Stream Table							
Name	201-LCH	202-NAOH	203-EFF	204-SOL	205-PRCP	206-PRCP	207-VAP
Flowrate	kg/hr	kg/hr	kg/hr	kg/hr	kg/hr	kg/hr	kg/hr
From	Leaching Block (was 106-LCH)	TK-NAOH	PRCP-201	FIL-201	FIL-201	PBR-201	PBR-201
To	PRCP-201	PRCP-201	FIL-201	Waste	PBR-201	Mn Extraction Block (becomes 301-AQFD)	GS-101
Fe(OH) ₃	0	0	195.8	195.8	0.0	0	0
Al(OH) ₃	0	0	371.9	371.9	0.0	0	0
Cu(OH) ₂	0	0	333.0	333.0	9.11E-09	0	0
Ni(OH) ₂	0	0	78.9	78.9	1.56E-05	0	0
OH ⁻	2.42E-09	0	0.01	5.51E-05	5.29E-03	0.01	0
F ⁻	42.1	0	20.4	0.2	20.1	20.1	0
SO ₄ ²⁻	1,788.5	0	58451.0	602.6	57848.4	57848.4	0
HSO ₄ ⁻	61934.6	0.0	0.6	0.0	0.6	0.6	0
H ₃ O ⁺	6819.0	0.0	0.0	0.0	0.0	0.0	0
Na ⁺	0.0	0.0	21142.7	218.0	20924.7	20924.7	0
Al ³⁺	128.6	0	6.80E-06	7.01E-08	6.73E-06	1.14E-05	0
AlOH ²⁺	0.002	0	5.81E-05	5.99E-07	5.75E-05	7.33E-05	0

Impurity Removal Block Full Stream Table							
Name	201-LCH	202-NAOH	203-EFF	204-SOL	205-PRCP	206-PRCP	207-VAP
Flowrate	kg/hr	kg/hr	kg/hr	kg/hr	kg/hr	kg/hr	kg/hr
From	Leaching Block (was 106-LCH)	TK-NAOH	PRCP-201	FIL-201	FIL-201	PBR-201	PBR-201
To	PRCP-201	PRCP-201	FIL-201	Waste	PBR-201	Mn Extraction Block (becomes 301-AQFD)	GS-101
Al(OH) ²⁺	3.00E-08	0	1.09E-03	1.13E-05	1.08E-03	1.05E-03	0
Co ²⁺	1,699.2	0	1,699.2	17.5	1,681.7	1,681.7	0
Mn ²⁺	1,714.5	0	1714.5	17.7	1,696.8	1,696.8	0
MnOH ⁺	1.18E-08	0	0.0	1.17E-04	0.0	0.0	0
Cu ²⁺	218.4	0.0	1.5	0.0	1.4	1.4	0
Li ⁺	560.8	0	560.8	5.8	555.0	555.0	0
Ca ²⁺	0	0	152.9	1.6	151.3	151.3	0
CaOH ⁺	0	0	2.87E-04	2.96E-06	2.84E-04	2.16E-04	0
Ni ²⁺	2683.5	0.0	2633.4	27.1	2606.3	2606.3	0
NiOH ⁺	9.77E-08	0	9.21E-02	9.50E-04	9.12E-02	6.93E-02	0
Fe ³⁺	102.3	0	1.70E-07	1.75E-09	1.68E-07	2.79E-07	0
FeOH ²⁺	8.40E-03	0	1.01E-05	1.04E-07	9.98E-06	1.25E-05	0

Impurity Removal Block Full Stream Table							
Name	201-LCH	202-NAOH	203-EFF	204-SOL	205-PRCP	206-PRCP	207-VAP
Flowrate	kg/hr	kg/hr	kg/hr	kg/hr	kg/hr	kg/hr	kg/hr
From	Leaching Block (was 106-LCH)	TK-NAOH	PRCP-201	FIL-201	FIL-201	PBR-201	PBR-201
To	PRCP-201	PRCP-201	FIL-201	Waste	PBR-201	Mn Extraction Block (becomes 301-AQFD)	GS-101
Fe(OH) ₂ ⁺	5.44E-08	0	6.28E-05	6.47E-07	6.21E-05	5.89E-05	0
Fe ₂ (OH) ₂	0.0	0	8.08E-09	8.33E-11	8.00E-09	1.33E-08	0

Manganese Extraction Block

Manganese Extraction Block Full Stream Table 1								
Name	301-AQFD	302-ACFD	303-AQEF	304-AQEE	305-OREE	306-AQEE	307-OREE	308-MNSF
Flowrate	kg/hr	kg/hr	kg/hr	kg/hr	kg/hr	kg/hr	kg/hr	kg/hr
From	Impurity Removal Block (was 206-PRCP)	TK-H2SO4	Mixed stream of 301-AQFD and 302-ACFD	EXT-301	EXT-301	EXT-302	EXT-302	Mix of 305-OREE and 307-OREE
To	Mixes with 302-ACFD	Mixes with 301-AQFD	EXT-301	EXT-302	Mixed with 307-OREE	Co Extraction Block (becomes 401-AQFD)	Mixed with 305-OREE	SCRB-301
Total	380,736.1	4800	385,536.5	384,166.3	320,872.4	383,745.5	319,923.1	87,454.5
O ₂	3.3	0	3.3	3.3	0	3.3	0	0
H ₂ O	295,246.1	3874.9	299,265.3	299,183.7	0	299,125.0	0	86,596.3
HF	8.25E-05	0	0.19	0.7	0	0.7	0	0
OH ⁻	0.01	0	2.80E-06	1.71E-07	0	7.22E-07	0	6.02E-08
F ⁻	20.1	0	20.0	19.5	0	19.4	0	0
SO ₄ ²⁻	57,848.4	85.5	57,166.4	52,447.0	0	51,252.4	0	546.0
HSO ⁴⁺	0.6	673.7	1,450.3	6,219.1	0	7,426.3	0	7.52E-03
H ₃ O ⁺	0	165.9	13.6	99.8	0	161.7	0	9.26E-04

Manganese Extraction Block Full Stream Table 1

Name	301-AQFD	302-ACFD	303-AQEF	304-AQEE	305-OREE	306-AQEE	307-OREE	308-MNSF
Flowrate	kg/hr	kg/hr	kg/hr	kg/hr	kg/hr	kg/hr	kg/hr	kg/hr
From	Impurity Removal Block (was 206-PRCP)	TK-H2SO4	Mixed stream of 301-AQFD and 302-ACFD	EXT-301	EXT-301	EXT-302	EXT-302	Mix of 305-OREE and 307-OREE
To	Mixes with 302-ACFD	Mixes with 301-AQFD	EXT-301	EXT-302	Mixed with 307-OREE	Co Extraction Block (becomes 401-AQFD)	Mixed with 305-OREE	SCRB-301
Na ⁺	20,924.7	0	20,924.6	20,924.6	0	20,924.6	0	0
Al ³⁺	1.14E-05	0	5.20E-04	8.28E-07	0	0	0	0
AlOH ²⁺	7.33E-05	0	1.34E-06	1.62E-10	0	0	0	0
Al(OH) ²⁺	1.05E-03	0	7.74E-09	7.45E-14	0	0	0	0
Co ²⁺	1,681.7	0	1,681.7	1,597.6	0	1,517.7	0	0
Mn ²⁺	1,696.8	0	1,696.8	509.0	0	152.7	0	312.2
MnOH ⁺	0.0	0	3.56E-06	1.74E-07	0	4.16E-07	0	3.47E-08
Cu ²⁺	1.4	0	1.7	0.5	0	0.2	0	0
Li ⁺	555.0	0	555.1	555.1	0	555.1	0	0
Ca ²⁺	151.3	0	151.3	0	0	0	0	0

Manganese Extraction Block Full Stream Table 1

Name	301-AQFD	302-ACFD	303-AQEF	304-AQEE	305-OREE	306-AQEE	307-OREE	308-MNSF
Flowrate	kg/hr	kg/hr	kg/hr	kg/hr	kg/hr	kg/hr	kg/hr	kg/hr
From	Impurity Removal Block (was 206-PRCP)	TK-H2SO4	Mixed stream of 301-AQFD and 302-ACFD	EXT-301	EXT-301	EXT-302	EXT-302	Mix of 305-OREE and 307-OREE
To	Mixes with 302-ACFD	Mixes with 301-AQFD	EXT-301	EXT-302	Mixed with 307-OREE	Co Extraction Block (becomes 401-AQFD)	Mixed with 305-OREE	SCRB-301
CaOH ⁺	2.16E-04	0	8.51E-08	1.77E-18	0	0	0	0
Ni ²⁺	2,606.3	0	2,606.3	2606.3	0	2,606.3	0	0
NiOH ⁺	6.93E-02	0	2.89E-05	4.71E-06	0	3.76E-05	0	0
Fe ³⁺	2.79E-07	0	4.57E-05	6.56E-07	0	0	0	0
FeOH ²⁺	1.25E-05	0	8.58E-07	2.20E-09	0	0	0	0
Fe(OH) ²⁺	5.89E-05	0	1.69E-09	7.07E-13	0	0	0	0
Fe ₂ (OH) ₂	1.33E-08	0	5.99E-11	2.74E-16	0	0	0	0
C ₁₂	0	0	0	0	281,162.1	0	281,162.1	0
D2EHPA	0	0	0	0	21,032.1	0	33,280.1	0
D2EHP-Mn	0	0	0	0	15,086.1	0	4,525.8	0

Manganese Extraction Block Full Stream Table 1

Name	301-AQFD	302-ACFD	303-AQEF	304-AQEE	305-OREE	306-AQEE	307-OREE	308-MNSF
Flowrate	kg/hr	kg/hr	kg/hr	kg/hr	kg/hr	kg/hr	kg/hr	kg/hr
From	Impurity Removal Block (was 206-PRCP)	TK-H2SO4	Mixed stream of 301-AQFD and 302-ACFD	EXT-301	EXT-301	EXT-302	EXT-302	Mix of 305-OREE and 307-OREE
To	Mixes with 302-ACFD	Mixes with 301-AQFD	EXT-301	EXT-302	Mixed with 307-OREE	Co Extraction Block (becomes 401-AQFD)	Mixed with 305-OREE	SCRB-301
D2EHP-Co	0	0	0	0	1,001.3	0	951.2	0
D2EHP-Al	0	0	0	0	1.91E-02	0	3.04E-05	0
D2EHP-Fe	0	0	0	0	8.35E-04	0	1.20E-05	0
D2EHP-Cu	0	0	0	0	13.1	0	3.9	0
D2EHP-Ca	0	0	0	0	2,577.7	0	1.02E-06	0

Manganese Extraction Block Full Stream Table 2

Name	309-ORSE	310-AQSE	311-AQTF	312-AQTE	313A/313B	314-CO3F	315-PRBF	316-PREF
Flowrate	kg/hr	kg/hr	kg/hr	kg/hr	kg/hr	kg/hr	kg/hr	kg/hr
From	SCRB-301	SCRB-301	TK-H2SO4	STRP-301	STRP-301	TK-NA2CO3	TK-NAOH	PRCP-301
To	STRP-301	Waste	STRP-301	PRCP-301	EXT-301 and EXT-302	PRCP-301	PRCP-301	FIL-301
Total	640,786.6	87,463.3	107,846.8	109,628.7	319,502.4	3217.8	5142.0	117988.5
H ₂ O	0	86,596.3	98,140.6	97,186.8	0	0	0	100,387.0
H ₂ SO ₄	0	0	9,706.2	7.09E-09	0	0	0	3.83E-19
NaOH	0	0	0	0	0	0	5142.0	0
Na ₂ CO ₃	0	0	0	0	0	3217.8	0	0
CaSO ₄ ⁻²	0	0	0	0	0	0	0	327.2
Fe(OH) ₃	0	0	0	0	0	0	0	8.80E-05
Cu(OH) ₂	0	0	0	0	0	0	0	2.4
MnCO ₃	0	0	0	0	0	0	0	3484.2
OH ⁻	0	1.97E-04	0	0	0	0	0	0.1
CO ₃ ²⁻	0	0	0	0	0	0	0	0.2
HCO ₃ ⁻	0	0	0	0	0	0	0	2.7
HSO ₄ ⁻	0	7.65E-03	0	7,345.2	0	0	0	0
SO ₄ ²⁻	0	546.0	0	2,237.8	0	0	0	9324.2

Manganese Extraction Block Full Stream Table 2

Name	309-ORSE	310-AQSE	311-AQTF	312-AQTE	313A/313B	314-CO3F	315-PRBF	316-PREF
Flowrate	kg/hr	kg/hr	kg/hr	kg/hr	kg/hr	kg/hr	kg/hr	kg/hr
From	SCRB-301	SCRB-301	TK-H2SO4	STRP-301	STRP-301	TK-NA2CO3	TK-NAOH	PRCP-301
To	STRP-301	Waste	STRP-301	PRCP-301	EXT-301 and EXT-302	PRCP-301	PRCP-301	FIL-301
H ₃ O ⁺	0	6.65E-04	0	1,006.0	0	0	0	4.32E-05
Na ⁺	0	0	0	0	0	0	0	4351.4
Al ³⁺	0	0	0	4.34E-04	0	0	0	2.94E-11
AlOH ²⁺	0	0	0	5.55E-08	0	0	0	1.36E-08
Al(OH) ²⁺	0	0	0	0	0	0	0	1.07E-05
Co ²⁺	0	131.2	0	32.8	0	0	0	32.8
Mn ²⁺	0	189.9	0	1,666.4	0	0	0	1.1
MnOH ⁺	0	7.35E-03	0	6.57E-07	0	0	0	3.28E-04
Cu ²⁺	0	0	0	1.5	0	0	0	3.45E-04
Ca ²⁺	0	0	0	151.3	0	0	0	75.2
CaOH ⁺	0	0	0	0	0	0	0	0
Fe ³⁺	0	0	0	4.64E-05	0	0	0	5.63E-13
FeOH ²⁺	0	0	0	2.33E-08	0	0	0	1.97E-09
Fe(OH) ²⁺	0	0	0	7.21E-13	0	0	0	5.51E-07
Fe ₂ (OH) ₂	0	0	0	1.66E-14	0	0	0	3.19E-16

Manganese Extraction Block Full Stream Table 2								
Name	309-ORSE	310-AQSE	311-AQTF	312-AQTE	313A/313B	314-CO3F	315-PRBF	316-PREF
Flowrate	kg/hr	kg/hr	kg/hr	kg/hr	kg/hr	kg/hr	kg/hr	kg/hr
From	SCRB-301	SCRB-301	TK-H2SO4	STRP-301	STRP-301	TK-NA2CO3	TK-NAOH	PRCP-301
To	STRP-301	Waste	STRP-301	PRCP-301	EXT-301 and EXT-302	PRCP-301	PRCP-301	FIL-301
C ₁₂	562,324.2	0	0	0	281,162.1	0	0	0
D2EHPA	54,312.2	0	0	0	38,340.3	0	0	0
D2EHP-Mn	21,165.0	0	0	0	0	0	0	0
D2EHP-Co	390.5	0	0	0	0	0	0	0
D2HEP-Al	1.91E-02	0	0	0	0	0	0	0
D2HEP-Fe	8.47E-04	0	0	0	0	0	0	0
D2HEP-Cu	17.0	0	0	0	0	0	0	0
D2HEP-Ca	2577.7	0	0	0	0	0	0	0

Manganese Extraction Block Full Stream Table 3

Name	317-FIWS	318-WETP	319-AIN	320-AOUT	321-PROD
Flowrate	kg/hr	kg/hr	kg/hr	kg/hr	kg/hr
From	FIL-301	FIL-301	Atmosphere	D-301	D-301
To	Waste	D-301	D-301	Waste	TK-MNPD
Total	112,534.7	5,453.8	93,600.0	95,110.4	3,943.4
O ₂	0	0	19,656.0	19,656.0	0
CO ₂	0.0	2.49E-04	0	0.0	0
H ₂ O	98,945.1	1,441.9	0	1,510.4	0
H ₂ SO ₄	3.59E-19	5.23E-21	0	6.16E-28	0
Na ₂ SO ₄	0	0	0	0	193.1
CaSO ₄ (S)	0	0	0	0	262.4
CaSO ₄ ²⁻	0	327.3	0	0	0
Fe(OH) ₃	0	8.80E-05	0	0	8.80E-05
Cu(OH) ₂	0	2.4	0	0	2.4
MnCO ₃	0	3,484.2	0	0	3,484.2
CoSO ₄ (S)	0	0	0	0	1.2
OH ⁻	0.1	1.19E-03	0	0	0
CO ₃ ²⁻	0.2	0.0	0	0	0
HCO ₃ ⁻	2.7	0.0	0	0	0

Manganese Extraction Block Full Stream Table 3

Name	317-FIWS	318-WETP	319-AIN	320-AOUT	321-PROD
Flowrate	kg/hr	kg/hr	kg/hr	kg/hr	kg/hr
From	FIL-301	FIL-301	Atmosphere	D-301	D-301
To	Waste	D-301	D-301	Waste	TK-MNPD
SO ₄ ²⁻	9,190.3	133.9	0	0	0
HSO ₄ ⁻	0.0	5.17E-05	0	0	0
H ₃ O ⁺	4.22E-05	6.15E-07	0	0	0
Na ⁺	4,288.9	62.5	0	0	0
Al ³⁺	2.93E-11	4.26E-13	0	0	0
AlOH ²⁺	1.35E-08	1.96E-10	0	0	0
Al(OH) ²⁺	1.05E-05	1.53E-07	0	0	0
Co ²⁺	32.3	0.5	0	0	0
Mn ²⁺	1.1	0.0	0	0	0
MnOH ⁺	3.26E-04	4.75E-06	0	0	0
Cu ²⁺	3.41E-04	4.97E-06	0	0	0
Ca ²⁺	74.1	1.1	0	0	0
CaOH ⁺	0.0	8.00E-05	0	0	0
Fe ³⁺	5.27E-13	7.72E-15	0	0	0
FeOH ²⁺	1.87E-09	2.74E-11	0	0	0

Manganese Extraction Block Full Stream Table 3

Name	317-FIWS	318-WETP	319-AIN	320-AOUT	321-PROD
Flowrate	kg/hr	kg/hr	kg/hr	kg/hr	kg/hr
From	FIL-301	FIL-301	Atmosphere	D-301	D-301
To	Waste	D-301	D-301	Waste	TK-MNPD
Fe(OH) ₂ ⁺	5.26E-07	7.71E-09	0	0	0
Fe ₂ (OH) ₂	2.89E-16	4.25E-18	0	0	0
N ₂	0	0	73,944.0	73,944.0	0

Cobalt Extraction Block

Cobalt Extraction Block Full Stream Table 1								
Name	401-AQFD	402-BSPH	403-AQEF	404-SPBF	405-RECY	406-OREF	407-AQEE	408-OREE
From	Mn Extraction Block (was 306-AQEE)	TK-NAOH	Mix of 401-AQFD and 402-BSFD	TK-NAOH	STRP-401	SAP-401	EXT-401	EXT-401
To	Mix with 402-BSPH	Mix with 401-AQFD	EXT-401	SAP-401	SAP-401	EXT-401	Ni Extraction Block (becomes 501-EFF)	SCRB-401
Flowrate	kg/hr	kg/hr	kg/hr	kg/hr	kg/hr	kg/hr	kg/hr	kg/hr
Total	383,745.5	3,397.4	387,143.0	6,422.6	249,212.0	255,634.7	391,440.4	251,337.2
O ₂	3.3	0.0	3.3	0.0	0.0	0.0	3.3	0
H ₂ O	299,125.0	0.0	300,808.3	3,211.3	0.0	4,657.7	305,466.0	0
H ₂ SO ₄	9.26E-08	0	1.89E-13	0	0	0	1.51E-13	0
HF	7.36E-01	0	9.47E-04	0	0	0	8.82E-04	0
NaOH	0	3,397.4	0	3,211.3	0	0.1	0	0
OH ⁻	6.02E-08	0	1.13E-04	0	0	0	8.71E-05	0
F ⁻	19.4	0	20.1	0	0	0	20.1	0
SO ₄ ²⁻	51,252.4	0	58,592.7	0	0	0	58,592.9	0

Cobalt Extraction Block Full Stream Table 1

Name	401-AQFD	402-BSPH	403-AQEF	404-SPBF	405-RECY	406-OREF	407-AQEE	408-OREE
From	Mn Extraction Block (was 306-AQEE)	TK-NAOH	Mix of 401-AQFD and 402-BSFD	TK-NAOH	STRP-401	SAP-401	EXT-401	EXT-401
To	Mix with 402-BSPH	Mix with 401-AQFD	EXT-401	SAP-401	SAP-401	EXT-401	Ni Extraction Block (becomes 501-EFF)	SCRB-401
Flowrate	kg/hr	kg/hr	kg/hr	kg/hr	kg/hr	kg/hr	kg/hr	kg/hr
HSO ₄ ⁻	7,426.3	0	9.0	0	0	0	8.8	0
H ₃ O ⁺	161.7	0	0.1	0	0	0	0.1	0
Na ⁺	20,924.6	0	22,877.3	0	0	0	24,197.0	0
Co ²⁺	1,517.7	0	1,517.7	0	0	0	106.2	0
Mn ²⁺	152.7	0	152.7	0	0	0	1.5	0
MnOH ⁺	3.47E-08	0	3.57E-05	0	0	0	3.40E-07	0
Cu ²⁺	0.2	0	1.51E-01	0	0	0	1.51E-01	0
Li ⁺	555.1	0	555.1	0	0	0	555.1	0
Ni ²⁺	2,606.3	0	2,606.3	0	0	0	2,489.1	0
NiOH ⁺	3.13E-06	0	0.0	0	0	0	0	0
C ₁₂	0	0	0	0	190,918.3	190,918.3	0	190,918.3

Cobalt Extraction Block Full Stream Table 1								
Name	401-AQFD	402-BSPH	403-AQEF	404-SPBF	405-RECY	406-OREF	407-AQEE	408-OREE
From	Mn Extraction Block (was 306-AQEE)	TK-NAOH	Mix of 401-AQFD and 402-BSFD	TK-NAOH	STRP-401	SAP-401	EXT-401	EXT-401
To	Mix with 402-BSPH	Mix with 401-AQFD	EXT-401	SAP-401	SAP-401	EXT-401	Ni Extraction Block (becomes 501-EFF)	SCRB-401
Flowrate	kg/hr	kg/hr	kg/hr	kg/hr	kg/hr	kg/hr	kg/hr	kg/hr
CYANEX	0	0	0	0	58,293.7	34,976.2	0	34,976.2
CYANEXNA	0	0	0	0	0	25,082.3	0	7,149.4
CYANEXCO	0	0	0	0	0	0	0	15,275.1
CYANEXNI	0	0	0	0	0	0	0	1,274.0
CYANEXMN	0	0	0	0	0	0	0	1,744.1

Cobalt Extraction Block Full Stream Table 2

Name	409-ACSF	410-COSF	411-AQSF	412-AQSE	413-ORSE	414-AQTF	415-AQTE	416-PRBF
From	TK-H2SO4	TK-COPD	Mix of 409-ACSF and 410-COSF	SCRB-401	SCRB-401	TK-H2SO4	STRP-401	TK-NAOH
To	Mix with 410-COSF	Mix with 409-ACSF	SCRB-401	Waste	STRP-401	STRP-401	PRCP-401	PRCP-401
Flowrate	kg/hr	kg/hr	kg/hr	kg/hr	kg/hr	kg/hr	kg/hr	kg/hr
Total	1,140.3	343,651.7	344,791.9	344,791.4	251,337.7	403,792.6	405,918.2	56,346.7
H ₂ O	0	342,571.0	342,989.9	342,989.9	0.0	337,408.1	325,309.7	0.0
H ₂ SO ₄	1,140.3	0	3.40E-20	3.88E-18	0	66,384.5	2.78E-06	0
NaOH	0	0	0	0	0	0	0	56,346.7
Co(OH) ₂	0	1,080.3	0	0	0	0	0	0
OH ⁻	0	0.1	0.0	4.05E-04	0	0	4.20E-10	0
SO ₄ ²⁻	0	0	1,116.8	1,116.8	0	0	7,205.4	0
HSO ₄ ⁻	0	0	1.57E-03	1.54E-02	0	0	58,421.7	0
H ₃ O ⁺	0	3.94E-06	2.65E-04	2.41E-03	0	0	12,774.9	0
Na ⁺	0	0	0	0	0	0	526.1	0
Co ²⁺	0	1.69E-01	685.1	568.5	0	0	1,528.1	0
Mn ²⁺	0	0	0	0	0	0	151.2	0

Cobalt Extraction Block Full Stream Table 2

Name	409-ACSF	410-COSF	411-AQSF	412-AQSE	413-ORSE	414-AQTF	415-AQTE	416-PRBF
From	TK-H2SO4	TK-COPD	Mix of 409-ACSF and 410-COSF	SCRB-401	SCRB-401	TK-H2SO4	STRP-401	TK-NAOH
To	Mix with 410-COSF	Mix with 409-ACSF	SCRB-401	Waste	STRP-401	STRP-401	PRCP-401	PRCP-401
Flowrate	kg/hr	kg/hr	kg/hr	kg/hr	kg/hr	kg/hr	kg/hr	kg/hr
MnOH ⁺	0	0	0	0	0	0	1.23E-09	0
Ni ²⁺	0	0	0	116.1	0	0	1.2	0
NiOH ⁺	0	0	0	3.07E-02	0	0	5.06E-11	0
C ₁₂	0	0	0	0	190,918.3	0	0	0
CYANEX	0	0	0	0	34,976.2	0	0	0
CYANEXNA	0	0	0	0	7,149.4	0	0	0
CYANEXCO	0	0	0	0	16,536.8	0	0	0
CYANEXNI	0	0	0	0	12.7	0	0	0
CYANEXMN	0	0	0	0	1,744.1	0	0	0

Cobalt Extraction Block Full Stream Table 3

Name	417-VENT	418-PREF	419-FIWS	420-WETP	421-AIN	422-AOUT	423-PROD
From	PRCP-401	PRCP-401	FIL-401	FIL-401	Atmosphere	D-401	D-401
To	Waste	FIL-401	Waste	D-401	D-401	Waste	TK-COPD
Flowrate	kg/hr	kg/hr	kg/hr	kg/hr	kg/hr	kg/hr	kg/hr
Total	11,353.3	450,911.6	447,462.6	3,449.0	46,400.0	47,206.9	2,642.1
O ₂	0	0	0	0	9744.0	9744.0	1.48E-06
H ₂ O	11,353.3	348,995.5	348,188.4	807.0	0	806.9	0.1
H ₂ SO ₄	2.10E-28	3.42E-23	3.42E-23	7.92E-26	0	0	1.35E-41
NaOH	0	0	0	0	0	0	6.5
Na ₂ SO ₄	0	0	0	0	0	0	222.3
Co(OH) ₂	0	2,410.1	0	2,410.1	0	0	2,410.1
Ni(OH) ₂	0	1.9	0	1.9	0	0	1.9
OH ⁻	0	1,414.6	1,411.4	3.3	0	0	3.96E-01
SO ₄ ²⁻	0	65,020.8	64,870.4	150.4	0	0	8.33E-05
HSO ₄ ⁻	0	4.22E-05	4.21E-05	9.76E-08	0	0	3.89E-19
H ₃ O ⁺	0	1.79E-07	1.79E-07	4.14E-10	0	0	6.58E-20
Na ⁺	0	32,912.6	32,836.5	76.1	0	0	0.4
Co ²⁺	0	1.80E-06	1.80E-06	4.16E-09	0	0	1.15E-18

Cobalt Extraction Block Full Stream Table 3

Name	417-VENT	418-PREF	419-FIWS	420-WETP	421-AIN	422-AOUT	423-PROD
From	PRCP-401	PRCP-401	FIL-401	FIL-401	Atmosphere	D-401	D-401
To	Waste	FIL-401	Waste	D-401	D-401	Waste	TK-COPD
Flowrate	kg/hr	kg/hr	kg/hr	kg/hr	kg/hr	kg/hr	kg/hr
Mn ²⁺	0	135.0	134.7	0.3	0	0	0.0
MnOH ⁺	0	21.2	21.2	0	0	0	4.54E-01
Ni ²⁺	0	2.81E-07	2.80E-07	6.49E-10	0	0	1.81E-19
NiOH ⁺	0	2.33E-07	2.33E-07	5.40E-10	0	0	1.37E-16
NITROGEN	0	0	0	0	36,656.0	36,656.0	1.50E-04

Nickel Extraction Block

Nickel Extraction Block Full Stream Table								
Name	501-EFF	502-NAOH	503-PRCP	504-AQ	505-SOL	506-AIN	507-AOUT	508-PROD
Flowrate	kg/hr	kg/hr	kg/hr	kg/hr	kg/hr	kg/hr	kg/hr	kg/hr
From	Cobalt Extraction Block (was 407-AQEE)	TK-NAOH	PRCP-501	FIL-501	FIL-501	Atmosphere	D-501	D-501
To	PRCP-501	PRCP-501	FIL-501	Lithium Extraction Block	D-501	D-501	Waste	TK-NIPD
Total	391,440.4	3,408.6	394,849.0	389,226.4	5,622.6	86,400.0	87,721.2	4,301.5
O ₂	3.3	0.0	3.3	3.3	0.0	18,144.0	18,144.0	3.24E-07
H ₂ O	305,466.0	0.0	305,467.9	304,146.8	1,321.2	0.0	1,321.1	0.0
H ₂ SO ₄	7.23E-14	0	5.37E-24	5.35E-24	2.32E-26	0	0	0
HF	7.16E-04	0	5.91E-09	5.88E-09	2.55E-11	0	1.15E-11	1.17E-18
NaOH	0	3,408.6	0	0	0	0	0	0
Na ₂ SO ₄	0	0	0	0	0	0	0	349.5
LiF(S)	0	0	0	0	0	0	0	0.1
Li ₂ SO ₄	0	0	0	0	0	0	0	18.7

Nickel Extraction Block Full Stream Table								
Name	501-EFF	502-NAOH	503-PRCP	504-AQ	505-SOL	506-AIN	507-AOUT	508-PROD
Flowrate	kg/hr	kg/hr	kg/hr	kg/hr	kg/hr	kg/hr	kg/hr	kg/hr
From	Cobalt Extraction Block (was 407-AQEE)	TK-NAOH	PRCP-501	FIL-501	FIL-501	Atmosphere	D-501	D-501
To	PRCP-501	PRCP-501	FIL-501	Lithium Extraction Block	D-501	D-501	Waste	TK-NIPD
Cu(OH) ₂	0.0	0.0	0.2	0.0	0.2	0.0	0.0	0.2
Ni(OH) ₂	0	0	3,931.7	0.0	3,931.7	0.0	0.0	3,931.7
OH ⁻	2.68E-05	0	5.0	5.0	2.18E-02	0	0	0.0
F ⁻	20.1	0	20.1	20.1	0.1	0	0	8.06E-06
SO ₄ ²⁻	58,593.2	0	58,601.6	58,348.2	253.5	0	0	0.7
HSO ₄ ⁻	8.5	0	6.54E-05	6.52E-05	2.83E-07	0	0	7.18E-14
H ₃ O ⁺	0.2	0	1.39E-06	1.38E-06	6.01E-09	0	0	3.20E-19
Na ⁺	24,197.0	0	26,156.2	26,043.0	113.1	0	0	0.0
Co ²⁺	106.2	0	106.2	105.8	0.5	0	0	0.5
Mn ²⁺	1.5	0	1.5	1.5	0.0	0	0	0.0
MnOH ⁺	2.51E-07	0	3.52E-02	3.51E-02	1.52E-04	0	0	0.0
Cu ²⁺	0.2	0	1.29E-06	1.28E-06	5.58E-09	0	0	7.05E-20

Nickel Extraction Block Full Stream Table

Name	501-EFF	502-NAOH	503-PRCP	504-AQ	505-SOL	506-AIN	507-AOUT	508-PROD
Flowrate	kg/hr	kg/hr	kg/hr	kg/hr	kg/hr	kg/hr	kg/hr	kg/hr
From	Cobalt Extraction Block (was 407-AQEE)	TK-NAOH	PRCP-501	FIL-501	FIL-501	Atmosphere	D-501	D-501
To	PRCP-501	PRCP-501	FIL-501	Lithium Extraction Block	D-501	D-501	Waste	TK-NIPD
Li ⁺	555.1	0	555.1	552.7	2.4	0	0	0.0
Ni ²⁺	2,489.1	0	0.0	0.0	3.01E-05	0	0	4.33E-17
NiOH ⁺	0.0	0	8.65E-04	8.61E-04	3.74E-06	0	0	6.85E-16
N ₂	0	0	0	0	0	68,256.0	68,256.0	3.31E-05